MCSHANE IDENTITIES FOR HIGHER TEICHMÜLLER THEORY AND THE GONCHAROV-SHEN POTENTIAL

YI HUANG AND ZHE SUN

ABSTRACT. In [GS15], Goncharov and Shen introduce a family of mapping class group invariant regular functions on their A-moduli space to explicitly formulate a particular homological mirror symmetry conjecture. Using these regular functions, we obtain McShane identities general rank positive surface group representations with loxodromic boundary monodromy and (non-strict) McShane-type inequalities for general rank positive representations with unipotent boundary monodromy. Our identities are expressed in terms of projective invariants, and we study these invariants: we establish boundedness and Fuchsian rigidity results for triple ratios. Moreover, we obtain McShane identities for finite-area cusped convex real projective surfaces by generalizing the Birman–Series geodesic scarcity theorem. We apply our identities to derive the simple spectral discreteness of unipotent bordered positive representations, collar lemmas, and generalizations of the Thurston metric.

1. Introduction

The aim of this paper is to generalize McShane identities for higher Teichmüller theory, a goal previously considered by Labourie and McShane in [LM09].

The starting point for our McShane identity is the *Goncharov–Shen potential* (Definition 2.9): a family of mapping class group invariant regular functions on the higher Teichmüller space $\mathcal{A}_{SL_n,S}$, first introduced by Goncharov and Shen in [GS15]. They utilize these potentials to formulate a precise homological mirror symmetry conjecture between Fock–Goncharov higher Teichmüller theoretic objects [GS15, Conjecture 1.16]. Goncharov–Shen potentials conjecturally correspond to *Landau-Ginzburg partial potentials* and contains data tantamount to specifying a compactification for the underlying space of the mirror dual. They are a natural higher rank generalization of horocycle length, and decomposing them leads to our family of McShane identities for positive surface group representations into PGL_n \mathbb{R} .

Our McShane identities are expressed in terms of geometric quantities such as simple root lengths and triple ratios, and naturally generalize those employed by Mirzakhani in her stunning proof [Mir07b] of the Witten–Kontsevich theorem. We establish geometric applications for our identities, yielding properties of simple root lengths and triple ratios along the way. We hope that this paper serves as an invitation for the community to further unravel the geometry underlying higher Teichmüller theory.

Date: May 19, 2019.

²⁰¹⁰ Mathematics Subject Classification. Primary 57M50, Secondary 32G15.

 $[\]it Key\ words\ and\ phrases.$ Mcshane's identity, Fock–Goncharov $\it A\ moduli\ space,$ Goncharov-Shen potential.

1.1. The McShane identity. Given a 1-cusped hyperbolic torus Σ , let $\mathcal{C}_{1,1}$ denote the collection of *unoriented* simple closed geodesics $\bar{\gamma}$ on Σ and let $\ell_{\bar{\gamma}}(\Sigma)$ denote the length of the (unoriented) simple closed geodesic $\bar{\gamma}$ on Σ . In his doctoral dissertation, McShane [McS91] established that:

(1)
$$\sum_{\bar{\gamma} \in \mathcal{C}_{11}} \frac{2}{1 + e^{\ell^{\Sigma}(\bar{\gamma})}} = 1.$$

McShane's prototypical identity has led to an ever-growing class of variant and generalized identities, including identities for the following hyperbolic manifolds:

- hyperbolic surfaces with differing topology and boundary monodromy [Hua15, McS98, Mir07a, Nor08, TWZ06],
- various hyperbolic 3-manifolds structures [AMS04, AMS06, Bow98, Bow97, Hua18, LS13, TWZ08],

not to mention the closely related Basmajian identity [Bas93], Bridgeman-Kahn identity [Bri11, BK10] and the Luo-Tan dilogarithm identity [LT11].

1.2. Cusped convex real projective surfaces. The theory of convex real projective surfaces is the simplest geometric example of a non-Fuchsian higher (rank) Teichmüller theory, and generalizes the Beltrami-Klein approach to hyperbolic surfaces. The monodromy representation $\rho:\pi_1(\Sigma)\to PGL_3(\mathbb{R})$ for a convex real projective surface Σ allows for multiple notions of *geodesic length*: an oriented closed geodesic γ on Σ corresponds to a conjugacy class in the fundamental group, and ratios of eigenvalues for $\rho(\gamma)$ are well-defined. Index the eigenvalues for $\rho(\gamma)$ so that $\frac{\lambda_1(\rho(\gamma))}{\lambda_2(\rho(\gamma))}, \frac{\lambda_2(\rho(\gamma))}{\lambda_3(\rho(\gamma))} > 1$ and define the *simple root lengths*

$$\ell_1(\gamma) := log\left(\frac{\lambda_1(\rho(\gamma))}{\lambda_2(\rho(\gamma))}\right) \text{ and } \ell_2(\gamma) := log\left(\frac{\lambda_2(\rho(\gamma))}{\lambda_3(\rho(\gamma))}\right) = \ell_1(\gamma^{-1}).$$

Throughout this article, we use $\bar{\gamma}$ to denote the unoriented geodesic underlying an oriented geodesic γ or γ^{-1} . Whereas simple root lengths are defined for *oriented* geodesics, the *Hilbert length*, given by

$$\ell(\bar{\gamma}) = \ell(\gamma) = \ell(\gamma^{-1}) = \ell_1(\gamma) + \ell_2(\gamma)$$

is well-defined for unoriented geodesics.

Ideal triangles are fundamental building pieces for hyperbolic and convex real projective surfaces. It is well-known that any two hyperbolic ideal triangles are isometric. In contrast, oriented convex real projective ideal triangles are geometrically richer and are classified by their *triple ratios* T (Figure 1) [FG06], which vary over $\mathbb{R}_{>0}$. We denote the logarithm of the triple ratio by $\tau(\Delta) := \log(T(\Delta)) \in \mathbb{R}$, and refer to this quantity as the *triangle invariant* [BD14, BD17].

In Section 7, we establish McShane identities for finite-area cusped convex real projective surfaces (Theorem 7.1). For 1-cusped tori, our result takes the form:

Theorem 1.1 (McShane identity for 1-cusped tori). Given a finite area convex real projective 1-cusped torus Σ , let $\vec{C}_{1,1}$ be the set of oriented simple closed geodesics on Σ . Then

(2)
$$\sum_{\gamma \in \vec{\mathcal{C}}_{1,1}} \frac{1}{1 + e^{\ell_1(\gamma) + \tau(\gamma)}} = 1,$$

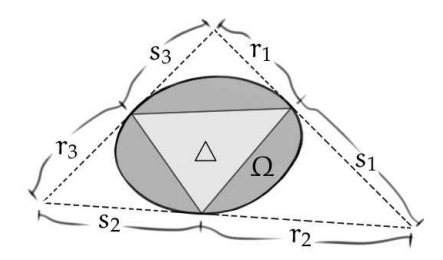


Figure 1. The triple ratio of the anticlockwise-oriented ideal triangle \triangle inside a convex domain $\Omega \subset \mathbb{R}^2 \subset \mathbb{R}P^2$, such as the universal cover of a convex real projective surface, is $T = \frac{s_1 s_2 s_3}{r_1 r_2 r_3}$.

where $\tau(\gamma)$ is the triangle invariant for either of the two embedded ideal triangles on Σ which has one side being the unique ideal geodesic disjoint from γ and the other two sides spiraling parallel to γ (see Figure 2).

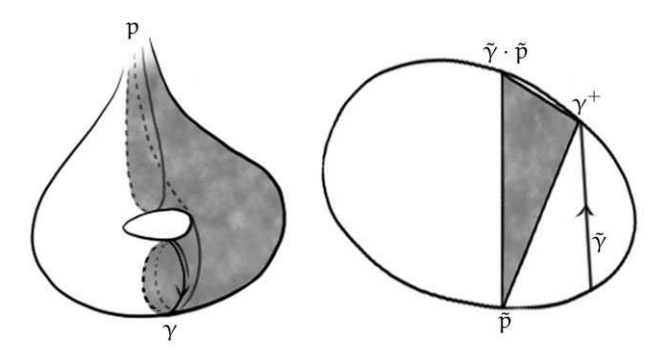


Figure 2. Cutting the shaded pair of half-pants on the left figure along the spiraling geodesic depicted (left figure) produces an ideal triangle \triangle_{γ} , and we use it to define $\tau(\gamma) = \tau(\triangle_{\gamma})$. The right figure depicts a single lift $(\tilde{p}, \gamma \cdot \tilde{p}, \gamma^+)$ of \triangle_{γ} to the universal cover of Σ , here γ denotes both the closed geodesic γ as well as an homotopy class representative chosen so that $\tilde{\gamma}$ is its invariant axis.

Remark 1.2. Triple ratios for ideal triangles on hyperbolic surfaces always equal 1. The Fuchsian case for the above identity therefore recovers the classical McShane identity after catering for the canonical 2:1 orientation-forgetting map between $\vec{\mathbb{C}}_{1,1}$ and $\mathbb{C}_{1,1}$.

1.3. **McShane identity proof strategy.** Each summand in the classical McShane identity is the probability that a geodesic shot out from the cusp p on Σ self-intersects before hitting $\bar{\gamma}$. This probability measure is the horocycle length measure induced from identifying the length 1 horocycle around p with the set of all directions emanating from p. The following two steps establish the identity:

Step 1:: one needs to show that there is 0 probability that a geodesic emanating from p is simple. This is due to the Birman–Series theorem [BS85].

Step 2:: the complement of the (uncountable) set of points on the length 1 horocycle corresponding to simple geodesics emanating from p is a countable union of open intervals. One needs to express the length of each interval in terms of geometric quantities intrinsic to the surface Σ .

For convex real projective surfaces, the probability measure we decompose is the *ratio* (4.13) derived from the *Goncharov–Shen potential* — an additive character introduced by Goncharov and Shen in [GS15]. The Goncharov–Shen potential measure can be manipulated and computed via Fock and Gocharov's \mathcal{A} -coordinates [FG06], and is perfectly suited for Step 2.

We further show that the probability measure induced by the Goncharov-Shen potential is a C¹-rescaling of the horocycle length probability measure, thus enabling us to use the following generalization of the Birman–Series theorem:

Theorem 1.3. *Given a finite-area convex real projective surface* Σ *, the* Birman–Series set *defined as*

$$BS(\Sigma) := \{x \in \Sigma \mid x \text{ lies on a complete simple geodesic on } \Sigma\}$$

is nowhere dense, closed and has 0 area.

1.4. Fock–Goncharov higher Teichmüller theory. In [Hit92], Hitchin discovered a special contractible component of $\operatorname{Hom}(\pi_1(S),\operatorname{PGL}_n(\mathbb{R})/\operatorname{PGL}_n(\mathbb{R}),$ called *Hitchin component*. It then becomes into the central object of higher Teichmüller theory. Labourie [Lab06] characterized the Hitchin components dynamically. Meanwhile Fock and Goncharov [FG06] characterized the Hitchin components algebraically, using the notion of positivity. In this paper, we concentrate on the Fock and Goncharov's approach to higher Teichmüller theory.

Positive representations $\rho:\pi_1(S)\to PGL_n(\mathbb{R})$ are central objects underpinning Fock and Goncharov's higher rank generalization of Teichmüller theory [FG06]. In particular, the composition of any Fuchsian representation with an irreducible representation from $PGL_2(\mathbb{R})$ to $PGL_n(\mathbb{R})$ is a positive representation. We refer to such representations as n-Fuchsian representations. When n=3, positive representations correspond precisely to monodromy representations for finite area cusped convex real projective surfaces and loxodromic bordered convex real projective surfaces [G90][CG93][FG07]. For rank n positive representations, there are n-1 linearly independent simple root lengths: one for each $i=1,\ldots,n-1$. The i-th simple root length for γ is given by:

(3)
$$\ell_{i}(\gamma) := \log \left(\frac{\lambda_{i}(\rho(\gamma))}{\lambda_{i+1}(\rho(\gamma))} \right),$$

here we again index eigenvalues by decreasing (absolute) value.

In [FG06], Fock and Goncharov describe the \mathcal{A} -moduli space and the \mathcal{X} -moduli space. These two "moduli spaces" are higher Teichmüller spaces in the following sense: the \mathcal{A} -moduli space and the \mathcal{X} -moduli space respectively generalize Penner's decorated Teichmüller space [Pen87] and Thurston's enhanced Teichmüller space [Bon96]. The \mathcal{A} -moduli space is associated with positive representations with unipotent boundary monodromy, whereas the \mathcal{X} -moduli space allows both unipotent and loxodromic boundary monodromy.

Fock–Goncharov A-coordinates parametrize the A-moduli space and generalize Penner's λ -length coordinates. On the other hand, the \mathcal{X} -moduli space is coordinatized by *edge functions* and triple ratios ([BD14] for closed surface case). Edge

Z: Added this paragraph for history background.

functions naturally generalize Thurston's shearing length coordinates, whereas triple ratios parameterize ideal triangles: precisely $\binom{n-1}{2}$ triple ratios are needed to specify each ideal triangle. In [SWZ17, SZ17, WZ18], starting from the elementary deformation of edge functions and triple ratios, Wienhard and Zhang and the second author provide a Darboux coordinate system for closed surface of genus g > 1.

- 1.5. **Triple ratio boundedness and rigidity.** We have hitherto only considered triple ratios as coordinates, i.e.: triple ratios for ideal triangles in ideal triangulations. We introduced triple ratios for convex real projective surfaces, and we see that they generalize to (Section 2.19):
 - Frenet curves in $\mathbb{R}P^{n-1}$ (including limit curves of positive representations)
 - and strictly convex domains in $\mathbb{R}^{n-1} \subset \mathbb{R}P^{n-1}$.

In [AC15], Adeboye–Cooper show that triangle invariants and Hilbert areas are related by the following inequality:

Theorem 1.4 ([AC15, Proposition 0.3]). *Given an embedded ideal triangle* $\triangle \subset \Sigma$ *on a finite-area convex real projective surface* Σ *, the Hilbert area Area*_H(\triangle) *of* \triangle *satisfies:*

$$Area_{\mathsf{H}}(\triangle) \geqslant \frac{1}{8}(\pi^2 + \tau(\triangle)^2).$$

An immediate consequence of this result is that the triangle invariant $\tau = \log(T)$ of any embedded ideal triangle on Σ is necessarily bounded between

$$\pm 2\sqrt{2Area_{\mathsf{H}}(\Sigma)-\pi^2|\chi(\Sigma)|}$$
.

We show, using topological arguments, that triple ratio/triangle-invariant boundeness is true for positive representations in general:

Theorem 1.5 (Triple ratio boundedness, Theorem 3.4). The set consisting of all triple ratios of all embedded ideal triangles for a (general rank) positive representation is bounded within some interval $[T_{\min}^{\rho}, T_{\max}^{\rho}]$.

Remark 1.6. Our proof for the above result is essentially topological and holds also for surfaces with quasihyperbolic boundary monodromy, for which it is known that immersed ideal triangles may have arbitrarily large triangle invariant. Furthermore, For finite-area convex real projective surfaces, it is possible to promote Theorem 1.5 to assert boundedness for all immersed ideal triangles using [BH13, Proposition 3.1].

Remark 1.7. In [Kim18], Kim shows that a strictly convex real projective surface has bounded triple ratio spectrum if and only if it has finite Hilbert area. One can derive Kim's claim for triangle invariants by combining Adeboye–Cooper's inequality with the last Corollary in Zhang's introduction [Zha15]. The issue that the formers uses Hilbert area and the latter uses the Busemann measure is resolved thanks (again) to [BH13, Proposition 3.1].

Theorem 1.8 (Fuchsian rigidity for n = 3, 4, 5, 6, Theorem 3.10). A positive representation ρ is Fuchsian if and only if every triple ratio X-coordinate (i.e.: with respect to every ideal triangulation of the underlying surface) is equal to 1.

Remark 1.9. This is equivalent to the (a. priori weaker) claim: a positive representation ρ is n-Fuchsian iff. every triple ratio for every embedded ideal triangle for ρ is equal to 1. The equivalence is because the set of ideal triangles which constitute an ideal triangulation is dense in the space of all ideal triangles.

Remark 1.10. We also obtain a similar rigidity criterion for edge functions (Theorem 3.12), namely that all edge functions along ideal geodesics being equal classifies n-Fuchsian representations.

Theorem 1.11 (Fuchsian rigidity for general rank). A positive representation ρ : $\pi_1(S) \to PGL_n(\mathbb{R})$ without loxodromic boundary monodromy (including S being a closed surface) is Fuchsian if and only if the triple ratio of every immersed ideal triangle is equal to 1.

The following immediate corollary is somewhat unrelated to the theme of our paper. We state it due to independent interest: ellipsoid characterization is a classical area of research with over a century's worth of history (see [Guo13] for a survey).

Corollary 1.12 (Ellipsoid characterization). *A* k-dimensional open convex set in \mathbb{R}^k is a k-dimensional ellipsoid iff all of its triple ratios are equal to 1.

1.6. **Goncharov–Shen potentials and their ratios.** For each cusp p of S, there are n-1 independent Goncharov–Shen potentials P_1^p, \ldots, P_{n-1}^p on the \mathcal{A} -moduli space $\mathcal{A}_{SL_n,S}$. Altogether, these potentials generate the ring of regular functions on the \mathcal{A} -moduli space [GS15, Theorem 10.7]. The Goncharov–Shen potential is a central object of this paper, and we dedicate Sections 4 and 5 to its study.

Goncharov–Shen potentials are defined for \mathcal{A} -moduli space and not \mathcal{X} -moduli space. They require, as input, decoration data in the same way that horocycle lengths in Penner's decorated Teichmüller theory necessitate the choice of decorating points in the Minkowski light cone [Pen87].

A change in decoration for cusp p rescales each Goncharov–Shen potential P_i^p by a constant factor. Therefore, ratios (see Definition 4.13) of potentials, of the same level i, of immersed subsurfaces containing p are decoration independent (Proposition 4.14). These ratios provide geometrically meaningful data about the underlying positive representation. In Proposition 4.16, we show that the exponentiated simple root lengths of a geodesic γ are equal to the ratio of the Goncharov–Shen potentials for a particular pair of ideal triangles related by Dehn twist in γ . We use the following quantity in the half-pants-based summation form of our Mc-Shane identities/inequality for unipotent bordered positive representations.

Definition 1.13 (Half-pants ratio). *let* $\bar{\mu} \subset S$ *be a pair of half-pants containing cusp* p. We define the i-th half-pants ratio $B_i^p(\bar{\mu})$ by

$$B_{\mathfrak{i}}(\bar{\mu}) := \frac{P_{\mathfrak{i}}^{\bar{\mu}}}{P_{\mathfrak{i}}^{p}},$$

where $P_i^{\bar{\mu}}$ is the i-th Goncharov–Shen potential at the unique cusp p of the half-pants $\bar{\mu}$. We refer to $B_i(\bar{\mu})$ as the i-th half-pants ratio for $\bar{\mu}$.

Remark 1.14. When S is not the once-punctured torus, pairs of half-pants $\bar{\mu}$ are uniquely specified by its (unoriented) cuff $\bar{\gamma}$ and its (unoriented) seam $\bar{\gamma}_p$ (see Figure 3). In these cases, we may write $B_i(\bar{\mu})$ as $B_i(\bar{\gamma}, \bar{\gamma}_p)$ or even as $B_i(\gamma, \gamma_p)$.

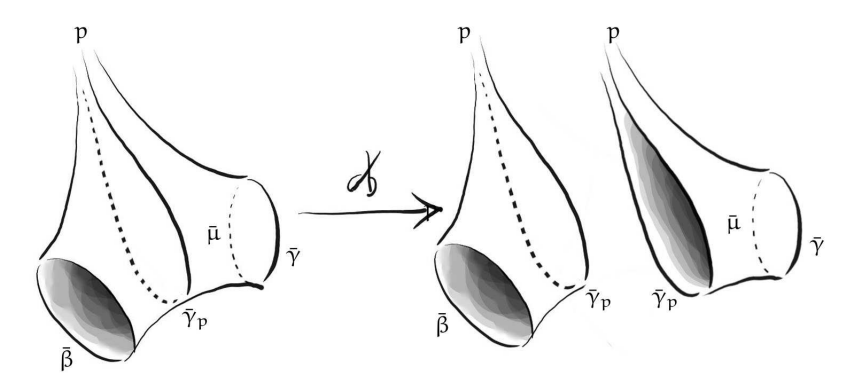


Figure 3. Cutting a surface S which is topologically a pair of pants into two pairs of half-pants $\bar{\mu} = (\bar{\gamma}, \bar{\gamma}_p)$ and $(\bar{\beta}, \bar{\gamma}_p)$.

1.7. Series for higher rank unipotent bordered representations. Benoist-Hulin show that the cusp geometry of finite-area convex real projective surfaces limits to a constant negative curve cusp as one penetrates deeper into the cusp [BH13, Proposition 3.1]. This fact is key to our proof of the Birman–Series theorem, enabling us to obtain our n = 3 identity (Theorem 7.1).

For higher rank positive representations with unipotent boundary monodromy, we currently lack an appropriate generalization of this key proposition, and instead obtain a McShane-type (non-strict) inequality. We first state the punctured torus result due to its relative simplicity:

Theorem 1.15 (General rank inequality for 1-cusped tori). *Consider a once-punctured* torus S, and let $\rho: \pi_1(S) \to PGL_n(\mathbb{R})$ be a positive representation with unipotent boundary monodromy. For each $i=1,\ldots,n-1$, we have the following inequality:

(5)
$$\sum_{\gamma \in \vec{C}_{1,1}} \frac{1}{1 + e^{\ell_1(\gamma) + \kappa_1(\gamma)}} \leq 1,$$

where the term $\kappa_i(\gamma)$ is the logarithm of a positive rational function of triple-ratios (see Theorem 1.17) of marked ideal triangles associated to \triangle_{γ} (see Figure 2).

We require different summation indices for surfaces topologically different to a 1-cusped torus. One corollary of [Hua14, Theorem 4.5] is an expression for the McShane identity summed over the set \mathcal{H}_p of embedded pairs of (ideal) halfpants $\bar{\mu}$ containing p.

We introduce a refinement of this summation index by introducing orientations on the boundary geodesics. In particular, we require the oriented boundaries γ and γ_p to be *parallel* in the sense that orientations agree with respect to isotopy on the annulus $\bar{\mu} \cup \{p\}$ (see Figure 4) .

Definition 1.16 (Boundary-parallel half-pants). An embedded boundary-parallel pair of half-pants μ containing p is an ordered pair (γ, γ_p) consisting of an oriented simple geodesic γ and an oriented simple bi-infinite geodesic γ_p so that $\bar{\gamma}, \bar{\gamma}_p$ bound a pair of half-pants on S and γ is parallel to γ_p . We denote the collection of all boundary-parallel pairs of half-pants on S containing p by $\overline{\mathcal{H}}_p$.

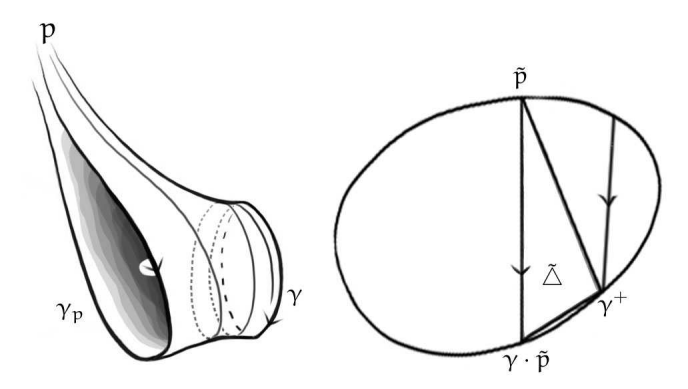


FIGURE 4. Cutting along the spiraling geodesic on the boundary-parallel pair of half-pants (γ, γ_p) (left figure) results in an ideal triangle $\triangle := \triangle_{\gamma, \gamma_p}$ oriented so that the marked triangle $\tilde{\triangle} = (\tilde{p}, \gamma \cdot \tilde{p}, \gamma^+)$ is a lift of \triangle (right figure).

For each pair of boundary-parallel half-pants $\mu=(\gamma,\gamma_p)$, the unique simple biinfinite geodesic which shoots out from p and spirals towards γ parallel to its orientation (see Figure 4) cuts the underlying pair of pants $\bar{\mu}=(\bar{\gamma},\bar{\gamma}_p)$ into an ideal triangle $\triangle_{\gamma,\gamma_p}$. We adopt the notation

(6)
$$T(\gamma, \gamma_p) := T(\triangle_{\gamma, \gamma_p}) \text{ and } \tau(\gamma, \gamma_p) := \tau(\triangle_{\gamma, \gamma_p}).$$

We emphasize that one needs to mark \triangle so that it is the projection of the triangle $\tilde{\triangle} = (\tilde{p}, \gamma \cdot \tilde{p}, \gamma^+)$ in the universal cover (Figure 4).

Theorem 1.17 (General rank inequality for cusped surfaces). Let $\rho: \pi_1(S) \to PGL_n(\mathbb{R})$ be a positive representation with unipotent boundary monodromy, and let p be a distinguished boundary of S. Then, for each $i=1,\ldots,n-1$, we have the following inequality:

(7)
$$\sum_{(\gamma,\gamma_{\mathfrak{p}})\in\overrightarrow{\mathcal{H}}_{\mathfrak{p}}} \frac{B_{\mathfrak{i}}(\gamma,\gamma_{\mathfrak{p}})}{1+e^{\ell_{\mathfrak{i}}(\gamma)+\kappa_{\mathfrak{i}}(\gamma,\gamma_{\mathfrak{p}})}} \leqslant 1,$$

the term $\kappa_i(\gamma, \gamma_p)$ is the logarithm of a positive rational function (see Theorem 8.5) of triple ratios of marked ideal triangles associated to $\triangle_{\gamma, \gamma_p}$.

Remark 1.18. The above formula is an equality for n = 3 positive representations.

1.8. **Pair of pants summation.** Our previous half-pants summation formula is a finer series than the classical McShane identity [McS98]. Which, in turn, is summed over the set

$$\mathcal{P}_p := \left\{ \begin{array}{c} \text{(isotopy classes of) embedded pairs of pants \bar{Y} on S} \\ \text{which contain cusp p as a boundary} \end{array} \right\}.$$

Here it is often convenient to denote a pair of pants $\bar{Y} \in \mathcal{P}_p$ by its cuffs $\{\bar{\beta}, \bar{\gamma}\}$.

We also have an identity summed over pairs of pants, but with oriented cuffs β, γ . Moreover, we need the orientations on β and γ to be *parallel* in the sense that their orientations agree with respect to isotopy on the annulus $\bar{Y} \cup \{p\}$ (see Figure 5).

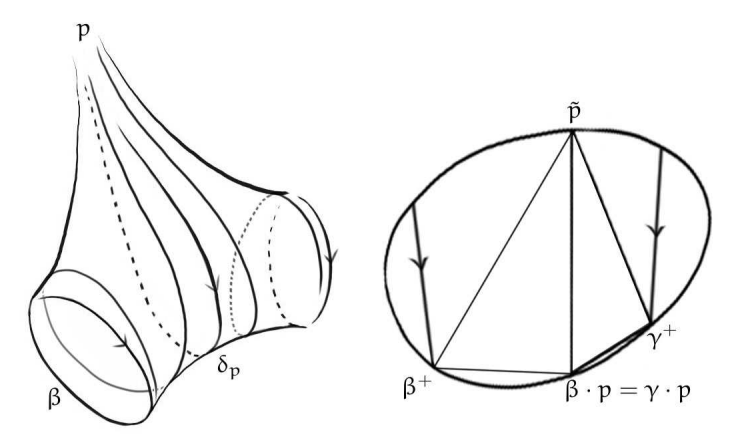


FIGURE 5. Cutting along the spiraling geodesics on the boundary-parallel pair of pants $\{\beta, \gamma\}$ (left figure) results in an ideal quadrilateral whose lift is the marked quadrilateral $(\tilde{p}, \beta^+, \beta \cdot \tilde{p} = \gamma \cdot \tilde{p}, \gamma^+)$ (right figure).

Definition 1.19 (Boundary-parallel pairs of pants). An embedded boundary-parallel pairs of pants Y containing p is an unordered pair $\{\beta,\gamma\}$ of (disjoint) oriented geodesics so that p, $\bar{\beta},\bar{\gamma}$ bound a pair of pants on S and β is parallel to γ . We denote the collection of all boundary-parallel pairs of pants on S containing p by $\vec{\mathbb{P}}_p$. Similar definition for $\vec{\mathbb{P}}_\alpha$ where p is replaced by a boundary component α .

Theorem 1.20 (Pants summation form). Given a positive representation $\rho : \pi_1(S) \to PGL_n(\mathbb{R})$ with unipotent boundary monodromy, then

(8)
$$\sum_{\{\beta,\gamma\}\in\vec{\mathcal{P}}_{p}} \left(1 + \frac{\cosh(\frac{1}{2}d_{2}(\beta,\gamma))}{\cosh(\frac{1}{2}d_{1}(\beta,\gamma))} \cdot e^{\frac{1}{2}(\ell_{i}(\beta) + \kappa_{i}(\beta,\delta_{p}) + \ell_{i}(\gamma) + \kappa_{i}(\gamma,\delta_{p}))}\right)^{-1} \leqslant 1, \text{ where}$$

- $\delta_p \subset \bar{Y} = \{\bar{\beta}, \bar{\gamma}\}$ is the unique oriented simple ideal geodesic on the pair of pants \bar{Y} with both ends tending to p and oriented so that it is parallel to p and p;
- and the $d_i(\beta, \gamma) = \log D_i(\tilde{p}, \gamma \cdot \tilde{p}, \beta^+, \gamma^+)$ are logarithms of (limiting) edge functions evaluated on the embedded ideal quadrilateral obtained from cutting \tilde{Y} along the two simple bi-infinite geodesics which emanate from p and respectively spiral towards β and γ (see Figure 5).

In particular, the above (non-strict) inequality is an equality for n=3, and the summand in this case takes the form:

$$\left(1 + \frac{\cosh\frac{d_2(\beta,\gamma)}{2}}{\cosh\frac{d_1(\beta,\gamma)}{2}} \cdot e^{\frac{1}{2}(\tau(\gamma,\delta_{\mathfrak{p}}) + \ell_1(\gamma) + \tau(\beta,\delta_{\mathfrak{p}}) + \ell_1(\beta))}\right)^{-1}$$

Remark 1.21. [Kim18, Theorem 1.2] shows that given a n=3 positive representation ρ , the quantities $\frac{\cosh(\frac{1}{2}d_2(\beta,\gamma))}{\cosh(\frac{1}{2}d_1(\beta,\gamma))}$ are bounded as one varies over $\{\beta,\gamma\} \in \overrightarrow{\mathcal{P}}_p$.

1.9. **Simple spectra discreteness.** One immediate corollary to triple ratio boundedness (Theorem 1.5) and our general rank inequality for 1-cusped tori (Theorem 1.15) is the discreteness of the simple root length spectrum of the simple

curves for a given unipotent bordered representation. For surfaces of general topological type, this is not immediate, because the $B_i(\gamma, \gamma_p)$ terms in (7) can (and do) become arbitrarily small. In Section 7.2, we show that:

Theorem 1.22 (Simple spectral discreteness). Let $\rho : \pi_1(S) \to PGL_n(\mathbb{R})$ be a positive representation with unipotent boundary monodromy. Then the simple ℓ_i -spectra and the simple Hilbert length spectrum for ρ are both discrete.

The above theorem is also proved in [Kim19] using a different method. For positive representations with (only) loxodromic boundary monodromy, the above result can be obtained via the Anosov property. However, positive representations with unipotent boundary monodromy are not Anosov. We emphasize that our proof requires only the cluster algebra structure of the Fock–Gocharov \mathcal{A} -moduli space.

For n=3 positive representations, we can say something stronger: our proof of the Birman–Series theorem implies that the simple Hilbert length spectrum grows at least polynomially. In order to extend this claim to simple root lengths, we require the following comparison result.

Theorem 1.23 (Hilbert vs. simple root length comparison). For any positive representation $\rho: \pi_1(S) \to PGL_3(\mathbb{R})$, there exists $K_{\rho} > 1$ such that for every simple closed curve γ on S, we have:

(10)
$$\ell_1(\gamma) < \ell(\gamma) < K_{\rho} \cdot \ell_1(\gamma).$$

We believe that the above result is due to Benoist-Hulin, and may be obtained by combining the proof of Benoist's [Ben01, Corollary 5.3] with Proposition 6.9. This is also proved in [Kim19]. Nonetheless, we provide a proof for this fact in Appendix A (just in case).

1.10. **McShane indentities for loxodromic bordered representations.** For higher rank positive representations with loxodromic boundaries, Labourie-McShane introduce a powerful and general machinery for establishing McShane-type identities via the language of cross-ratios [LM09]. We require a mild generalization of their work to allow for "asymmetric" versions of cross-ratios.

Definition 1.24 (Ratio). Consider the following space of 4-tuples of of ideal points

$$\vartheta_\infty\pi_1(S)^{4*}=\left\{(x,y,z,t)\in\vartheta_\infty\pi_1(S)^4\mid x\neq t \text{ and } y\neq z\right\}.$$

A ratio $\mathbb{B}: \mathfrak{d}_{\infty}\pi_1(S)^{4*} \to \mathbb{R}$ is a $\pi_1(S)$ -invariant Hölder function function satisfying the following axioms:

- (1) (normalization): B(x, y, z, t) = 0 iff. y = t,
- (2) (normalization): B(x, y, z, t) = 1 iff. z = t,
- (3) (cocycle): $B(x, y, z, t) = B(x, y, z, w) \cdot B(x, y, w, t)$,

An ordered ratio is a ratio B on S which satisfies the condition that for any four distinct ideal points $x, y, z, t \in \partial_{\infty} \pi_1(S)$:

- (1) if z, t lie on the same side of xy, then B(x, y, z, t) > 0,
- (2) if x, y, z, t are cyclically ordered, then B(x, y, z, t) > 1.

We also require a new summation index for our:

Definition 1.25. Let $\overline{\mathcal{H}}_{\alpha}$ denotes the collection of (embedded) boundary-parallel pairs of half-pants on $S_{g,m}$ with both ends of its seam emanating from α^- (see Figure 6). Moreover, let $\overline{\mathcal{H}}_{\alpha}^0 \subset \overline{\mathcal{H}}_{\alpha}$ denote the subset of half-pants with a peripheral cuff.

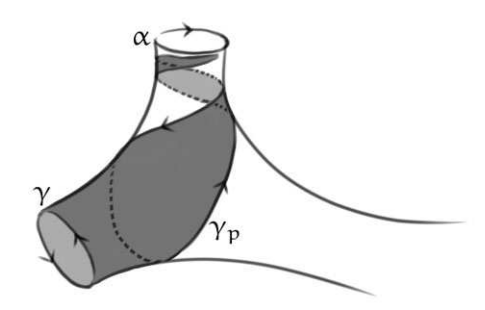


Figure 6. An example of a boundary-parallel pair of pants (γ, γ_p) with both ends of the seam $\bar{\gamma}_p$ emanating from p where $p = \alpha^-$ denotes the repelling fixed point of α .

Remark 1.26. Given a boundary-parallel pair of half-pants $(\gamma, \gamma_{\alpha_{-}}) \in \overrightarrow{\mathcal{H}}_{\alpha}^{\mathfrak{d}}$, there is a unique boundary-parallel pair of pants in $\overrightarrow{\mathcal{P}}_{\alpha}$ that contains $(\gamma, \gamma_{\alpha_{-}})$ and agrees with its boundary orientations. We thereby identify $\overrightarrow{\mathcal{H}}_{\alpha}^{\mathfrak{d}}$ with the subset $\overrightarrow{\mathcal{P}}_{\alpha}^{\mathfrak{d}} \subset \overrightarrow{\mathcal{P}}_{\alpha}$ of boundary-parallel pairs of pants with a peripheral cuff.

Proposition 1.27 (A variation of [LM09, Theorem 5.1.1]). Let α be a distinguished boundary component for $S = S_{q,m}$, we have the following identity:

$$\ell_{\mathbb{B}}(\alpha) = \sum_{(\gamma,\gamma_{\alpha^{-}}) \in \overrightarrow{\mathcal{H}}_{\alpha}} \left| \log B(\alpha^{-},\alpha^{+},\gamma(\alpha^{-}),\gamma^{+}) \right| + \sum_{(\gamma,\gamma_{\alpha^{-}}) \in \overrightarrow{\mathcal{H}}_{\alpha}^{\circ}} \log B(\alpha^{-},\alpha^{+},\gamma^{-},\gamma^{+}).$$

We now state the explicit form that these summands take, but only for $S_{g,1}$ — this is for simplicity as there are no $\overrightarrow{\mathcal{H}}^{\mathfrak{d}}_{\alpha}$ summands.

Theorem 1.28 (half-pants summation identity). Consider a positive representation $\rho: \pi_1(S_{g,1}) \to PGL_n(\mathbb{R})$, and let α be a distinguished boundary component of $S_{g,m}$. Then we have the following pants summation form of the McShane identity:

$$(11) \qquad \ell_{\mathfrak{i}}(\alpha) = \sum_{(\gamma,\gamma_{\alpha^{-}}) \in \overrightarrow{\mathcal{H}}_{\alpha}} \left| \log \left(\frac{e^{R_{\mathfrak{i}}(\gamma,\gamma_{\alpha^{-}}) \cdot \ell_{\mathfrak{i}}(\alpha)} + e^{\ell_{\mathfrak{i}}(\gamma) + \kappa_{\mathfrak{i}}(\gamma,\gamma_{\alpha^{-}})}}{1 + e^{\ell_{\mathfrak{i}}(\gamma) + \kappa_{\mathfrak{i}}(\gamma,\gamma_{\alpha^{-}})}} \right) \right|.$$

Note that we show that these summands limit to the punctured case (Theorem 1.17) summands as one deforms from a positive representation with loxodromic boundary monodromy to one with unipotent boundary monodromy. We also obtain the pants summation form of the above identity:

Theorem 1.29 (pants summation identity). Consider a positive representation ρ : $\pi_1(S_{g,1}) \to PGL_n(\mathbb{R})$, and let α be a distinguished boundary component of $S_{g,1}$. Then

we have the following half-pants summation form of the McShane identity:

(12)

$$\ell_{\mathfrak{i}}(\alpha) = \sum_{\{\beta,\gamma\} \in \overrightarrow{\mathcal{P}}_{\alpha}} \log \left(\frac{e^{\frac{1}{2}\ell_{\mathfrak{i}}(\alpha)} + \frac{\cosh\frac{d_{2}(\beta,\gamma)}{2}}{\cosh\frac{d_{1}(\beta,\gamma)}{2}} \cdot e^{\frac{1}{2}(\kappa_{\mathfrak{i}}(\gamma,\gamma_{\alpha^{-}}) + \ell_{\mathfrak{i}}(\gamma) + \kappa_{\mathfrak{i}}(\beta,\beta_{\alpha^{-}}) + \ell_{\mathfrak{i}}(\beta))}}{e^{-\frac{1}{2}\ell_{\mathfrak{i}}(\alpha)} + \frac{\cosh\frac{d_{2}(\beta,\gamma)}{2}}{\cosh\frac{d_{1}(\beta,\gamma)}{2}} \cdot e^{\frac{1}{2}(\kappa_{\mathfrak{i}}(\gamma,\gamma_{\alpha^{-}}) + \ell_{\mathfrak{i}}(\gamma) + \kappa_{\mathfrak{i}}(\beta,\beta_{\alpha^{-}}) + \ell_{\mathfrak{i}}(\beta))}} \right).$$

Remark 1.30. The pants summation identities more apparently generalize Mirzakhani and Tan-Wong-Zhang's bordered hyperbolic surface identities. Whereas the half-pants summations are more convenient for our applications.

Notation 1.31. At various points in this paper we alternate between topological, geometric and representation theoretic vernacular, and we shall adapt our notation to these varying contexts. For example, the set $\vec{C}_{g,m}$ of oriented simple closed geodesics γ on a genus g surface with m cusps is equivalent to the set of conjugacy classes of homotopy classes in $\pi_1(S_{g,n})$ with simple curve representatives. In geometric contexts, we might use γ to denote a simple closed geodesic, whereas in representation theoretic contexts we use γ to denote a particular representative $\gamma \in \pi_1(S_{g,m})$ of the conjugacy class. The level of notational flexibility extends also to notation for pairs of pants: we use $\{\beta,\gamma\}$ in geometric contexts versus $(\alpha,\beta^{-1},\gamma)\in\pi_1(S_{g,m})^3$ in representation theoretic contexts when it is convenient to have the precise homotopy classes of α , β and γ .

1.11. **Applications.** We are aware of the following applications for McShane-type identities in the literature:

- various authors [AMS04, AMS06, Bow98, Bow97, Hua18, LS13] use them
 to study the geometry of the convex core or the cuspidal tori for various
 hyperbolic 3-manifolds;
- Miyachi uses them to bound the Teichmüller distance between two marked surfaces [Miy05];
- and most spectacularly, Mirzakhani [Mir07a] uses them to derive a recursive algorithm for computing moduli space volumes.

We illustrate several novel applications of the McShane identity. We see in Section 7.2 that even McShane inequalities give us useful information: simple length spectrum discreteness. In fact, the inequality also allows us to derive the following useful fact:

Theorem 1.32 (Collar lemma [LZ17], Theorem 7.7). *Given any finite-area convex projective surface* Σ *, any two intersecting simple closed geodesics* β *, \gamma satisfy the following inequality:*

(13)
$$(e^{\frac{1}{2}\ell(\beta)} - 1)(e^{\frac{1}{2}\ell(\gamma)} - 1) > 4.$$

The remaining applications are all related to asymmetric ratio metrics on various Teichmüller spaces. These results require the full strength of the McShane identity and not just an inequality. We begin with our results for Fuchsian representations:

Theorem 1.33 (Fuchsian non-domination). Given two marked hyperbolic surfaces $\Sigma_1, \Sigma_2 \in \mathit{Teich}_{g,m}(L_1,\ldots,L_m)$ with fixed boundary lengths $L_1,\ldots,L_n \geqslant 0$. Then the marked simple geodesic spectrum for Σ_1 dominates the marked simple geodesic spectrum Σ_2 if and only if $\Sigma_1 = \Sigma_2$.

Non-domination fails when the boundary length is allowed to vary [PT10], meaning that the naive generalization of Thurston's length ratio metric does not satisfy positivity (compare with [Thu98, Theorem 3.1]). Liu–Papadopoulos–Su–Théret resolve this by introducing the arc metric. We do so by fixing the boundary length:

Corollary 1.34 (Length ratio metric for fixed bordered surfaces). The non-negative real function $d_{\mathit{Th}}: \mathit{Teich}_{g,m}(L_1,\ldots,L_m) \times \mathit{Teich}_{g,m}(L_1,\ldots,L_m) \to \mathbb{R}_{\geqslant 0}$ defined by

(14)
$$d_{\mathit{Th}}(\Sigma_{1}, \Sigma_{2}) := \log \sup_{\bar{\gamma} \in \mathfrak{C}(S_{g,m})} \frac{\ell^{\Sigma_{1}}(\bar{\gamma})}{\ell^{\Sigma_{2}}(\bar{\gamma})},$$

is a mapping class group invariant asymmetric metric on the Teichmüller space Teich_{g,m} $(L_1, ..., L_m)$ of genus g surfaces with m boundaries of fixed lengths $L_1, ..., L_m$.

Non-domination is also a problem for convex real projective surfaces. We propose the following candidate for a metric on the space $Conv_{1,1}^*$ of finite-area convex real projective 1-cusped tori:

(15)
$$d_{\textit{Gap}}(\Sigma_1, \Sigma_2) := \log \sup_{\gamma \in \overrightarrow{\mathcal{C}}_{1,1}} \frac{\log(1 + e^{\ell_1^{\Sigma_1}(\gamma) + \tau^{\Sigma_1}(\gamma)})}{\log(1 + e^{\ell_1^{\Sigma_2}(\gamma) + \tau^{\Sigma_2}(\gamma)})}.$$

Theorem 1.35 (Gap metric for $Conv_{1,1}^*$). The non-negative function d_{Gap} defines a mapping class group invariant aymmetric metric on $Conv_{1,1}^*$. Moreover, the restriction of the metric d_{Gap} to the Fuchsian locus of $Conv_{1,1}^*$ is equal to the Thurston metric.

We also generalize the notion of a gap metric to include finite-area cusped convex real projective surfaces of general topological type (Definitions 7.16 and 7.17). The resulting asymmetric metric is mapping class group invariant, but we are unsure if it is a strictly larger distance function than the Thurston metric on the Fuchsian locus.

1.12. **Section overview and reading guide.** This paper consists of the following sections:

Section 2: Fock–Goncharov moduli spaces and coordinates. We construct Fock and Goncharov's higher Teichmüller spaces (Definitions 2.6 and 2.9), before defining coordinates (Definitions 2.15 and 2.21) and explicit coordinate transforms (Definition 2.24) for them. We conclude by defining the positive subset of the Fock–Goncharov moduli spaces and positive representations (Definition 2.27) — these are the central object of our studies.

Section 3: Properties of \mathcal{X} **-coordinates.** We study the set of all triple ratios and edge functions for any given positive representation. We use topological arguments to show that the set of triple ratios is bounded (Theorem 3.4). We then employ algebraic and geometric techniques to show that triple ratios all being equal to 1 or edge functions along the same edge being all the same are characterizing properties for n-Fuchsian representations (Theorem 3.10 for n = 3,4, Theorem 3.12 for n = 3 and Theorem 3.16 for general n with no loxodromic boundaries).

Section 4: Goncharov–Shen potentials. We define and study Goncharov–Shen potentials. In particular, we show that ratios of Goncharov–Shen potentials are projective invariants (Proposition 4.14), and we dub these objects i-ratios and

relate them to weak cross ratios (Corollary 4.15) and simple root lengths (Proposition 4.19).

Section 5: Goncharov–Shen splitting technique. We compute the behavior of \mathcal{A} -coordinates under Dehn-twists (Proposition 5.4). We combine this with the Goncharov–Shen potential splitting mechanism to compute McShane identity summands. We derive two variant McShane–type inequalities: the half-pants summation form (Theorem 5.9) and the pants summation form (Theorem 5.10).

Section 6: Geodesic sparsity for convex real projective surfaces. We give an introduction to the theory of convex real projective surfaces before proving a Birman–Series geodesic sparsity theorem for convex real projective surfaces (Theorem 6.11).

Section 7: McShane identities for convex real projective surfaces and applications. We utilize the Birman–Series geodesic sparsity theorem obtained in Section 6 to show that the McShane-type inequality we obtained in Section 5 is in fact an equality (Theorem 7.1). We then employ these identities to show the discreteness of simple length spectra (Theorem 7.4), to demonstrate the collar lemma (Theorem 7.7) and to generalize the Thurston metric (Theorem 7.14 and Definition 7.16) for convex real projective surfaces.

Section 8: McShane-type identities for higher Teichmüller space. We adapt (Theorem 8.4) Labourie and McShane's ideas from [LM09] to derive McShane identities for loxodromic bordered positive representations of arbitrary rank (Theorems 8.17 and 8.20). We conclude by deforming these identities from loxodromic bordered representations to unipotent bordered ones to obtain a McShane-type inequality for unipotent bordered positive representations of arbitrary rank (8.5).

Remark 1.36. Readers mainly interested in convex real projective surfaces may wish to focus on Sections 6 and 7. On the other hand, those with background in and predominantly interested in (arbitrary rank) Fock–Goncharov higher Teichmüller theory may be primarily interested in Sections 3, 4, 5 and 8, with secondary interests in our McShane identity applications in Section 7.

2. Fock-Goncharov moduli spaces and coordinates

Fock and Goncharov's version of higher Teichmüller theory [FG06] is deep and applies to a *very* broad context. We do not require the full force of their machinery, and concern ourselves with higher Teichmüller spaces of the form $\mathfrak{X}_{PGL_n,S_{g,m}}$ and $\mathcal{A}_{SL_n,S_{g,m}}$, where $S_{g,m}$ is a negative Euler characteristic (open) Riemann surface of genus g with $m \geqslant 1$ holes. We either regard the boundaries of $S_{g,m}$ as:

- holes, often when dealing with $\mathcal{X}_{PGL_n,S_{q,m}}$;
- punctures, often when dealing with $A_{SL_n,S_{q,m}}$.

2.1. A reductionist approach: ideal triangles and flags. Since our surface has $m \ge 1$ punctures, the negative Euler characteristic condition allows for ideal triangulations:

Definition 2.1 (Ideal triangulations). Let \mathfrak{m}_p denote the set of punctures of $S_{g,\mathfrak{m}}$, regarded as a punctured surface. An ideal triangulation \mathfrak{T} of $S_{g,\mathfrak{m}}$ is a maximal collection of (unoriented) essential arcs which join the elements of \mathfrak{m}_p , such that these arcs are:

- pairwise disjoint on the interior of $S_{g,m}$ and
- non-homotopic with respect to homotopies of $S_{q,m}$.

We regard ideal triangulations up to isotopy. Moreover, we identify an ideal triangulation $\mathfrak T$ with the graph $(V_{\mathfrak T}, E_{\mathfrak T})$, where $V_{\mathfrak T} = \mathfrak m_p$ is the set of vertices of $\mathfrak T$ and $E_{\mathfrak T}$ is the set of (unoriented) edges of $\mathfrak T$.

Ideal triangulations are key to both Thurston's enhanced Teichmüller theory and Penner's decorated Teichmüller theory [Pen87] — the respective classical archetypes for Fock–Goncharov's $\chi_{PGL_n,S_{g,m}}$ and $A_{SL_n,S_{g,m}}$ moduli space theory. The central idea is that surface representations may be described in terms of:

- (1) data specifying the representation at the level of each ideal triangle;
- (2) data specifying how to reconstitute the above data together into a higher rank surface representation.

Crucially, Fock and Gocharov realized that all of these necessary data may be stored in terms of flags (and decorated flags) assigned to the ideal vertices of ideal triangles.

We consider a vector space \mathbb{E} and endow it with a distinguished volume form Ω . We generally take $\mathbb{E} = \mathbb{R}^n$ and Ω to be the standard Euclidean form.

Definition 2.2 (Flags and the decorated flags). *A* flag F in \mathbb{E} is a maximal filtration of vector subspaces of \mathbb{E} :

$$\{0\} = F_0 \subset F_1 \subset \cdots \subset F_{n-1} \subset F_n = \mathbb{E}, \quad \dim F_i = i.$$

A basis for a flag F is an ordered basis (f_1, \ldots, f_n) for the vector space \mathbb{E} such that the first i basis vectors form a basis for F_i , for $i=1,\ldots,n$.

A decorated flag (F,ϕ) is pair consisting of a flag F and a collection ϕ of (n-1) non-zero vectors

$$\phi = \left\{ \check{f}_i \in F_i/F_{i-1} \right\}_{i=1,\dots,n-1}.$$

A basis for a decorated flag (F,ϕ) is an ordered basis (f_1,\ldots,f_n) for the vector space $\mathbb E$ such that

$$f_i + F_{i-1} = \check{f}_i \in F_i / F_{i-1}$$
 for $i = 1, \dots, n-1$.

We refer to the set $\mathbb B$ of flags on $\mathbb E$ as the flag variety and the set $\mathcal A$ of decorated flags on $\mathbb E$ as the principal affine space. We note the obvious "forgetful" projection map

(16)
$$\pi: \mathcal{A} \to \mathcal{B}, (\mathsf{F}, \varphi) \mapsto \mathsf{F}.$$

Notation 2.3. Given a basis $(f_1, ..., f_n)$, we use f^i to denote:

$$f^{i} := f_{1} \wedge f_{2} \wedge \cdots \wedge f_{i-1} \wedge f_{i}.$$

In particular, we set $f^0 = 1$ by convention.

Definition 2.4 (generic position). We say that triple X, Y, Z of flags are in generic position if for any non-negative integers i, j, k satisfying $i + j + k \le n$, the sum $X_i + Y_j + Z_k$ is direct. Likewise, a triple of decorated flags are in generic position if their underlying flags are in generic position.

2.2. Fock–Goncharov moduli spaces $\mathcal{X}_{PGL_n,S_{g,m}}$ and $\mathcal{A}_{SL_n,S_{g,m}}$. We now fix a collection of m (based-)homotopy classes α_1,\ldots,α_m , respectively winding the punctures $p_1,\ldots,p_m\in\mathfrak{m}_p$.

Notation 2.5. In latter sections of this paper, we perform computations involving objects determined by ideal points (e.g.: ideal triangles), and we shall find it convenient to canonically identify p_1, \ldots, p_m with the subset in $\partial_\infty \pi_1(S_{g,m})$ consisting of the respective fixed points of $\alpha_1, \ldots, \alpha_m$. This allows us to adopt notation such as $(p, \gamma p, \gamma^+)$ that is more convenient for explicit computation.

Definition 2.6 ([FG06, Definition 2.1] X-moduli space $X_{PGL_n,S_{g,m}}$). A framed PGL_n local system on $S_{g,m}$ is a pair (ρ, ξ) consisting of

- a representation $\rho \in Hom(\pi_1(S_{q,m}), PGL_n)$, and
- a map $\xi: m_p \to \mathcal{B}$, such that $\rho(\alpha_i)$ fixes the flag $\xi(p_i) \in \mathcal{B}$ for each $i=1,\ldots,m$.

Two framed PGL_n -local systems $(\rho_1, \xi_1), (\rho_2, \xi_2)$ are equivalent iff. there exists some $g \in PGL_n$ such that $\rho_2 = g\rho_1g^{-1}$ and $\xi_2 = g\xi_1$. We denote the moduli space (ie.: space of equivalence classes) of all framed PGL_n -local systems on $S_{g,m}$ by $\mathfrak{X}_{PGL_n,S_{g,m}}$.

Remark 2.7. Although the elements of the X-moduli space $\mathfrak{X}_{PGL_{\pi},S_{g,m}}$ are equivalence classes, we choose to conflate notation and denote them by (ρ,ξ) . We also adopt this convention later for the elements of the A-moduli space.

Definition 2.8 (Farey set). Let us assume for the moment that surface $S = S_{g,m}$ is cusped, and let $\widetilde{\mathfrak{m}}_p$ denote the set consisting of all the lifts $\widetilde{\mathfrak{m}}_p$ of \mathfrak{m}_p in the ideal boundary of the universal cover \widetilde{S} of S. We refer to $\widetilde{\mathfrak{m}}_p$ as the Farey set. The data contained in $(\rho, \xi) \in \mathfrak{X}_{PGL_n, S_{g,m}}$ is equivalent to that contained in the map $\xi_\rho : \widetilde{\mathfrak{m}}_p \to \mathbb{B}$ induced by deck-transformation $(\rho$ -action) applied to ξ .

The analogous definition for the \mathcal{A} -moduli space is slightly more involved. Let $\mathsf{T}^1\mathsf{S}$ denote the unit tangent bundle over S and fix an arbitrary point $\hat{\mathsf{x}} \in \mathsf{T}^1_\mathsf{x}\mathsf{S} \subset \mathsf{T}^1\mathsf{S}$ over $\mathsf{x} \in \mathsf{S}$. Consider the short exact sequence for the unit tangent bundle fibration:

$$1 \to \pi_1(T^1_xS) = \mathbb{Z} = \langle \sigma_S \rangle \to \pi_1(T^1S,\hat{x}) \to \pi_1(S,x),$$

where σ_S is either of the two generators for $\pi_1(T^1_\chi S)$. Define the quotient group $\bar{\pi}_1(S) = \bar{\pi}_1(S, x) := \pi_1(T^1 S, \hat{x})/\langle \sigma_S^2 \rangle$, and observe that $\bar{\pi}_1(S)$ is a 2:1 covering group for $\pi_1(S, x)$. We fix lifts $\hat{\alpha}_1, \ldots, \hat{\alpha}_m \in \bar{\pi}_1(S, x)$ respectively covering $\alpha_1, \ldots, \alpha_m$.

Definition 2.9 ([FG06, Definition 2.4, page 38] A-moduli space $A_{SL_n,S_{g,m}}$). A decorated twisted SL_n -local system on $S_{g,m}$ is a pair $(\bar{\rho},\bar{\xi})$ consisting of

- a representation $\bar{\rho} \in \text{Hom}(\bar{\pi}_1(S_{g,m}), SL_n)$ with unipotent boundary monodromy for each boundary, such that $\bar{\rho}(\bar{\sigma}_S) = (-1)^{n-1} Id_{n \times n}$, and
- a map $\bar{\xi}: m_p \to \mathcal{A}$, such that each $\bar{\rho}(\hat{\alpha}_i)$ fixes the decorated flag $\bar{\xi}(p_i) \in \mathcal{A}$.

Two decorated twisted SL_n -local systems $(\bar{\rho}_1,\bar{\xi}_1),(\bar{\rho}_2,\bar{\xi}_2)$ are equivalent iff. there exists some $g\in SL_n$ such that $\bar{\rho}_2=g\bar{\rho}_1g^{-1}$ and $\bar{\xi}_2=g\bar{\xi}_1$. We denote the moduli space of all decorated twisted SL_n -local systems on $S_{g,m}$ by $\mathcal{A}_{SL_n,S_{g,m}}$.

Remark 2.10. We refer to the unique representation $\rho : \pi_1(S_{g,m}) \to SL_n$ which lifts to $\bar{\rho}$ as the monodromy representation underlying $(\bar{\rho}, \bar{\xi})$.

Remark 2.11. By deck transformation, the data in a pair $(\bar{\rho}, \bar{\xi})$ is equivalent to a map $\bar{\xi}_{\bar{\rho}}$ from all 2:1 double cover of $\tilde{\mathfrak{m}}_p$ in the double cover $\partial_{\infty}\bar{\pi}_1(S)$ of the ideal boundary $\partial_{\infty}\pi_1(S)$ into the principle affine space \mathcal{A} . Note that $\pi \circ \bar{\xi}_{\bar{\rho}}$ is equal to the map ξ_{ρ} associated to $(\rho, \xi) := (\rho, \pi \circ \bar{\xi})$, and this in turn induces a map from $\mathcal{A}_{SL_n, S_{g,m}}$ to $\mathfrak{X}_{PGL_n, S_{g,m}}$ whose image consists of all points (ρ, ξ) with unipotent boundary monodromy.

We now introduce coordinate for the \mathcal{X} and \mathcal{A} -moduli spaces. Going forward, we only consider ξ_{ρ} which satisfy the following generic position condition: any pairwise distinct triple $(x, y, z) \in (\partial_{\infty} \pi_1(S_{g,m}))^3$ is mapped to a triple $(\xi_{\rho}(x), \xi_{\rho}(y), \xi_{\rho}(z))$ of flags (decorated flags resp.) in generic position (Definition 2.4).

2.3. Fock-Goncharov A-coordinates.

Definition 2.12 (n-Triangulations). Given an ideal triangulation $\mathfrak{T}=(V_{\mathfrak{T}}, E_{\mathfrak{T}})$ of $S_{g,m}$, we define the n-triangulation \mathfrak{T}_n of \mathfrak{T} to be the triangulation of $S_{g,m}$ obtained by subdividing each triangle of \mathfrak{T} into \mathfrak{n}^2 triangles (as per Figure 7). We also identify \mathfrak{T}_n with the graph $(V_{\mathfrak{T}_n}, E_{\mathfrak{T}_n})$, just as we did for ideal triangulations.

Notation 2.13 (vertex notation). We define the following vertex sets.

$$\mathbb{J}_n:=\left\{\begin{array}{c|c}V\in V_{\mathbb{J}_n}\setminus V_{\mathbb{J}}\mid V \text{ lies on an edge }e\in E_{\mathbb{J}}\end{array}\right\} \text{ and } \mathbb{J}_n:=V_{\mathbb{J}_n}\setminus (V_{\mathbb{J}}\cup \mathbb{J}_n)\,.$$

We also adopt the following vertex labeling conventions:

- we denote a vertex $V \in \mathbb{J}_n \in \mathbb{J}_n$ on an oriented ideal edge (x,y) by $v_{i,n-i}^{x,y} = v_{n-i,i}^{y,x}$, where $i \geqslant 1$ is the least number of $E_{\mathbb{J}_n}$ edges from V to x (see Figure 7).
- we denote a vertex $V \in J_n \cup J_n$ on a triangle (x,y,z) by $v_{i,j,k}^{x,y,z}$, where $i \ge 0$, $j \ge 0$ and $k = n i j \ge 0$ respectively denote: the least number of E_{J_n} edges from V to \overline{yz} , from V to \overline{xz} and from V to \overline{xy} (see Figure 7).

Definition 2.14 (Quivers). Consider the largest subgraph of \mathfrak{T}_n with vertex set $\mathfrak{I}_n \cup \mathfrak{J}_n$. By placing orientations on this graph as per Figure 7, we obtain a quiver $\Gamma_{\mathfrak{T}_n}$.

Quivers are combinatorially useful both in defining Fock–Goncharov coordinates, as well as in describing their coordinate transformations. We now describe Fock–Goncharov \mathcal{A} -coordinates.

Definition 2.15 ([FG06, Section 9] Fock–Goncharov A-coordinates). Fix an ideal triangulation \mathfrak{T} of $S_{g,m}$ and its n-triangulation \mathfrak{T}_n . Given a vertex $V \in \mathfrak{I}_n \cup \mathfrak{J}_n$, let (f,g,h) denote the ideal vertices of an idea triangle in $\widetilde{\mathfrak{T}}$ containing a lift of $V = \nu_{i,j,k}$. For $(\bar{\rho},\bar{\xi}) \in \mathcal{A}_{SL_n,S_{g,m}}$, choose bases

$$(f_1,...,f_n), (g_1,...,g_n), (h_1,...,h_n)$$

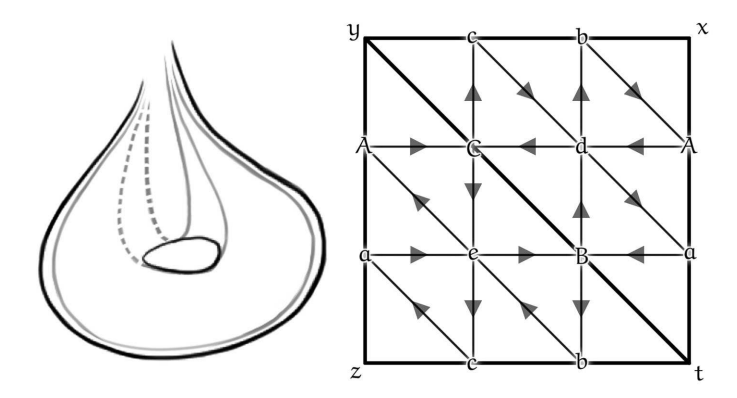


Figure 7. Left: an ideal triangulation for $S_{1,1}$. Right: a (lift of a) 3-triangulation \mathfrak{T}_3 for $S_{1,1}$, with opposite edges identified. Edges endowed with arrows constitute edges of the quiver $\Gamma_{\mathfrak{T}_3}$. The edge vertices $v_{1,2}^{x,y}$ and $v_{2,1}^{z,t}$ identify to the same vertex b when projected to $S_{1,1}$. The interior vertices $v_{1,1,1}^{x,y,t}$ and $v_{1,1,1}^{y,z,t}$ respectively correspond to the vertices d and e.

for the respective decorated flags $\bar{\xi}_{\bar{\rho}}(\bar{f})$, $\bar{\xi}_{\bar{\rho}}(\bar{g})$, $\bar{\xi}_{\bar{\rho}}(\bar{h})$, where $\bar{f}, \bar{g}, \bar{h}$ are lifts of f, g, h consecutive along $\partial_{\infty}\bar{\pi}_{1}(S)$. The vertex function Δ_{V} is defined by

$$\Delta_{V} := \Delta \left(f^{i} \wedge g^{j} \wedge h^{k} \right).$$

The Fock–Goncharov A-coordinate A_V *is equal to* Δ_V *up to sign.*

Remark 2.16. *The choice of sign for* A_V *is technical and dependent upon a choice of spin structure on* $S_{q,m}$ [FG06].

2.4. Fock-Goncharov χ -coordinates.

Notation 2.17. We henceforth adopt the following notation conventions:

- \overline{xy} denotes the unoriented edge between x and y;
- xyz denotes an unoriented triangle;
- \overrightarrow{xyz} denotes an oriented triangle;
- (x,y) denotes the oriented edge from x to y;
- (x, y, z) denotes a marked triangle;
- \tilde{X} denotes the union of all the lifts of a set $X \subset S$ to the universal cover \tilde{S} of S.

We continue to use this notation throughout the paper except when explicitly stated otherwise, especially when carrying out computations.

Definition 2.18 (Edge functions). *Let* (X,Y,Z,T) *be quadruple of flags in generic position, choose their bases*

$$(x_1, \dots, x_n), (y_1, \dots, y_n), (z_1, \dots, z_n), (t_1, \dots, t_n).$$

For the positive integer i < n, the edge function defined by

$$D_{\mathfrak{i}}(X,Y,Z,T) := \frac{\Delta \left(x^{n-\mathfrak{i}} \wedge y^{\mathfrak{i}-1} \wedge z^{1} \right)}{\Delta \left(x^{n-\mathfrak{i}-1} \wedge y^{\mathfrak{i}} \wedge z^{1} \right)} \cdot \frac{\Delta \left(x^{n-\mathfrak{i}-1} \wedge y^{\mathfrak{i}} \wedge t^{1} \right)}{\Delta \left(x^{n-\mathfrak{i}} \wedge y^{\mathfrak{i}-1} \wedge t^{1} \right)}$$

is a projective invariant.

Definition 2.19 (triple ratios). *Consider a triple of flags* (F, G, H) *in generic position, with bases*

$$(f_1, \dots, f_n), (g_1, \dots, g_n), (h_1, \dots, h_n).$$

Then for any triple of non-negative integers (i,j,k) with i+j+k=n, the triple ratio $T_{i,i,k}(F,G,H)$ is defined by:

$$T_{i,j,k}(F,G,H) := \frac{\Delta \left(f^{i+1} \wedge g^j \wedge h^{k-1} \right) \Delta \left(f^{i-1} \wedge g^{j+1} \wedge h^k \right) \Delta \left(f^i \wedge g^{j-1} \wedge h^{k+1} \right)}{\Delta \left(f^{i+1} \wedge g^{j-1} \wedge h^k \right) \Delta \left(f^i \wedge g^{j+1} \wedge h^{k-1} \right) \Delta \left(f^{i-1} \wedge g^j \wedge h^{k+1} \right)}.$$

Remark 2.20. For n = 3, the triple (i, j, k) is necessarily equal to (1, 1, 1), so we often omit the indices and simply write T(F, G, H).

There are two types of Fock–Goncharov $\mathfrak X$ coordinates respectively corresponding to edge functions and triple ratios. The former are labeled by vertices in $\mathfrak I_n$, correspond to degree four vertices in the quiver $\Gamma_{\mathcal I_n}$, and generalize Thurston's shear coordinate [Thu98]. The latter are labeled by vertices in $\mathfrak I_n$ and are degree 6 vertices in $\Gamma_{\mathcal I_n}$.

Definition 2.21 ([FG06, Section 9] \mathfrak{X} -coordinates). We define one \mathfrak{X} -coordinate for each vertex in $\mathfrak{I}_n \cup \mathfrak{J}_n$. For a vertex $V \in \mathfrak{I}_n$, let (x,y) denote an (oriented) edge in $E_{\widetilde{\mathfrak{T}}}$ containing a lift $\widetilde{V} = \nu_{x,y}^{n-i,i}$ of V. Further let \overline{xyz} and \overline{xty} denote the two anticlockwise oriented ideal triangles in $\widetilde{\mathfrak{T}}$ which contain the edge \overline{xy} . The Fock–Goncharov \mathfrak{X} -coordinate X_V , evaluated at $(\rho,\xi) \in \mathfrak{X}_{PGL_n,S_{n,m}}$, is defined as the edge function:

$$X_{V} := D_{\mathfrak{t}}(x, y, z, t) := D_{\mathfrak{t}}(\xi_{\rho}(x), \xi_{\rho}(y), \xi_{\rho}(z), \xi_{\rho}(t)).$$

For a vertex $V \in \mathfrak{J}_n$, let (f,g,h) denote an ideal triangle in $\widetilde{\mathfrak{T}}$ containing a lift $\widetilde{V} = \mathfrak{V}_{i,j,k}^{f,g,h}$ of V. The Fock–Goncharov \mathfrak{X} -coordinate X_V , evaluated at $(\rho,\xi) \in \mathfrak{X}_{PGL_n,S_{g,m}}$, is defined as the triple ratio:

$$X_{V} := T_{i,i,k}(f, g, h) := T_{i,i,k}(\xi_{\rho}(f), \xi_{\rho}(g), \xi_{\rho}(h)).$$

Fock–Goncharov \mathcal{X} -coordinates are crucial examples of projective invariants for higher rank surface representations, they are rational functions of \mathcal{A} -coordinates and define rational functions on the \mathcal{X} -moduli space. Before moving on, we give an alternative interpretation for the triple ratio which is more geometric in flavor:

Remark 2.22 ([FG07] Geometric definition for the triple ratio). Consider three flags

$$A = (a, L_1), B = (b, L_2), C = (c, L_3)$$

in \mathbb{RP}^2 in generic position. Let $u=L_2\cap L_3$, $v=L_1\cap L_3$, $w=L_1\cap L_2$ (see Figure 8), and let $|\cdot|$ denote the Euclidean distance. We stated in the introduction that the triple ratio $T\equiv T_{1,1,1}$ function is given by

(17)
$$T(A, B, C) := \frac{|wb| \cdot |uc| \cdot |va|}{|bu| \cdot |cv| \cdot |aw|},$$

To interpret triple ratios for flags A, B, $C \in \mathcal{B}$ in higher rank contexts, we project \mathbb{E} down to the following 3-dimensional vector space

$$\mathbb{E}/\left(A_{i-1} \oplus B_{i-1} \oplus C_{k-1}\right)$$

and then use the previous (i.e.: n = 3) interpretation for $T(A, B, C) := T_{i,j,k}(A, B, C)$.

Remark 2.23. Ceva's theorem asserts that T(A, B, C) = 1 iff. the lines $\overline{\alpha u}$, $\overline{b \nu}$, $\overline{c w}$ intersect at one point.

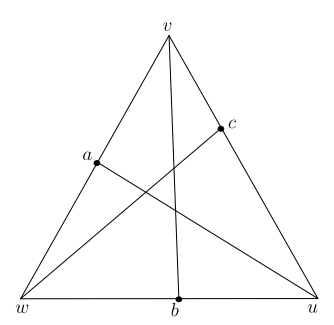


FIGURE 8. Triple ratio.

2.5. Coordinate transformations and the cluster ensemble structure. One key advantage of the Fock-Goncharov approach to higher Teichmüller theory is that we can explicitly write down rational functions specifying the transition maps between coordinate patches. Moreover, this aspect of the story is an example of the powerful theory of cluster ensembles:

Definition 2.24 ([FG06, Section 10] Cluster ensemble structure for $(\mathfrak{X}, \mathcal{A})$). A seed for $(\mathfrak{X}_{PGL_n,S_{q,m}},\mathcal{A}_{SL_n,S_{q,m}})$ is a pair

$$\mathbf{I} = (\mathfrak{I}_{\mathfrak{n}} \cup \mathfrak{J}_{\mathfrak{n}}, \varepsilon),$$

where ε is a skew-symmetric function

$$(\mathfrak{I}_{\mathfrak{n}}\cup\mathfrak{J}_{\mathfrak{n}})\times(\mathfrak{I}_{\mathfrak{n}}\cup\mathfrak{J}_{\mathfrak{n}})\to\mathbb{Z}$$

defined by the following equation:

$$\varepsilon_{VW} = \#\{ arrows from V to W \} - \#\{ arrows from W to V \}$$

for $V,W\in J_n\cup J_n$. A mutation at $V\in J_n\cup J_n$ changes the seed I to a new one $I'=(J_n\cup J_n,\epsilon')$, where we identify the new vertex V' with V and

$$\epsilon_{I,J}' = \begin{cases} -\epsilon_{I,J}, & V \in \{I,J\}; \\ \epsilon_{I,J} + [\epsilon_{I,V}]_+ \cdot [\epsilon_{V,J}]_+ - [-\epsilon_{I,V}]_+ \cdot [-\epsilon_{V,J}]_+, & V \notin \{I,J\}, \end{cases}$$

where $[x]_{+} = \max\{x, 0\}.$

A cluster transformation is a composition of mutations at $\mathfrak{I}_n \cup \mathfrak{J}_n$ and permutations of $\mathfrak{I}_n \cup \mathfrak{J}_n$. And the cluster modular group is the collection of cluster transformations that preserve the quiver $\Gamma_{\mathfrak{T}_n}$.

We assign the split torus X_I (A_I resp.) parameterized by the Fock–Goncharov coordinates $\{X_I\}_{I \in \mathfrak{I}_n \cup \mathfrak{J}_n} \ (\{A_I\}_{I \in \mathfrak{I}_n \cup \mathfrak{J}_n} \ resp.) \ to \ the \ seed \ I. \ The \ transition \ map \ \mu_V^X: \ \mathfrak{X}_I \to \mathfrak{X}_{I'}$ corresponds to a mutation at $V \in \mathfrak{I}_n \cup \mathfrak{J}_n$, with map $\mu_V^{X*}: \mathbb{Q}(\mathfrak{X}_{I'}) \to \mathbb{Q}(\mathfrak{X}_I)$ given by $\mu_V^{X*}(X_I') = \begin{cases} X_I X_V^{[\epsilon_{I,V}]_+} (1+X_V)^{-\epsilon_{I,V}}, & I \neq V; \\ X_V', & I = V. \end{cases}$

$$\mu_V^{X*}(X_I') = \begin{cases} X_I X_V^{[\epsilon_{I,V}]_+} (1+X_V)^{-\epsilon_{I,V}}, & I \neq V; \\ X_V^{-1}, & I = V. \end{cases}$$

The transition map $\mu_V^A: A_I \to A_{I'}$ corresponds to a mutation at $V \in \mathfrak{I}'_n \cup \mathfrak{J}_n$, with map $\mu_V^{A*}: \mathbb{Q}(\mathcal{A}_{\mathbf{I}'}) \to \mathbb{Q}(\mathcal{A}_{\mathbf{I}})$ given by

$$\mu_V^{A*}(A_I') = \begin{cases} A_I, & I \neq V; \\ A_V^{-1}(\prod_{J \mid \epsilon_{V,J} > 0} A_J^{\epsilon_{V,J}} + \prod_{J \mid \epsilon_{V,J} < 0} A_J^{-\epsilon_{V,J}}), & I = V. \end{cases}$$

The coordinate transformations given in Definition 2.24 are crucial in our derivation of our McShane identities — especially the A-coordinate transformations.

Definition 2.25 (Flip). Consider two adjacent ideal triangles \overline{xyt} and \overline{yzt} sharing a common edge \overline{yt} . A flip along \overline{yt} produces a new triangulation by replacing \overline{yt} with \overline{xz} .

The corresponding coordinate change for a flip is a sequence of (n-1) successive mutations ([FG06, Section 10.3, pg. 147]). We write out the n=3 (Figure 9) computation explicitly in Figure 9 as an example: denote the Fock–Goncharov \mathcal{A} -coordinates for $\mathcal{A}_{SL_3,S_{1,1}}$ by $\{a,b,c,d,r,s,q,w\}$. After successive mutations at the vertices corresponding to r,s,p,q, we obtain new coordinates $\{a,b,c,d,r',s',q',w'\}$ given by:

$$r' = \frac{b\,q + c\,w}{r}, \quad s' = \frac{a\,w + d\,q}{s}, \quad w' = \frac{a\,s' + c\,r'}{w}, \quad q' = \frac{b\,r' + d\,s'}{q}.$$

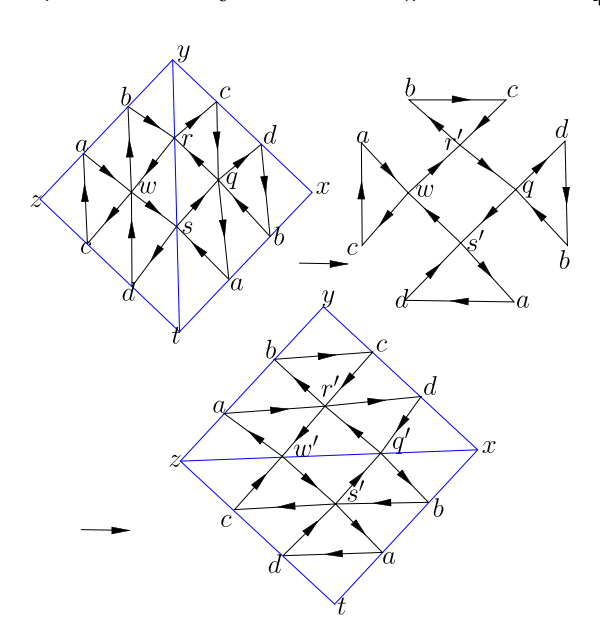


Figure 9. For $\mathcal{A}_{SL_3,S_{1,1}}$, given an ideal triangulation \mathfrak{T} with $V_{\mathfrak{T}}=\{x,y,z,t\}$ and $E_{\mathfrak{T}}=\{\overline{xy},\overline{yt},\overline{tx},\overline{yz},\overline{zt}\}$, we have its n-triangulation \mathfrak{T}_{-}

Remark 2.26. Note that these are all degree four mutations: two vertices point toward the mutating vertex, and the mutation vertex points out at two vertices. Each of these mutations comes from a Plücker relation for $(n \times n)$ determinants. These Plücker relations are also known as Ptolemy relations in certain geometric contexts [Pen87].

2.6. **Positivity.** The moduli space $\chi_{PGL_n,S_{g,m}}$ ($\mathcal{A}_{SL_n,S_{g,m}}$ resp.) is birationally equivalent to the *cluster* χ (\mathcal{A} resp.) variety obtained by gluing all the possible algebraic tori $\chi_{\mathbf{I}}$ ($\mathcal{A}_{\mathbf{I}}$ resp.) according to the above transition maps. These transition maps are all *positive* in sense that transition functions send positive coordinates to positive coordinates.

Definition 2.27 (Positive higher Teichmüller spaces). *The* positive Fock–Goncharov higher Techmüller space $\mathcal{A}_{\mathrm{SL}_n,S_{q,m}}(\mathbb{R}_{>0})$ and $\mathfrak{X}_{\mathrm{PGL}_n,S_{q,m}}(\mathbb{R}_{>0})$ are the respective subsets

of $A_{SL_n,S_{g,m}}$ and $\mathfrak{X}_{PGL_n,S_{g,m}}$ consisting of points which are positive in every coordinates with respect to some A or X coordinate chart. We refer to monodromy representations for positive points of either the X or A moduli space as positive representations.

Positivity is more than just an algebraic condition, but has geometric consequences. One important geometric property of positive representations is that their respective associated maps $\xi_\rho:\widetilde{m}_p\to \mathcal{B}$ (Definition 2.8) extend to Frenet maps (see Definition 3.13). More precisely, for a positive representation with only unipotent boundary monodromy, there exists a unique Frenet map $\xi: \vartheta_\infty \pi_1(S_{g,m}) \to \mathcal{B}$ which restricts to ξ_ρ on $\widetilde{m}_p \subset \vartheta_\infty \pi_1(S_{g,m})$. The uniqueness here owes to the fact that \widetilde{m}_p is dense in $\vartheta_\infty \pi_1(S_{g,m})$, in particular, this also asserts that ξ is ρ -equivariant.

For positive representations with at least one loxodromic boundary, let dS denote the topological double of $S_{g,m}$ along all of its loxodromic boundaries, then there exists a Frenet map $d\xi:\partial_\infty\pi_1(dS)\to \mathcal{B}$ which restricts to ξ_ρ on $\tilde{\mathfrak{m}}_p\subset\partial_\infty\pi_1(S_{g,m})\subset\partial_\infty\mathcal{B}_1(dS)$. Note that the set of map satisfying this restriction condition is not unique, but $d\xi$ can be made canonical if considers the associated restriction condition to do with the Hitchin double representation $d\rho$ [LM09, Definition 9.2.2.3].

3. Properties of χ -coordinates

- 3.1. **Uniform boundedness of the triple ratio.** Given a surface S with hyperbolic fundamental group $\pi_1(S)$, we denote its *boundary at infinity* or its *ideal boundary* by $\partial_\infty \pi_1(S)$ (see, for example, [LM09, Section 2, pg. 284]).
 - When S is a closed or punctured, its boundary at infinity $\partial_{\infty} \pi_1(S)$ is homeomorphic to \mathbb{S}^1 ;
 - when S has holes (with or without punctures), its boundary at infinity is homeomorphic to the Cantor set of ends of any Cayley graph of $\pi_1(S)$.

Whichever the case, the orientation of S imposes a canonical anti-clockwise ordering on $\partial_{\infty}\pi_1(S)$.

Definition 3.1 (marked ideal triangles). We define the set of marked (oriented) ideal triangles on the universal cover \tilde{S} of S as:

$$\textit{Tri}(\tilde{S}) := \left\{ (a,b,c) \in (\mathfrak{d}_{\infty}\pi_1(S))^3 \,\middle|\, \begin{array}{l} a,b,c \text{ are distinct elements arranged} \\ \text{in anticlockwise order along } \mathfrak{d}_{\infty}\pi_1(S). \end{array} \right\}$$

The ideal boundary $\partial_{\infty}\pi_1(S)$ is naturally endowed with a (diagonal) $\pi_1(S)$ -action, and we define the set of ideal triangles on S as

$$Tri(S) := Tri(\tilde{S})/\pi_1(S).$$

Moreover, we denote the $\pi_1(S)$ orbit of (a,b,c) representing an element in Tri(S) by $[a,b,c]_S$. We regard each $[a,b,c]_S$ as an immersed ideal triangle on S and denote its sides by $[a,b]_S$, $[b,c]_S$ and $[c,a]_S$.

Fact 3.2 (e.g.: [BCS18, Section 4.1, pg. 7]). When S is closed or cusped, the set Tri(S) of (oriented) marked ideal triangles on S is homeomorphic to the unit tangent bundle T^1S on S.

Definition 3.3 (k-intersecting ideal triangle). Let Σ be a model hyperbolic surface for S, we say that an ideal triangle $[a,b,c]_S$ on S is k-intersecting if the (unique) geodesic representatives on Σ of each of the three sides $[a,b]_S$, $[b,c]_S$, $[c,a]_S$ of $[a,b,c]_S$ have:

- at most k self-intersections, and
- at most k pairwise intersections.

We denote the set of k-intersecting ideal triangle on S by $Tri_k(S)$ and the set of lifts of k-intersecting ideal triangles to the universal cover \tilde{S} is denoted by $Tri_k(\mathfrak{d}_{\infty}(\pi_1(S)))$.

The goal of this subsection is to prove the following result:

Theorem 3.4. Let $\rho: \pi_1(S) \to PGL_n(\mathbb{R})$ be a positive representation, and fix a triple ratio function $T^{\rho}: Tri(\tilde{S}) \to \mathbb{R}_{>0}$ of the form:

(18)
$$T^{\rho}(x,y,z) = T^{\rho}_{i,i,k}(x,y,z), \text{ for } i+j+k=n.$$

Then the restriction of $T^{\rho}(\cdot)$ to the set of k-intersecting ideal triangles on \tilde{S} , is bounded within some interval $[T^{\rho}_{min,k},T^{\rho}_{max,k}]\subset\mathbb{R}_{>0}$.

We first consider the special case when S is closed. We learned the following argument from François Labourie and Tengren Zhang (independently):

Proposition 3.5 (Labourie, Zhang). When S is a closed surface, the triple ratio function T^{ρ} is bounded within some interval $[T^{\rho}_{\min}, T^{\rho}_{\max}] \subset \mathbb{R}_{>0}$.

Proof. The function T^{ρ} is $\pi_1(S)$ -invariant and hence descends to a continuous function on $Tri(S) \cong T^1S$. The rest follows from the compactness of T^1S .

We now turn to the case when $S = S_b$ has boundary holes and punctures. Our proof in this case is also based on compactness, with the adjustment that the role of Tri(S) is supplanted by $Tri_k(S_b)$. We first establish the following:

Proposition 3.6. The set $Tri_k(S_b)$ of k-intersecting ideal triangles on S_b is a compact subset of $Tri(S_b)$.

Proof. The case when all the boundary components of S_b are holes is straightforward. Let dS_b denote the closed double of S_b , then the embedding

$$\iota: S_b \hookrightarrow dS_b$$

of surfaces induces an embedding of ideal triangles $\iota_*: Tri(S_b) \hookrightarrow Tri(dS_b)$. Observe that $\iota_*(Tri(S_b))$ is precisely the set of ideal triangles on dS_b which lie completely on $\iota(S_b)$. Both the property of being contained on $\iota(S_b)$ and the property of being a k-intersecting ideal triangle are closed conditions. Therefore $Tri_k(S_b)$ is compact.

When all of the boundary components of S_b are all punctures, we remove small disjoint horocycle-bounded neighborhoods around each puncture and reuniformize the resulting surface to obtain a surface S_h where all of its boundary components are holes. This gives us a smooth embedding map

$$unif: S_h \hookrightarrow S_b$$

given by the inclusion function.

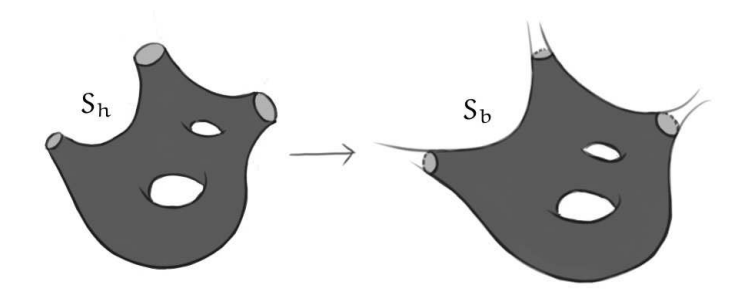


Figure 10. An example of the map $unif: S_h \rightarrow S_b$, geodesic boundaries are mapped to horocycles.

This in turn induces a map on the level of the fundamental group and hence on the ideal boundaries:

$$u: \partial_{\infty} \pi_1(S_h) \to \partial_{\infty} \pi_1(S_b).$$

First observe that u identifies the two end points of every lift of the boundary geodesics of S_h to \tilde{S}_h to obtain the lift of a cuspidal ideal point in \tilde{S}_b , because every geodesic boundary of S_h maps to some horocycle on S_b . In fact, we see that there are no other identifications by combining the following facts:

• the induced ordering on $u(\partial_{\infty}\pi_1(S_h))$ and the ordering on $\partial_{\infty}\pi_1(S_b)$ agree;

• ideal points in $\partial_{\infty} \pi_1(S_h)$ which are not endpoints to some peripheral geodesic cannot map to cuspidal ideal points in $\partial_{\infty} \pi_1(S_b)$ — this is because such ideal points correspond ideal limit points of (lifts of) leaves of (interior) geodesic laminations and laminations on S_h map to laminations on S_b (up to isotopy).

The (continuous) identification map u in turn induces a continuous map u_* : $Tri_k(S_h) \to Tri_k(S_b)$. It is important to note that u_* is well-defined but does not extend to a map $Tri(S_h) \to Tri(S_b)$. This is because

$$u_*([a, b, c]_{S_h}) = [u(a), u(b), u(c)]_{S_h}$$

does not produce a triangle if u(a), u(b) and u(c) are not pairwise distinct. This cannot happen to a triangle $[a,b,c]_{S_h} \in Tri_k(S_h)$: if (without loss of generality) a and b are the two endpoints of a lift of a boundary geodesic of S_h , then the geodesics $[b,c]_{S_h}$ and $[c,a]_{S_h}$ spiral toward the same boundary in opposite directions and hence intersect infinitely often.

Further observe that u_* is a surjective map which is at most 8 to 1. The preimage of a triangle $\triangle \in \mathfrak{d}_{\infty}\pi_1(S_h)$ has 2^j pre-images if the ideal vertices of \triangle are based at j distinct cusps. Since $Tri_k(S_b)$ is the image of a compact set, it is compact.

Finally, if S_b has a combination of boundary holes and punctures, we double S_b to a surface dS_b with punctures only. Then by our punctured case argument, the set of ideal triangles $Tri_k(dS_b)$ on dS_b is compact. And by our holed case argument, the set of ideal triangles $Tri_k(S_b)$ is homeomorphic to a closed subset of $Tri_k(dS_b)$ and is hence compact.

Theorem 3.4, surfaces with both boundary holes and cusps case. The triple ratio function $\mathsf{T}^\rho: \mathit{Tri}(\mathsf{S}_{\mathfrak{b}}) \to \mathbb{R}_{>0}$ restricts to a positive continous function $\mathsf{T}^\rho|_{\mathit{Tri}_k(\mathsf{S}_{\mathfrak{b}})}$ defined over the compact set $\mathit{Tri}_k(\mathsf{S}_{\mathfrak{b}})$. We then take $\mathsf{T}^\rho_{\min}(k)$ and $\mathsf{T}^\rho_{\max}(k)$ to be the respective minimum and the maximum for the restricted function $\mathsf{T}^\rho|_{\mathit{Tri}_k(\mathsf{S}_{\mathfrak{b}})}$. \square

Remark 3.7. Our proof is sufficiently topological that Theorem 3.4 holds true even for convex real projective surface with quasihyperbolic boundary monodromy (see [Mar12]) — note that the area of the surface is infinite in this case.

3.2. n-Fuchsian rigidity conditions. We now shift from the study of triple ratio boundedness to that of fuchsian rigidity. Our goal in this section is to prove two characterizing conditions for a positive point $(\rho,\xi)\in \mathfrak{X}_{PGL_n,S_{g,m}}(\mathbb{R}_{>0})$ to lie on the n-Fuchsian locus.

Definition 3.8. *The two proposed* n-Fuchsian-characterizing conditions are:

- (1) every triple ratio coordinate is equal to 1.
- (2) for every edge, the edge function coordinates along that edge are all equal.

We say that triple ratio rigidity holds if condition 1 is a characterizing condition for the n-Fuchsian locus, and we say that edge function rigidity holds if condition 2 is a characterizing condition.

Remark 3.9. It is well-known that all triple ratio coordinates being equal to 1 is a necessary condition. Conversely, these two properties combine to give the defining equations for n-Fuchsian slice of the relevant positive \mathfrak{X} -moduli space (including the universal higher Teichmüller space $\mathfrak{X}^+_{PGL_n}$). Therefore, to show that triple ratio rigidity holds, we need only

show that the triple ratio equal 1 condition implies the equal edge function condition. Vice versa for edge function rigidity.

We begin in lower rank examples, where direct computation yields algebraic proofs. The advantage of such a proof is not merely in simplicity, but also in their extensibility to the universal higher Teichmüller space context [FG07, Definition 1.9] and also to general coefficient fields.

Theorem 3.10 (Triple ratio rigidity for n = 3,4). For n = 3,4, the triple ratio rigidity condition characterizes when a positive point $(\rho, \xi) \in \mathfrak{X}_{PGL_n,S_{g,m}}(\mathbb{R}_{>0})$ is n-Fuchsian.

Proof. We invoke Remark 3.9, and also lift our discussion to the universal cover to avoid dealing with different cases involving topologically distinct triangulations of the surface. Given any ideal triangulation \mathfrak{T} , consider an ideal edge \overline{xz} common to two ideal triangles (x, y, z) and (x, z, t) in $\widetilde{\mathfrak{T}}$ as depicted in Figure 11.

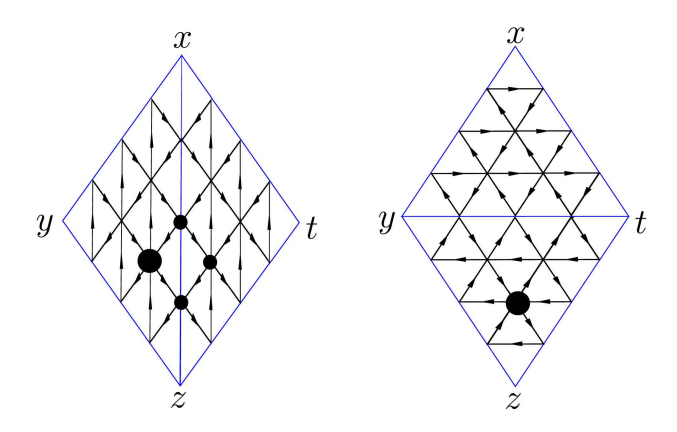


FIGURE 11. flip at \overline{xz}

We compute $X'_{v_{t,y,z}^{1,l,n-2}}$ after flipping at edge \overline{xz} via the cluster transformation formula in Definition 2.24:

$$(19) \qquad \frac{X'_{\nu_{1,l,n-2}^{t,y,z}}}{X_{\nu_{1,l,n-2}^{x,y,z}}} = \frac{1 + X_{\nu_{2,n-2}^{x,z}} + X_{\nu_{1,n-2,l}^{x,z,t}} X_{\nu_{2,n-2}^{x,z}} + X_{\nu_{1,n-1}^{x,z}} X_{\nu_{1,n-2,l}^{x,z,t}} X_{\nu_{2,n-2}^{x,z}} X_{\nu_{1,n-2}^{x,z}} X_{\nu$$

By assumption, triple ratios are all equal to 1, and the equation above tells us that

(20)
$$X_{\nu_{2,n-2}^{x,z}} = X_{\nu_{1,n-1}^{x,z}}.$$

By symmetry, we also have

(21)
$$X_{\nu_{n-2,2}^{x,z}} = X_{\nu_{n-1,1}^{x,z}}.$$

For n = 3, 4 there are at most 3 coordinates along \overline{xz} , and hence must all be equal. Since this applies to any arbitrary edge, we see that ρ is n-Fuchsian.

Remark 3.11. For n=5, 6, we can express $X_{v_{i,1}^{t,y,z}}$ in the Fock–Goncharov coordinates for the n-triangulation of Figure 11 (left). By explicit computation, we obtain $X_{v_{3,n-3}^{x,z}} = X_{v_{2,n-2}^{x,z}}$ and symmetry again ensures that $X_{v_{n-3,3}^{x,z}} = X_{v_{n-2,2}^{x,z}}$. However, the number of mutations needed to compute flips increases significantly as n increases and this is a stumbling block for extend this strategy for all ranks.

Theorem 3.12 (Edge function rigidity for n=3). For n=3, the edge function rigidity condition characterizes when a positive point $(\rho, \xi) \in \mathfrak{X}_{PGL_n, S_{g,m}}(\mathbb{R}_{>0})$ is n-Fuchsian.

Proof. We again invoke Remark 3.9, and we again work in the universal cover (see Figure 11). By assumption, we have $X_{\nu_{1,2}^{x,z}} = X_{\nu_{2,1}^{x,z}}$. After flipping the edge \overline{xz} , we obtain

$$(22) \qquad X'_{\nu_{1,2}^{x,y}} = \frac{X_{\nu_{1,2}^{x,y}} X_{\nu_{1,1,1}^{x,y,z}} X_{\nu_{1,2}^{x,z}} (1 + X_{\nu_{1,2}^{x,z}})}{1 + X_{\nu_{1,2}^{x,z}} + X_{\nu_{1,2}^{x,z}} X_{\nu_{1,1,1}^{x,y,z}} + X_{\nu_{1,2}^{x,y,z}} X_{\nu_{1,1,1}^{x,y,z}} X_{\nu_{1,2}^{x,y,z}}} = \frac{X_{\nu_{1,2}^{x,y}} X_{\nu_{1,1,1}^{x,y,z}} X_{\nu_{1,2}^{x,z}}}{1 + X_{\nu_{1,1,1}^{x,y,z}} X_{\nu_{1,2}^{x,z}}},$$

and

(23)
$$X'_{\nu_{2,1}^{x,y}} = \frac{X_{\nu_{2,1}^{x,y}} X_{\nu_{2,1}^{x,z}}}{1 + X_{\nu_{2,1}^{x,z}}} = \frac{X_{\nu_{1,2}^{x,y}} X_{\nu_{1,2}^{x,z}}}{1 + X_{\nu_{1,2}^{x,z}}},$$

which satisfies $X'_{\nu_{1,2}^{x,y}}=X'_{\nu_{2,1}^{x,y}}$ by asumption. Solving for $X_{\nu_{1,1,1}^{x,y,z}}$ yields $X_{\nu_{1,1,1}^{x,y,z}}=1$ as desired. \Box

We now turn to the geometry of Frenet curves to help establish these rigidity conditions.

Definition 3.13 (Frenet curves and osculating curves). *A curve* $\xi^1 : \mathbb{S}^1 \to \mathbb{R}P^{n-1}$ *is called a* Frenet curve *if there is an curve* $\xi = (\xi^1, \dots, \xi^n) : \mathbb{S}^1 \to \mathbb{B}$ *such that*

• For every ordered partition $(n_1, ..., n_k)$ of n and every k-tuple of distinct points $x_1, ..., x_k \in \mathbb{S}^1$, the following sum is direct:

$$\bigoplus_{i=1}^k \xi^{n_i}(x_i) = \mathbb{R}^n.$$

• For every ordered partition $(j_1, ..., j_k)$ of a positive integer $j \le n$, and for every $x \in \mathbb{S}^1$, then:

$$\lim_{(x_i)\to x}\bigoplus_{i=1}^k \xi^{j_i}(x_i)=\xi^j(x),$$

where the limit is taken over k-tuples $(x_1, ..., x_k)$ of pairwise distinct points x_i . We refer to $\xi = (\xi^1, ..., \xi^n)$ as the osculating curve for the Frenet curve ξ^1 .

To begin with, we note that (for n=3) the Fuchsian-characterizing nature of simultaneously having both the triple ratio unicity and the edge function equality properties applies to the entire higher Teichmüller space, and not just on the subspace of positive points. This is of independent interest to our aims in this subsection.

Remark 3.14. For n=3, we demonstrate that if an ideal quadrilateral satisfies the properties that the two edge functions on its cross-edges are equal and all triple ratios for the ideal triangles constituting this ideal quadrilateral equal 1 is equivalent to having the four vertices x_1, x_2, x_3, x_4 being on the sam ellipse. Since $T(\xi(x_1), \xi(x_2), \xi(x_3)) = 1$, there is a unique projective transformation sending the flags $\xi(x_1), \xi(x_2), \xi(x_3)$ to $(A, l_{EF}), (B, l_{FG}), (C, l_{EG})$ arranged as per Figure 12 with \overline{EFG} equilateral and with A, B, C being midpoints. Further let $\xi(x_4) = (D, l_D), H = AD \cap BE, I = AC \cap BE, L = BD \cap AG$ and $M = BC \cap AG$. Then the edge function equality

(24)
$$C_1(\xi(x_1), \xi(x_2), \xi(x_3), \xi(x_4)) = C_2(\xi(x_1), \xi(x_2), \xi(x_3), \xi(x_4))$$

is equivalent to

$$(25) \qquad \qquad -\frac{|\mathsf{EH}|}{|\mathsf{BH}|} = -\frac{|\mathsf{EH}| \cdot |\mathsf{BI}|}{|\mathsf{BH}| \cdot |\mathsf{EI}|} = -\frac{|\mathsf{AL}| \cdot |\mathsf{GM}|}{|\mathsf{GL}| \cdot |\mathsf{AM}|} = -\frac{|\mathsf{AL}|}{|\mathsf{GL}|}$$

Combined with |EI| = |IB| = |AM| = |MG|, we get |HI| = |LM|. Since |AI| = |BM|, $AI \perp HI$ and $BM \perp ML$, and we obtain $\angle \alpha = \angle \beta$ and hence A, B, C, D lie on the same circle as $\angle \alpha$ and $\angle \beta$ are angles subtended on the same arc.

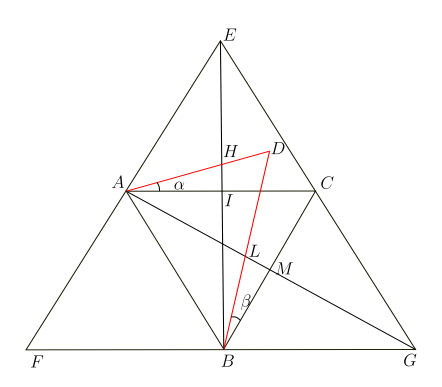


FIGURE 12. Normalized position

We now present a different approach for establishing triple ratio or edge function rigidity via the geometry of the Frenet curves. The method allows us to establish triple ratio rigidity to arbitrary rank positive representations of closed surfaces and punctured surfaces (i.e.: positive representations with unipotent monodromy). The limitation is that this method does not apply for arbitrary Frenet curves (i.e.: elements of universal higher Teichmüller space) or if there is a loxodromic boundary component.

The following lemma is key to our proof strategy:

Lemma 3.15. Consider the restricted osculating curve $\xi = (\xi^1, \xi^2) : [0, 1] \to \mathbb{B}$ for the subarc ξ^1 of a Frenet curve. If the triple ratio $\mathsf{T}(\xi(0), \xi(1), \xi(s))$ is equal to 1 for every $s \in (0,1)$, then the image of ξ^1 in $\mathbb{R}\mathsf{P}^2$ is the subarc of an ellipse.

Proof. We first observe that we may freely apply $PGL_3(\mathbb{R})$ to ξ without affecting the smoothness of ξ or its triples ratios. Therefore, we may assume without loss of generality that

- (1) the subarc maps to $\mathbb{R}^2 = \{(x,y)\} = \{[x,y:1]^t \in \mathbb{R}P^2\} \subset \mathbb{R}P^2$;
- (2) $\xi^1(0)$ and $\xi^1(1)$ are respectively positioned at (0,0) and (0,1);
- (3) $\xi^2(0)$ and $\xi^2(1)$ are vertical lines;
- (4) and ξ^1 is parameterized so that $\xi^1(s) = (s, f(s))$ for some C^1 function f(s).

This final condition is possible because Frenet curves are necessarily hyperconvex. The triple ratio

$$T(\xi(0), \xi(1), \xi(s)) = 1.$$

Explicitly writing out this condition for a C^1 curve (t, f(t)) yields the following:

$$\frac{(1-s)(f(s)-sf'(s))}{s(f(s)+(1-s)f'(s))}=1.$$

The family of half-ellipses of the form $y^2 = Ax(1-x)$ constitute the full set of possible solutions for this ODE.

We are now well-prepared to prove the following:

Theorem 3.16. Triple ratio rigidity holds for positive points $(\rho, \xi) \in \mathfrak{X}_{PGL_n, S_{g,m}}(\mathbb{R}_{>0})$ for which the boundaries (if any) of $S_{g,m}$ are all unipotent.

Proof. The statement is trivially true for n=2, so consider $n\geqslant 3$. Our goal is to show that the Frenet curve for (ρ,ξ) has smooth image and thus invoke [PS17, Theorem D] (or [Ben01, Proposition 6.1] for the n=3 case) to conclude that ρ is n-Fuchsian. To demonstrate the desired smoothness, we compute the projection (a smooth lift) of the Frenet curve into 3-dimensional subspaces for which a certain set of ideal triangles retain their triple ratios and then apply Lemma 3.15.

Let $X:[0,1]\to\mathbb{R}P^{n-1}$ be a subarc of ξ^1 . By applying the action of $PGL_n(\mathbb{R})$, we assume without loss of generality that:

- the (ordered) standard basis (e_1, e_2, \dots, e_n) is a basis for the flag $\xi(0)$;
- the reversed standard basis $(e_n, e_{n-1}, \dots, e_1)$ is a basis for the flag $\xi(1)$.

We identify X(t) with the following lift to \mathbb{R}^n :

$$X(t) = x_1(t)e_1 + ... + x_{n-1}(t)e_{n-1} + x_n(t)e_n.$$

The first axiom for Frenet curves (Definition 3.13) ensures that:

- $x_n(t) \neq 0$ for $t \neq 0$;
- $x_i(t)$ and $x_{i+1}(t)$ cannot simultaneously equal 0 for $t \neq 0, 1$;
- and $x_i(t)$ cannot identically zero.

We renormalize X(t) by setting $x_n(t) = t$.

Step 1: we know from the given assumption that $T_{n-2,1,1}(X(0),X(1),X(t))=1$. Remark 2.22 tells us that these triple ratios are still equal to 1 after projecting X(t) into the orthogonal complement \mathbb{V}_1^{\perp} of

(26)
$$\mathbb{V}_1 := \operatorname{Span}\{e_1, e_2, \dots, e_{n-3}\}.$$

By Lemma 3.15, the projected image

$$(27) \quad \textit{proj}_{\mathbb{V}_{1}^{\perp}}(X(t)) = x_{n-2}(t)e_{n-2} + x_{n-1}(t)e_{n-1} + x_{n}(t)e_{n}, \quad \text{where } x_{n}(t) = t,$$

defines a subsegment of an ellipse when further projected into $\mathbb{R}P^2.$ Thus there is a reparametrization $s:[0,1]\to[0,1]$ of t such that $\frac{x_{n-2}(t(s))}{t(s)},\frac{x_{n-1}(t(s))}{t(s)}$ are both real analytic functions in s. We also observe that it at least one of $x_{n-2}(t),x_{n-1}(t)$ needs to be non-zero or else the projected image of X(t) in $\mathbb{R}P^2$ would just be a single point. Analyticity further asserts that $x_{n-2}(t)$ and $x_{n-1}(t)$ either have finitely many zeroes, as they cannot be identically zero. We now show that $x_{n-k-1}(t(s))/t(s)$ is real analytic in s, inductively over $k=2,\ldots,n-2.$

Step k: we know from the given assumption that the triple ratios

$$T_{n-1-k,k,1}(X(0),X(1),X(t)) = 1$$
 for all t

and remain equal to 1 after projecting into the orthogonal complement \mathbb{V}_k^{\perp} of

(28)
$$V_k := \operatorname{Span}\{e_1, e_2, \dots, e_{n-k-2}, e_{n-k+2}, \dots, e_n\}.$$

The projected image of X(t) is given by

(29)
$$proj_{\mathbb{V}_{\nu}^{\perp}}(X(t)) = x_{n-k-1}(t)e_{n-k-1} + x_{n-k}(t)e_{n-k} + x_{n-k+1}(t)e_{n-k+1}.$$

Further projecting in the e_{n-k-1}, e_{n-k} direction, Lemma 3.15 ensures that $\frac{x_{n-k+1}}{x_{n-k}}$ is real analytic with respective to some reparametrization t_k of t. However, we already know that this quantity is real analytic with respect to s, which implies that t_k and s are real analytically compatible reparametrizations of t. Hence, the functions $\frac{x_{n-k-1}(t(s))}{x_{n-k}(t(s))}$ is a real analytic function in s, and

$$\frac{x_{n-k-1}(\mathsf{t}(s))}{\mathsf{t}(s)} = \frac{x_{n-k-1}(\mathsf{t}(s))}{x_{n-k}(\mathsf{t}(s))} \cdot \frac{x_{n-k}(\mathsf{t}(s))}{\mathsf{t}(s)}$$

is also real analytic with respect to s. Note that this argument applies when $\frac{x_{n-k-1}(t(s))}{x_{n-k}(t(s))}$ is well-defined. For the remaining finitely many points where $x_{n-k}(t(s))$ equals 0, we may project $\operatorname{proj}_{\mathbb{V}_k^\perp}(X(t))$ in the e_{n-k-1}, e_{n-k+1} direction and run the same argument. This is always doable because $x_{n-k}(t)$ and $x_{n-k+1}(t)$ cannot simultaneously equal 0.

We have now shown that $\frac{x_1(t(s))}{t(s)}, \ldots, \frac{x_{n-1}(t(s))}{t(s)}$ are real analytic functions in s, and hence X(t) has smooth image in $\mathbb{R}P^{n-1}$.

4. Goncharov-Shen potentials

The \mathcal{A} -moduli space $\mathcal{A}_{SL_2,S_{1,1}}(\mathbb{R}_{>0})$ is equivalent to Penner's decorated Teichmüller space, whose element correspond to marked hyperbolic surfaces decorated with a horocycle around its solitary cusp. Penner showed that the length P of this horocycle is a rational function of his λ -length coordinates $(\lambda_x,\lambda_y,\lambda_z)$ for $\mathcal{A}_{SL_2,S_{1,1}}(\mathbb{R}_{>0})$. In particular, it takes the form:

$$P = 2\left(\frac{\lambda_x}{\lambda_y \lambda_z} + \frac{\lambda_y}{\lambda_z \lambda_x} + \frac{\lambda_z}{\lambda_x \lambda_y}\right).$$

Moreover, choosing the length P = 6 horocycle yields the Markoff equation.

Goncharov and Shen generalize this construct to $\mathcal{A}_{SL_n,S_{g,m}}$ in [GS15]. Their construction is based on the following key observation:

Fact 4.1. For any triple of decorated flags $(F,G,H) \in \mathcal{A}^3$ if (F,G,H) are in generic position, there is a unique upper triangular unipotent matrix g, upper triangular with respect to any basis for F, such that $(F,\pi(G)) \cdot g = (F,\pi(H))$.

Definition 4.2 (i-th Character). Let the above linear transformation g take the form (g_{ij}) with respect to any basis for the decorated flag F. For $i=1,\cdots,n-1$, we define the i-th character

$$P_i(F; G, H)$$
 of (F, G, H) to be $g_{n-i,n-i+1}$.

The i-th character satisfies the following additive properties:

$$P_{i}(F; G, H) = P_{i}(F; G, W) + P_{i}(F; W, H);$$

 $P_{i}(F; G, H) = -P_{i}(F; H, G).$

Consider $(\rho, \xi) \in \mathcal{A}_{SL_n, S_{g,m}}$ and an ideal triangulation \mathfrak{T} of $S_{g,m}$. For any marked triangle (f,g,h) in $\widetilde{\mathfrak{T}}$ (\mathfrak{T} resp.), we denote the i-th character $P_i(\xi_\rho(f);\xi_\rho(g),\xi_\rho(h))$ $(P_i(\xi(f);\xi(g),\xi(h))$ resp.) by $P_i(f;g,h)$.

Remark 4.3. Given $(\rho, \xi) \in A_{SL_n, S_{q,m}}(\mathbb{R}_{>0})$ and the ideal triangulation \mathfrak{T} ,

(1) for any anticlockwise oriented (e,f,g,h), these additive characters satisfy the following positivity property:

$$\frac{P_{i}(e;f,g)}{P_{i}(e;g,h)} > 0;$$

(2) by the above definition, for any marked ideal triangle (x,y,z) and any $\delta \in \pi_1(S_{g,m})$, we have

$$P_i(x; y, z) = P_i(\delta x; \delta y, \delta z).$$

For general $\mathfrak{X}_{PGL_n,S_{q,m}}(\mathbb{R}_{>0})$, we have Proposition 4.16 instead.

Definition 4.4 ([GS15] Goncharov–Shen potential). Given $(\bar{\rho}, \bar{\xi}) \in \mathcal{A}_{SL_n,S_{g,m}}$, we fix an ideal triangulation \mathfrak{T} of $S_{g,m}$ and fix one fundamental domain Ω of $\widetilde{\mathfrak{T}}$ composed of ideal triangles in $\widetilde{\mathfrak{T}}$. Given $\mathfrak{p} \in \mathfrak{m}_{\mathfrak{p}}$, let $\Theta_{\mathfrak{p}}$ denote the set of marked anticlockwise-oriented ideal triangles $(\mathfrak{f},\mathfrak{g},\mathfrak{h})$ in Ω with \mathfrak{f} being a lift of \mathfrak{p} . For each $\mathfrak{i}=1,\cdots,\mathfrak{n}-1$, the \mathfrak{i} -th Goncharov–Shen potential at \mathfrak{p} , denoted by $P_{\mathfrak{i}}^{\mathfrak{p}}$, on the \mathcal{A} -moduli space $\mathcal{A}_{SL_n,S_{g,m}}$ is given by:

(31)
$$P_{i}^{p} := \sum_{(f,g,h)\in\Theta_{p}} P_{i}(f;g,h).$$

For $[\mu] \in \overrightarrow{\mathcal{H}}_p$ (Recall Definition 1.16), let Θ_{μ} be a subset of Θ_p that contained in a lift of μ . We define (μ,i) -Goncharov–Shen potential to be

(32)
$$P_{\mathfrak{i}}^{\mu} := P_{\mathfrak{i}}^{\bar{\mu}} := \sum_{(f,g,h) \in \Theta_{\mathfrak{u}}} P_{\mathfrak{i}}(f,g,h).$$

For the case (n, g, m) = (2, 1, 1), the Goncharov–Shen potential P_1^p is the same as P_1^p in Equation (30). Goncharov and Shen show that P_i^p is well-defined, independent of the chosen ideal triangulation $\mathcal T$ and hence mapping class group invariant. They further demonstrate the following beautiful fact:

Theorem 4.5 ([GS15, Theorem 10.7]). These $\mathfrak{m}(\mathfrak{n}-1)$ Goncharov–Shen potentials $\{P_i^p\}_{p,i}$ generate the algebra of mapping class group invariant regular functions on the moduli space $\mathcal{A}_{SL_n,S_{\mathfrak{a},\mathfrak{m}}}$.

Remark 4.6. Goncharov and Shen refer to their potentials as Landau—Ginzberg partial potentials because an important aspect of their hitherto unproven homological mirror symmetry conjecture asserts that their potentials should correspond to Landau—Ginzburg partial potentials from Landau-Ginzburg theory. We opt to refer to their potentials as Goncharov—Shen potentials both to acknowledge their contribution in discovering this geometrically fascinating object, as well as to avoid implying the open conjecture that Goncharov—Shen potentials are Landau-Ginzburg partial potentials.

We now give explicit algebraic manipulations of $P_i(F;G,H)$. This is essentially taken from [GS15, Section 3], but is included both for expositional completeness and because many of our computations and derivations depend upon these foundational computations.

Remark 4.7. The following computation differs from Goncharov–Shen's: we are computing g such that $(F, \pi(G)) \cdot g = (F, \pi(H))$, they are computing g' such that $(F, \pi(H)) \cdot g' = (F, \pi(G))$. This accounts for the difference in sign in Lemma 4.8.

Consider a triple of decorated flags $(F,G,H) \in \mathcal{A}^3$ is in generic position with respective bases (f_1,\cdots,f_n) , (g_1,\cdots,g_n) , and (h_1,\cdots,h_n) . For any non-negative integers a,b,c with a+b+c=n, define a one dimensional vector space

$$L_a^{b,c} := F^{a+1} \cap (G^b \oplus H^c),$$

and choose $e_{\alpha}^{b,c}\in L_{\alpha}^{b,c}$ such that $e_{\alpha}^{b,c}-f_{\alpha+1}\in F^{\alpha}$. Define $\alpha_{\alpha,b,c}^{F;G,H}\in \mathbb{R}$ so that

(33)
$$e_a^{b-1,c+1} - e_a^{b,c} = \alpha_{a,b,c}^{F;G,H} \cdot e_{a-1}^{b,c+1}.$$

Lemma 4.8 ([GS15, Lemma 3.1]).

$$\alpha^{\text{F;G,H}}_{\alpha,b,c} = \frac{\Delta \left(f^{\alpha-1} \wedge h^{c+1} \wedge g^b \right) \cdot \Delta \left(f^{\alpha+1} \wedge h^c \wedge g^{b-1} \right)}{\Delta \left(f^{\alpha} \wedge h^c \wedge g^b \right) \cdot \Delta \left(f^{\alpha} \wedge h^{c+1} \wedge g^{b-1} \right)}.$$

Notation 4.9. By definition $e_0^{i,n-i} = f_1$ for every $i = 0, \dots, n$.

Equation (33) tells us that there is a change of (ordered) bases

$$\begin{split} &\left(e_{0}^{\alpha+b-1,c+1},\cdots,e_{\alpha-1}^{b,c+1},e_{\alpha}^{b,c},e_{\alpha+1}^{b-1,c},\cdots,e_{\alpha+b-1}^{1,c},e_{\alpha+b}^{0,c},\cdots,e_{n-1}^{0,1}\right)\cdot\mathsf{N}_{\alpha}(\alpha_{\alpha,b,c}^{\mathsf{F};\mathsf{G},\mathsf{H}})\\ &=\left(e_{0}^{\alpha+b-1,c+1},\cdots,e_{\alpha-1}^{b,c+1},e_{\alpha}^{b-1,c+1},e_{\alpha+1}^{b-1,c},\cdots,e_{\alpha+b-1}^{1,c},e_{\alpha+b}^{0,c},\cdots,e_{n-1}^{0,1}\right) \end{split}$$

encoded by unipotent matrices of the form

$$N_{\mathfrak{a}}(x) = \left(\begin{array}{cccc} Id_{\mathfrak{a}-1} & 0 & 0 & 0 \\ 0 & 1 & x & 0 \\ 0 & 0 & 1 & 0 \\ 0 & 0 & 0 & Id_{\mathfrak{b}+\mathfrak{c}-1} \end{array} \right).$$

For c = 0, using the above transformation n - 1 times, we have

$$\left(f_1,e_1^{n-1,0},\cdots,e_{n-1}^{1,0}\right)\cdot N_1(\alpha_{1,n-1,0}^{F;G,H})\cdots N_{n-1}(\alpha_{n-1,1,0}^{F;G,H}) = \left(f_1,e_1^{n-2,1},\cdots,e_{n-1}^{0,1}\right).$$

For $1 \leqslant c = k \leqslant n-2$, applying the above transformation n-1-k times, we have

$$\begin{split} &\left(f_{1},e_{1}^{n-1-k,k},\cdots,e_{n-k-1}^{1,k},e_{n-k'}^{0,k},\cdots,e_{n-1}^{0,1}\right)\cdot N_{1}(\alpha_{1,n-1-k,k}^{F;G,H})\cdots N_{n-1-k}(\alpha_{n-1-k,1,k}^{F;G,H}) \\ &=\left(f_{1},e_{1}^{n-2-k,k+1},\cdots,e_{n-k-1}^{0,k+1},e_{n-k'}^{0,k},\cdots,e_{n-1}^{0,1}\right). \end{split}$$

Composing the above n-1 transformations, starting from c=0, we get:

$$\left(e_0^{n,0},e_1^{n-1,0},\cdots,e_{n-1}^{1,0}\right)\cdot g=\left(e_0^{0,n},e_1^{0,n-1},\cdots,e_{n-1}^{0,1}\right).$$

We refer to the unipotent matrix

(35)
$$g = \prod_{c=0}^{n-2} \prod_{\alpha=1}^{n-c-1} N_{\alpha}(\alpha_{\alpha,b,c}^{F;G,H}), \text{ as the rotation matrix.}$$

Observe that $(F, \pi(G)) \cdot g = (F, \pi(H))$. Since g may be explicitly written out, and satisfies the criterion for Fact 4.1, we see that:

(36)
$$P_{i}(F;G,H) = \sum_{c=0}^{i-1} \alpha_{n-i,i-c,c}^{F;G,H}.$$

Example 4.10. When n=3 (see Figure 13), we denote $\alpha_{2,1,0}^{F;G,H}$ by $R_{g,h}^f$, $\alpha_{1,2,0}^{F;G,H}$ by $S_{g,h}^f$, $\alpha_{1,1,1}^{F;G,H}$ by $C_{g,h}^f$, we obtain

(37)
$$g = N_1(S_{g,h}^f) \cdot N_2(R_{g,h}^f) \cdot N_1(T_{g,h}^f) = \begin{pmatrix} 1 & S_{g,h}^f + T_{g,h}^f & S_{g,h}^f R_{g,h}^f \\ 0 & 1 & R_{g,h}^f \\ 0 & 0 & 1 \end{pmatrix},$$

and hence $P_1(F;G,H)=R_{g,h}^f$ and $P_2(F;G,H)=S_{g,h}^f+T_{g,h}^f$

By direct computation, we obtain the following relationships among the quantities $\alpha_{a,b,c}^{F;G,H}$, $P_i(F;G,H)$ and $T_{i,j,k}(F,G,H)$.

Lemma 4.11. For positive integers a, b, c with a + b + c = n, we have

(38)
$$\frac{\alpha_{a,b+1,c-1}^{F;G,H}}{\alpha_{a,b,c}^{F;G,H}} = T_{a,b,c}(F,G,H).$$

Proposition 4.12.

(39)
$$P_{i}(F;G,H) = \alpha_{n-i,i,0}^{F;G,H} \left(1 + \sum_{c=1}^{i-1} \prod_{j=1}^{c} \frac{1}{T_{n-i,i-j,j}(F,G,H)} \right).$$

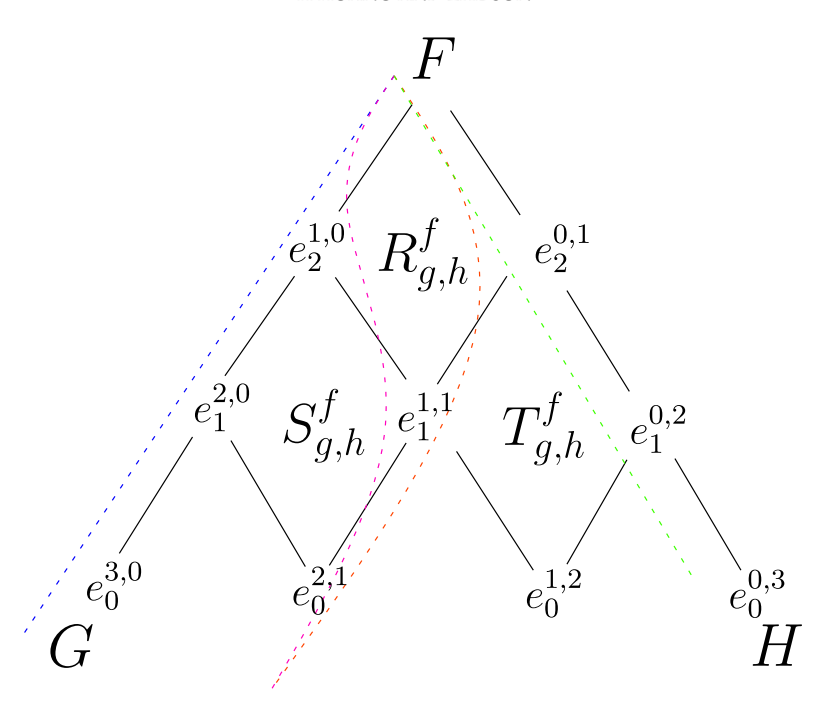


FIGURE 13. The above figures encodes how one constructs the unipotent matrix taking $(F, \pi(G))$ to $(F, \pi(H))$. Basis 1 is blue, basis 2 is mangenta, basis 3 is red, and basis 4 is green.

Proof. Iteratively applying Lemma 4.11 c times, we obtain

(40)
$$\alpha_{n-i,i-c,c}^{F;G,H} = \alpha_{n-i,i,0}^{F;G,H} \cdot \prod_{j=1}^{c} \frac{1}{T_{n-i,i-j,j}(F,G,H)}.$$

Re-expressing Equation (36), we get:

$$(41) \quad P_{i}(F;G,H) = \sum_{c=0}^{i-1} \alpha_{n-i,i-c,c}^{F;G,H} = \alpha_{n-i,i,0}^{F;G,H} \left(1 + \sum_{c=1}^{i-1} \prod_{j=1}^{c} \frac{1}{T_{n-i,i-j,j}(F,G,H)}\right).$$

The i-th character $P_i(f;g,h)$ depends on the choice of basis for F. For elements of \mathcal{A} -moduli space, this is canonically assigned, but not so for $\mathfrak{X}_{PGL_n,S_{g,m}}(\mathbb{R}_{>0})$. To resolve this issue, we consider taking ratios of two i-th characters, thereby providing a well-defined regular function on $\mathfrak{X}_{PGL_n,S_{g,m}}(\mathbb{R}_{>0})$. This is an idea previously used in [Sun15] in considering the ratio of two $(n \times n)$ determinants.

Definition 4.13 (i-th ratio). Given $(\rho, \xi) \in \mathfrak{X}_{PGL_{\pi}, S_{g, \pi}}(\mathbb{R}_{>0})$ and $x, y, z, t \in \widetilde{\mathfrak{m}}_{p}$, suppose that $(\xi_{\rho}(x), \xi_{\rho}(y), \xi_{\rho}(z))$ and $(\xi_{\rho}(x), \xi_{\rho}(y), \xi_{\rho}(t))$ are in generic position. Choose respective bases

$$(x_1, \dots, x_n), (y_1, \dots, y_n), (z_1, \dots, z_n), (t_1, \dots, t_n)$$

for $(\xi_{\rho}(x), \xi_{\rho}(y), \xi_{\rho}(z), \xi_{\rho}(t))$ and fix a lift X of $\xi_{\rho}(x)$ to A. We define the i-th ratio of (x, y, z, t) as:

(42)
$$B_{i}(x;y,z,t) := \frac{P_{i}(x;y,t)}{P_{i}(x;y,z)} := \frac{P_{i}(X;\xi_{\rho}(y),\xi_{\rho}(t))}{P_{i}(X;\xi_{\rho}(y),\xi_{\rho}(z))}.$$

We show (Proposition 4.14) that the i-th ratio is independent of the choice of X.

The well-definedness of i-th ratio also insures that $\frac{P_i(x;w,t)}{P_i(x;y,z)}$ is also well defined if $(\xi_\rho(x),\xi_\rho(w),\xi_\rho(t))$ is in generic position.

Proposition 4.14. The i-th ratio $B_i(x; y, z, t)$ is expressed as follows:

(43)
$$B_{i}(x;y,z,t) = \frac{1 + \sum_{c=1}^{i-1} \prod_{j=1}^{c} \frac{1}{T_{n-i,i-j,j}(x,y,t)}}{1 + \sum_{c=1}^{i-1} \prod_{j=1}^{c} \frac{1}{T_{n-i,j-j,j}(x,y,z)}} \cdot D_{i}(x,y,z,t),$$

and the i-th ratio does not depend on the lift X of $\xi_{\rho}(x)$.

Proof. By Proposition 4.12, we have

(44)
$$P_{i}(x;y,t) = \alpha_{n-i,i,0}^{x;y,t} \left(1 + \sum_{c=1}^{i-1} \prod_{j=1}^{c} \frac{1}{T_{n-i,i-j,j}(x,y,t)} \right),$$

and

(45)
$$P_{i}(x;y,z) = \alpha_{n-i,i,0}^{x;y,z} \left(1 + \sum_{c=1}^{i-1} \prod_{j=1}^{c} \frac{1}{T_{n-i,i-j,j}(x,y,z)} \right).$$

Moreover, by Lemma 4.8, we get

$$(46) \begin{split} \frac{\alpha_{n-i,i,0}^{x;y,t}}{\alpha_{n-i,i,0}^{x;y,z}} &= \frac{\frac{\Delta\left(x^{n-i-1}\wedge t^{1}\wedge y^{i}\right)\cdot\Delta\left(x^{n-i+1}\wedge y^{i-1}\right)}{\Delta\left(x^{n-i}\wedge y^{i}\right)\cdot\Delta\left(x^{n-i}\wedge t^{1}\wedge y^{i-1}\right)}}{\frac{\Delta\left(x^{n-i-1}\wedge z^{1}\wedge y^{i}\right)\cdot\Delta\left(x^{n-i+1}\wedge y^{i-1}\right)}{\Delta\left(x^{n-i}\wedge y^{i}\right)\cdot\Delta\left(x^{n-i}\wedge z^{1}\wedge y^{i-1}\right)}} \\ &= \frac{\Delta\left(x^{n-i-1}\wedge t^{1}\wedge y^{i}\right)}{\Delta\left(x^{n-i}\wedge t^{1}\wedge y^{i-1}\right)} \cdot \frac{\Delta\left(x^{n-i}\wedge z^{1}\wedge y^{i-1}\right)}{\Delta\left(x^{n-i-1}\wedge z^{1}\wedge y^{i}\right)} \\ &= D_{i}(x,y,z,t). \end{split}$$

Thus we obtain

(47)
$$B_{i}(x;y,z,t) = \frac{P_{i}(x;y,t)}{P_{i}(x;y,z)} = \frac{1 + \sum_{c=1}^{i-1} \prod_{j=1}^{c} \frac{1}{T_{n-i,i-j,j}(x,y,t)}}{1 + \sum_{c=1}^{i-1} \prod_{j=1}^{c} \frac{1}{T_{n-i,i-j,j}(x,y,z)}} \cdot \frac{\alpha_{n-i,i,0}^{x;y,t}}{\alpha_{n-i,i,0}^{x;y,z}} = \frac{1 + \sum_{c=1}^{i-1} \prod_{j=1}^{c} \frac{1}{T_{n-i,i-j,j}(x,y,t)}}{1 + \sum_{c=1}^{i-1} \prod_{j=1}^{c} \frac{1}{T_{n-i,i-j,j}(x,y,z)}} \cdot D_{i}(x,y,z,t).$$

Since edge functions and triple ratios are projective invariants, we conclude that $B_i(x; y, z, t)$ is independent of the lift X of $\xi_\rho(x)$.

Recall the weak cross ratio in [LM09, Theorem 10.3.1]

(48)
$$\mathbb{B}(x,y,z,t) := \frac{\Delta \left(x^{n-1} \wedge z^1 \right)}{\Delta \left(x^{n-1} \wedge t^1 \right)} \cdot \frac{\Delta \left(y^{n-1} \wedge t^1 \right)}{\Delta \left(u^{n-1} \wedge z^1 \right)}.$$

By Proposition 4.14, we have

$$\mathbb{B}(x,y,z,t) = \prod_{i=1}^{n-1} \frac{\Delta \left(x^{n-i-1} \wedge t^{1} \wedge y^{i} \right)}{\Delta \left(x^{n-i} \wedge t^{1} \wedge y^{i-1} \right)} \cdot \frac{\Delta \left(x^{n-i} \wedge z^{1} \wedge y^{i-1} \right)}{\Delta \left(x^{n-i-1} \wedge z^{1} \wedge y^{i} \right)}$$

$$= \prod_{i=1}^{n-1} D_{i}(x,y,z,t)$$

$$= \prod_{i=1}^{n-1} \left(B_{i}(x,y,z,t) \cdot \frac{1 + \sum_{c=1}^{i-1} \prod_{j=1}^{c} \frac{1}{T_{n-i,i-j,j}(x,y,z)}}{1 + \sum_{c=1}^{i-1} \prod_{j=1}^{c} \frac{1}{T_{n-i,i-j,j}(x,y,t)}} \right).$$

We therefore obtain:

Corollary 4.15. *The weak cross-ratio and the* i*-th ratio is related by:*

(50)
$$\mathbb{B}(x,y,z,t) = \prod_{i=1}^{n-1} B_i(x,y,z,t) \cdot \prod_{i=1}^{n-1} \left(\frac{1 + \sum_{c=1}^{i-1} \prod_{j=1}^{c} \frac{1}{T_{n-i,i-j,j}(x,y,z)}}{1 + \sum_{c=1}^{i-1} \prod_{j=1}^{c} \frac{1}{T_{n-i,i-j,j}(x,y,t)}} \right).$$

The above corollary allows us to relate Labourie–McShane's identities [LM09] to the McShane-type identities/inequalities in this paper.

Proposition 4.16. Consider an element $(\rho, \xi) \in \mathfrak{X}_{PGL_n, S_{g,m}}(\mathbb{R}_{>0})$ and its associated osculating map ξ_{ρ} . Suppose that for any homotopy class $\gamma \in \pi_1(S_{g,m})$ representing a closed curve with loxodromic monodromy, there exist a lift of $\rho(\gamma)$ into SL_n with eigenvectors $\delta_1, \dots, \delta_n$ and positive eigenvalues $\lambda_1, \dots, \lambda_n$ respectively. Further let δ^+, δ^- respectively denote the attracting and repelling fixed points of δ . Suppose that $(\delta_1, \dots, \delta_n)$ $((\delta_n, \dots, \delta_1)$ resp.) is the basis of the flag $\xi_{\rho}(\delta^+)$ $(\xi_{\rho}(\delta^-)$ resp.). Now, given a marked ideal triangle (x, y, z), (arbitrarily) fix respective bases

$$(x_1, \dots, x_n), (y_1, \dots, y_n)$$
 and (z_1, \dots, z_n)

for $\xi_{\rho}(x)$, $\xi_{\rho}(y)$, $\xi_{\rho}(z)$. Then, for integers a, $b\geqslant 1$ and $c=n-a-b\geqslant 0$, the following ratio is indepent of our basis choice and satisfies

(51)
$$\frac{\alpha_{a,b,c}^{x;y,z}}{\alpha_{a,b,c}^{x;\delta y,\delta z}} = \begin{cases} \frac{\lambda_{a+1}}{\lambda_a} & \text{if } x = \delta^+\\ \frac{\lambda_{n-a}}{\lambda_{n-a+1}} & \text{if } x = \delta^-. \end{cases}$$

In addition, we also obtain that:

(52)
$$\frac{P_{n-\alpha}(\delta^+; y, z)}{P_{n-\alpha}(\delta^+; \delta y, \delta z)} = \frac{\lambda_{\alpha+1}}{\lambda_{\alpha}} \quad and \quad \frac{P_{\alpha}(\delta^-; y, z)}{P_{\alpha}(\delta^-; \delta y, \delta z)} = \frac{\lambda_{\alpha}}{\lambda_{\alpha+1}}.$$

Proof. We only derive the δ^+ case, the other is essentially the same. Recall the notation $x^a := x_1 \wedge \cdots \wedge x_a$. For any non-negative integer u, v with a + u + v = n, we obtain

(53)
$$\Delta(\delta^{\alpha} \wedge z^{u} \wedge y^{v}) = \Delta(\rho(\delta)\delta^{\alpha} \wedge \rho(\delta)z^{u} \wedge \rho(\delta)y^{v})$$

$$= \lambda_1 \cdots \lambda_\alpha \cdot \Delta(\delta^\alpha \wedge (\delta z)^u \wedge (\delta y)^\nu).$$

Then

$$(55) \quad \alpha_{a,b,c}^{\delta^{+};y,z} = \frac{\Delta \left(\delta^{a-1} \wedge z^{c+1} \wedge y^{b}\right) \cdot \Delta \left(\delta^{a+1} \wedge z^{c} \wedge y^{b-1}\right)}{\Delta \left(\delta^{a} \wedge z^{c} \wedge y^{b}\right) \cdot \Delta \left(\delta^{a} \wedge z^{c+1} \wedge y^{b-1}\right)}$$

$$(56) \qquad \qquad = \frac{\lambda_{\alpha+1} \cdot \Delta \left(\delta^{\alpha-1} \wedge (\delta z)^{c+1} \wedge (\delta y)^{b}\right) \cdot \Delta \left(\delta^{\alpha+1} \wedge (\delta z)^{c} \wedge (\delta y)^{b-1}\right)}{\lambda_{\alpha} \cdot \Delta \left(\delta^{\alpha} \wedge (\delta z)^{c} \wedge (\delta y)^{b}\right) \cdot \Delta \left(\delta^{\alpha} \wedge (\delta z)^{c+1} \wedge (\delta y)^{b-1}\right)}$$

(57)
$$= \frac{\lambda_{a+1}}{\lambda_a} \cdot \alpha_{a,b,c}^{\delta^+;\delta y,\delta z}.$$

This lets us obtain that $\frac{\alpha_{a,b,c}^{\delta^+;y,z}}{\alpha_{a,b,c}^{\delta^+;\delta y,b,z}} = \frac{\lambda_{a+1}}{\lambda_a}$. The basis-independence of $\frac{\lambda_{a+1}}{\lambda_a}$ again ensures that our initial choice of bases is irrelevant. To further obtain that

$$\frac{P_{n-\alpha}(\delta^+;y,z)}{P_{n-\alpha}(\delta^+;\delta y,\delta z)} = \frac{\lambda_{\alpha+1}}{\lambda_{\alpha}},$$

we apply Proposition 4.14 with the observation that

$$(\delta^+, \delta x, \delta y) = \delta \cdot (\delta^+, x, y)$$

and the fact that triple ratios are projective invariants.

Definition 4.17 (Canonical lift). For any positive $\rho \in \text{Hom}(\pi_1(S_{g,m}), PGL_n)/PGL_n$ with loxodromic monodromy around each boundary component, there is a canonical lift (ρ, ξ) into $\mathfrak{X}_{PGL_n, S_{g,m}}(\mathbb{R}_{>0})$ such that for any homotopy class $\delta \in \pi_1(S_{g,m})$ representing a boundary component of $S_{g,m}$, there exist a lift of $\rho(\delta)$ into SL_n with eigenvectors $\delta_1, \dots, \delta_n$ and eigenvalues $\lambda_1, \dots, \lambda_n$ respectively satisfying $\lambda_1 > \dots > \lambda_n > 0$, and $(\delta_1, \dots, \delta_n)$ $((\delta_n, \dots, \delta_1)$ resp.) is a basis for the flag $\xi_\rho(\delta^+)$ $(\xi_\rho(\delta^-)$ resp.).

Remark 4.18. We use δ_i to represent an eigenvector only here. Later in Section 8, we use $\delta^i := \delta_1 \wedge \cdots \wedge \delta_i$ for computation as in Proposition 4.16 and avoid using δ_i .

Proposition 4.19. With respect to the canonical lift (ρ, ξ) of a loxodromic bordered positive representation ρ , the i-th period of α is the i-th simple root length of α :

(58)
$$\log B_{\mathfrak{i}}\left(\alpha^{-};\alpha^{+},\alpha(y),y\right) = \log \frac{\lambda_{\mathfrak{i}}(\rho(\alpha))}{\lambda_{\mathfrak{i}+1}(\rho(\alpha))} = \ell_{\mathfrak{i}}(\alpha), \quad \textit{for } y \neq \alpha^{\pm}.$$

Proof. Apply Proposition 4.16.

5. Goncharov-Shen potential splitting technique

5.1. **The** $A_{SL_3,S_{1,1}}(\mathbb{R}_{>0})$ **Case.** The goal of this section is to prove the following McShane-type inequality, before we promote it to an equality in Section 7.

Remark 5.1. For $(\bar{\rho}, \bar{\xi}) \in \mathcal{A}_{SL_3,S_{g,m}}(\mathbb{R}_{>0})$, the representation of the twist $\sigma_{S_{g,m}}$ is identity by Definition 2.9. Thus we use $(\rho, \bar{\xi}) \in \mathcal{A}_{SL_3,S_{g,m}}(\mathbb{R}_{>0})$ instead.

Theorem 5.2. Given $(\rho, \bar{\xi}) \in \mathcal{A}_{SL_3,S_{1,1}}(\mathbb{R}_{>0})$, let \mathfrak{p} be the puncture of $S_{1,1}$, let $\vec{\mathfrak{C}}_{1,1}$ be the collection of oriented simple closed curves up to homotopy on $S_{1,1}$. Then

(59)
$$\sum_{\gamma \in \overrightarrow{\mathcal{C}}_{1,1}} \frac{1}{1 + e^{\ell_1(\gamma) + \tau(\gamma)}} \leqslant 1,$$

where $\tau(\gamma)$ is defined in the description of Figure 2.

We obtain the above result by splitting the Goncharov–Shen potential P_1^p . As such, we first explain the splitting procedure.

Let $(\rho, \bar{\xi}) \in \mathcal{A}_{SL_3,S_{1,1}}(\mathbb{R}_{>0})$. Given an ideal triangulation \mathfrak{T} of $S_{1,1}$, we lift \mathfrak{T} into the universal cover $\widetilde{\mathfrak{T}}$. We denote the Fock–Goncharov \mathcal{A} coordinates as in Figure 9. Same as the case of $\mathcal{A}_{SL_2,S_{1,1}}(\mathbb{R}_{>0})$, the flips along the edges \overline{yt} , \overline{tx} , \overline{xy} generate the extended mapping class group of $S_{1,1}$. Such dynamic is described by an infinite tree with degree three for each vertex expanding to infinity starting from one vertex. For $\mathcal{A}_{SL_3,S_{1,1}}(\mathbb{R}_{>0})$, the flip at the edge \overline{yt} is composed of four successive cluster mutations. This is shown in the description adjacent to Figure 9.

By Equation (36), we have

(60)
$$P_1^p = \frac{w}{br} + \frac{w}{ds} + \frac{q}{ac} + \frac{q}{cr} + \frac{q}{bd} + \frac{q}{as},$$

(61)
$$P_2^p = \frac{bc}{aw} + \frac{rd}{ws} + \frac{bs}{wr} + \frac{ad}{wc} + \frac{ar}{bw} + \frac{cs}{dw} + \frac{ar}{sq} + \frac{cb}{dq} + \frac{dr}{cq} + \frac{bs}{aq} + \frac{ad}{bq} + \frac{cs}{rq}$$

For P_1^p and P_2^p , we have similar combining and splitting properties given by mutations as that of Markoff equation: flips cause a third of the summands each to split into two new summands, whilst for the remaining two-thirds pairs of summands reconsistute to form new summands. This phenomenon is easily checked by explicitly computing the mutation formulas (see Figure 9). We adopt to use additivity of i-th character as follows.

Lemma 5.3. *Set up as in Figure 9, we have*

(62)
$$P_1(y;z,t) + P_1(y;t,x) = \frac{w}{br} + \frac{q}{cr} = \frac{r'}{bc} = P_1(y;z,x),$$

(63)
$$P_1(t; x, y) + P_1(t; y, z) = \frac{q}{sa} + \frac{w}{ds} = \frac{s'}{ad} = P_1(t; x, z),$$

(64)
$$P_1(z;t,y) = \frac{w}{ac} = \frac{s'}{cw'} + \frac{r'}{aw'} = P_1(z;t,x) + P_1(z;t,y),$$

(65)
$$P_1(x;y,t) = \frac{q}{bd} = \frac{r'}{dq'} + \frac{s'}{bq'} = P_1(x;y,z) + P_1(x;z,t).$$

These formulas generalize the splitting of horocycle length for a hyperbolic structure. Similarly, we have formulas for P_2 .

5.2. **Asymptotic behavior.** For each oriented simple closed geodesic γ , we study the effect of arbitrarily iterated Dehn twists along γ on functions such as i-ratios and triple ratios.

Given $(\rho, \bar{\xi}) \in \mathcal{A}_{SL_3,S_{1,1}}(\mathbb{R}_{>0})$, recall the continuous map ξ_ρ into the flag variety defined with respect to $(\rho, \xi = \pi \circ \bar{\xi})$. Given an oriented closed geodesic γ and the corresponding γ_p , let \mathfrak{T}^0 be an ideal triangulation that contains γ_p as an ideal edge. In one fundamental domain of $\widetilde{\mathfrak{T}}^0$, suppose x,y_0,t_0,t are the vertices of the fundamental domain where $x = \tilde{p}$ is a lift of p such that $\xi(p) = \xi_\rho(x)$ and (x,t) is a lift of γ_p . After doing Dehn twist k ($k \in \mathbb{Z}$) times around γ on \mathfrak{T}^0 , suppose \mathfrak{T}^k is the resulting ideal triangulation. The fundamental domain of $\widetilde{\mathfrak{T}}^k$ is shown in Figure 14 left with the vertices x,y_k,t_k,t . Let $(x_1,x_2),(y_{k,1},y_{k,2}),(z_{k,1},z_{k,2}),(t_1,t_2)$ be the bases of the images of x,y_k,z_k,t under ξ_ρ respectively, which induce the Fock–Goncharov $\mathcal A$ coordinates $(a_1,a_2,b_{k-1},c_{k-1},c_k,b_k,d_{k-1},e_{k-1})$.

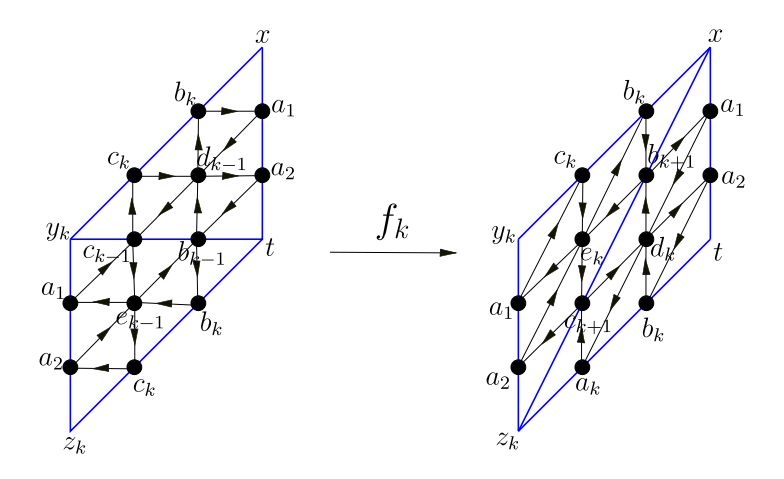


FIGURE 14. flip at $\overline{y_k t}$

Then as shown in Figure 14, the Dehn twist tw_{γ} induces the map from $V_{\mathbb{T}^k}$ to $V_{\mathbb{T}^{k+1}}$

$$\{x, y_k, z_k, t\} \rightarrow \{x, \gamma y_k, \gamma z_k, t\},$$

the corresponding map for the Fock–Goncharov A coordinates gives:

$$(a_1, a_2, b_{k-1}, c_{k-1}, c_k, b_k, d_{k-1}, e_{k-1}) \rightarrow (a_1, a_2, b_k, c_k, c_{k+1}, b_{k+1}, d_k, e_k).$$

Let f_k be the flip around the edge $\overline{ty_k}$. Let $\Gamma_{\mathcal{T}_3^k}$ be the quiver for \mathcal{T}_3^k . Then $tw_{\gamma}(\Gamma_{\mathcal{T}_3^k}) = (y_k z_k) \circ f_k(\Gamma_{\mathcal{T}_3^k}) = \Gamma_{\mathcal{T}_3^{k+1}}$, where $(y_k z_k)$ is the permutation of the vertices in $\Gamma_{\mathcal{T}_3^k}$ corresponding to permutation of y_k, z_k in \mathcal{T}^k . Moreover, $f_{k+1} \circ f_k = tw_{\gamma}^2$.

In [Hua14], for $\mathcal{A}_{SL_2,S_{1,1}}$, each gap of the McShane identity is interpreted as the limit of $\frac{\lambda_b}{\lambda_a\lambda_c}$ under the sequence $\{tw_\gamma^k\}_{k=-\infty}^{+\infty}$. Since we can express P_1^p as a positive rational function of Fock–Goncharov \mathcal{A} -coordinates, we begin by studying the asymptotic behavior of these coordinates under the Dehn twists.

Proposition 5.4. Suppose that the eigenvalues of $\rho(\gamma)$ satisfying $\lambda_1(\rho(\gamma)) > \lambda_2(\rho(\gamma)) > \lambda_3(\rho(\gamma)) > 0$. Under the sequence $\{tw_{\gamma}^k\}_{k=-\infty'}^{+\infty}$ we have:

$$(66) \qquad \lim_{k\to +\infty}\frac{b_{k+1}}{b_k}=\lim_{k\to +\infty}\frac{d_{k+1}}{d_k}=\lim_{k\to -\infty}\frac{c_k}{c_{k+1}}=\lim_{k\to -\infty}\frac{e_k}{e_{k+1}}=\lambda_1(\rho(\gamma)),$$

and conversely, we have:

(67)
$$\lim_{k \to +\infty} \frac{c_{k+1}}{c_k} = \lim_{k \to +\infty} \frac{e_{k+1}}{e_k} = \lim_{k \to -\infty} \frac{b_k}{b_{k+1}} = \lim_{k \to -\infty} \frac{d_k}{d_{k+1}} = \lambda_1(\rho(\gamma^{-1})).$$

Moreover, the following limits exist:

(68)
$$\lim_{k \to +\infty} \frac{b_k}{d_k}, \lim_{k \to -\infty} \frac{b_k}{d_k}, \lim_{k \to +\infty} \frac{c_k}{e_k}, \lim_{k \to -\infty} \frac{c_k}{e_k}$$

Proof. When k=0 in Figure 14, suppose that $y_0=\beta x$ where $\beta\in\pi_1(S_{1,1})$. For $k\in\mathbb{Z}$ in general, by definition, $t=\gamma\cdot x$, $y_k=\gamma^k\beta\cdot x$, $z_k=\gamma^{k+1}\beta\cdot x$. Let the bases of the flag $\xi_\rho(x)$ be (x_1,x_2,x_3) . Since ξ_ρ is ρ -equivariant, we have

$$\frac{d_{k+1}}{d_k} = \left| \frac{\Delta \left(x_1 \wedge \rho(\gamma^{k+1}\beta) x_1 \wedge \rho(\gamma) x_1 \right)}{\Delta \left(x_1 \wedge \rho(\gamma^k\beta) x_1 \wedge \rho(\gamma) x_1 \right)} \right|.$$

It is the ratio of the length of two vectors $\rho(\gamma) \cdot \rho(\gamma^k \beta) x_1$, $\rho(\gamma^k \beta) x_1$ projecting down to the plan spanned by $x_1, \rho(\gamma) x_1$ When k converges to $+\infty$, $\rho(\gamma^k \beta) x_1$ converge to the attracting fix point γ^+ . The ratio $\frac{d_{k+1}}{d_k}$ is then converge to $\lambda_1(\rho(\gamma))$. Suppose ν_1, ν_2, ν_3 are eigenvectors of $\lambda_1(\rho(\gamma)) > \lambda_2(\rho(\gamma)) > \lambda_3(\rho(\gamma))$ respectively. We have

$$\lim_{k \to +\infty} \frac{b_k}{d_k} = \lim_{k \to +\infty} \left| \frac{\Delta \left(x_1 \wedge x_2 \wedge \rho(\gamma^k \beta) x_1 \right)}{\Delta \left(x_1 \wedge \rho(\gamma^k \beta) x_1 \wedge \rho(\gamma) x_1 \right)} \right| = \left| \frac{\Delta \left(x_1 \wedge x_2 \wedge \nu_1 \right)}{\Delta \left(x_1 \wedge \nu_1 \wedge \rho(\gamma) x_1 \right)} \right|,$$

which does not depend on the eigenvector v_1 that we choose in the eigenspace. Thus $\lim_{k\to+\infty}\frac{b_k}{d_k}$ exists.

The proof of the other cases in Equations (66), (67) and (68) are similar, we leave them to the reader. \Box

Monodromy computation We compute hw_0 explicitly in [GS15, Section 6.2] using formulas in [GS15, page 566], then we have

$$(\xi_{\rho}(z_k), \pi(\xi_{\rho}(y_k))) \cdot \begin{pmatrix} 0 & 0 & \frac{1}{\alpha_2} \\ 0 & -\frac{\alpha_2}{\alpha_1} & 0 \\ \alpha_1 & 0 & 0 \end{pmatrix} = (\xi_{\rho}(y_k), \pi(\xi_{\rho}(z_k))).$$

Remark 5.5 (monodromy). The monodromy matrix g, in the conjugacy class of $\rho(\gamma)$, such that $(\xi_{\rho}(z_k), \pi(\xi_{\rho}(t))) \cdot g = (\xi_{\rho}(y_k), \pi(\xi_{\rho}(x)))$ is

$$\begin{pmatrix} 1 & S_{t,y_k}^{z_k} + T_{t,y_k}^{z_k} & S_{t,y_k}^{z_k} R_{t,y_k}^{z_k} \\ 0 & 1 & R_{t,y_k}^{z_k} \\ 0 & 0 & 1 \end{pmatrix} \begin{pmatrix} 0 & 0 & \frac{1}{a_2} \\ 0 & -\frac{a_2}{a_1} & 0 \\ a_1 & 0 & 0 \end{pmatrix} \begin{pmatrix} 1 & S_{z_k,x}^{y_k} + T_{z_k,x}^{y_k} & S_{z_k,x}^{y_k} R_{z_k,x}^{y_k} \\ 0 & 1 & R_{z_k,x}^{y_k} \\ 0 & 0 & 1 \end{pmatrix},$$

$$= \begin{pmatrix} 1 & \frac{b_{k-1}c_k}{b_ke_{k-1}} + \frac{a_2c_{k-1}}{a_1e_{k-1}} & \frac{b_{k-1}}{a_2b_k} \\ 0 & 1 & \frac{e_{k-1}}{a_2c_k} \\ 0 & 0 & 1 \end{pmatrix} \begin{pmatrix} 0 & 0 & \frac{1}{a_2} \\ 0 & -\frac{a_2}{a_1} & 0 \\ 0 & 0 & 0 \end{pmatrix} \begin{pmatrix} 1 & \frac{a_1c_{k+1}}{a_2e_k} + \frac{b_{k+1}c_k}{b_ke_k} & \frac{c_{k+1}}{a_2c_k} \\ 0 & 1 & \frac{e_k}{a_1c_k} \\ 0 & 0 & 1 \end{pmatrix}.$$

And

$$(70) \qquad \mathsf{Tr}(g) = -\frac{a_2}{a_1} + a_1 \cdot (R^{z_k}_{t,y_k} S^{z_k}_{t,y_k} + R^{y_k}_{z_k,x} S^{y_k}_{z_k,x} + R^{z_k}_{t,y_k} S^{y_k}_{z_k,x} + R^{z_k}_{t,y_k} T^{y_k}_{z_k,x}),$$

$$(71) \quad \operatorname{Tr}(g^{-1}) = -\frac{a_1}{a_2} + a_2 \cdot (R^{y_k}_{z_k,x} S^{z_k}_{t,y_k} + R^{z_k}_{t,y_k} T^{z_k}_{t,y_k} + R^{y_k}_{z_k,x} T^{z_k}_{t,y_k} + R^{y_k}_{z_k,x} T^{y_k}_{z_k,x}).$$

5.3. Goncharov-Shen potential for half pants.

Remark 5.6. Given $(\rho, \bar{\xi}) \in \mathcal{A}_{SL_3,S_{1,1}}$, as in Figure 14, the surface $S_{1,1}$ is cut into two half pairs of pants μ and μ' along γ and γ_p . Recall the (μ,i) -Goncharov–Shen potential in Definition 4.4. By the additivity of i-th character, we have P_i^{μ} and $P_i^{\mu'}$ are invariant under the Dehn twist around γ . More explicitly, we have

$$\begin{split} P_1^{\mu} &= R_{y_k,t}^x + R_{x,z_k}^t = \frac{d_{k-1}}{b_k a_1} + \frac{d_k}{b_k a_2}, \\ P_1^{\mu'} &= R_{t,y_k}^{z_k} + R_{z_k,x}^{y_k} = \frac{e_{k-1}}{c_k a_2} + \frac{e_k}{c_k a_1}, \\ P_2^{\mu} &= S_{y_k,t}^x + T_{y_k,t}^x + S_{x,z_k}^t + T_{x,z_k}^t = \frac{b_k c_{k-1}}{c_k d_{k-1}} + \frac{a_1 b_{k-1}}{d_{k-1} a_2} + \frac{a_2 b_{k+1}}{a_1 d_k} + \frac{b_k c_{k+1}}{d_k c_k}, \\ P_2^{\mu'} &= S_{t,y_k}^{z_k} + T_{t,y_k}^{z_k} + S_{z_k,x}^{y_k} + T_{z_k,x}^{y_k} = \frac{c_k b_{k-1}}{b_k e_{k-1}} + \frac{a_2 c_{k-1}}{a_1 e_{k-1}} + \frac{a_1 c_{k+1}}{a_2 e_k} + \frac{c_k b_{k+1}}{e_k b_k}, \end{split}$$

do not depend on $k \in \mathbb{Z}$.

Proof of Theorem 5.2. McShane's identity [McS91] is established by dividing up a horocycle into countable many disjoint open intervals and a Cantor set. Each such interval takes the form as shown in Figure 15, and there is a canonical 2:1 correspondence between these open intervals and oriented simple closed geodesics on $S_{1,1}$. Specifically, the intervals I_1 , I_2 correspond to $\gamma \in \vec{\mathcal{C}}_{1,1}$ and the intervals $I_3 \cup I_4$ correspond to γ^{-1} . This correspondence is purely topological, and applies also to the higher rank context.

For $\mathcal{A}_{SL_3,S_{1,1}}(\mathbb{R}_{>0})$, the role of the horocycle is supplanted by the Goncharov–Shen potential P_1^p . Using the Fock–Goncharov \mathcal{A} coordinates in Figure 14, we compute the gap terms for I_1 , I_2 , thereby allowing us to obtain

(72)
$$\sum_{\substack{\longrightarrow\\\chi\in\mathcal{C}_{1,1}}} \left(\lim_{k\to+\infty} \frac{d_{k-1}}{b_k a_1} + \lim_{k\to-\infty} \frac{e_k}{c_k a_1} \right) \leqslant P_1^p,$$

where the inequality is due to the potential measure theoretic contribution of the remnant Cantor set.

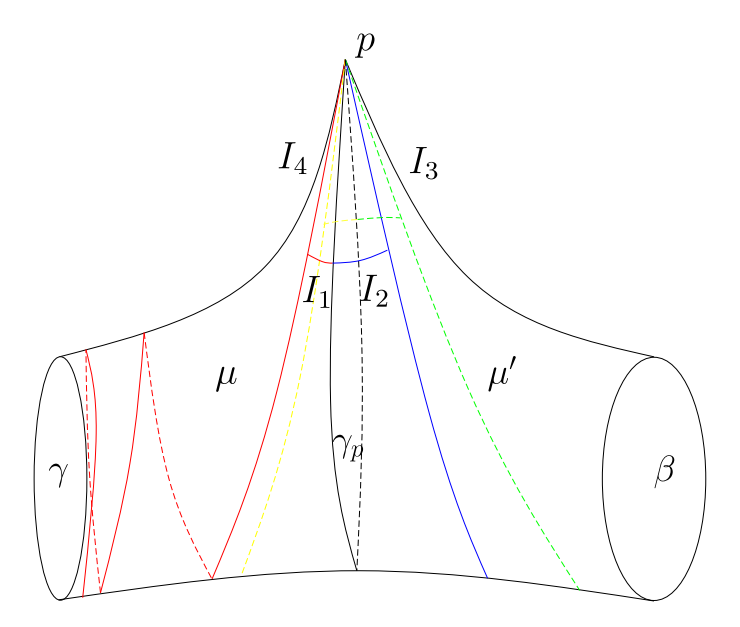


FIGURE 15. The red and yellow simple curves spiral around the left side hole to the infinity in two different directions, while the blue and the green simple curves spiral around the right side hole to the infinity.

Renormalizing this summation by dividing through by P_1^p , Proposition 5.4 tells us that we have

$$(73) \quad \begin{array}{l} \lim\limits_{k \to +\infty} \frac{d_{k-1}}{b_k a_1 P_1^p} = \lim\limits_{k \to +\infty} \frac{\frac{d_{k-1}}{b_k a_1}}{\frac{d_{k-1}}{b_k a_1} + \frac{d_k}{b_k a_2}} \cdot \frac{P_1^{\mu}}{P_1^p} = \lim\limits_{k \to +\infty} \frac{1}{1 + \frac{a_1 d_k}{a_2 d_{k-1}}} \cdot \frac{P_1^{\mu}}{P_1^p} \\ = \frac{1}{1 + \frac{a_1}{a_2} \lambda_1(\rho(\gamma))} \cdot \frac{P_1^{\mu}}{P_1^p}. \end{array}$$

Similarly,

(74)
$$\lim_{k \to -\infty} \frac{e_k}{c_k a_1 P_1^p} = \frac{1}{1 + \frac{a_1}{a_2} \lambda_1(\rho(\gamma))} \cdot \frac{P_1^{\mu'}}{P_1^p}.$$

Since $P_1^p = P_1^{\mu} + P_1^{\mu'}$, we obtain

(75)
$$1 \geqslant \sum_{\gamma \in \overrightarrow{\mathcal{C}}_{1,1}} \left(\lim_{k \to +\infty} \frac{d_{k-1}}{b_k a_1 P_1^p} + \lim_{k \to -\infty} \frac{e_k}{c_k a_1 P_1^p} \right)$$
$$= \sum_{\gamma \in \overrightarrow{\mathcal{C}}_{1,1}} \frac{1}{1 + \frac{a_1(\gamma_p)}{a_2(\gamma_p)} \lambda_1(\rho(\gamma))}.$$

Moreover, by Proposition 5.4, observe that

(76)
$$\mathsf{T}(\tilde{\mathfrak{p}},\gamma\tilde{\mathfrak{p}},\gamma^+) = \lim_{k \to +\infty} \frac{a_1b_{k-1}c_k}{a_2c_{k-1}b_k} = \frac{a_1(\gamma_{\mathfrak{p}})\lambda_2(\rho(\gamma))}{a_2(\gamma_{\mathfrak{p}})}.$$

Thus

(77)
$$\sum_{\substack{\overrightarrow{\gamma} \in \mathcal{C}_{1,1}}} \frac{1}{1 + \mathsf{T}(\widetilde{\mathfrak{p}}, \gamma \widetilde{\mathfrak{p}}, \gamma^+) \cdot \frac{\lambda_1(\rho(\gamma))}{\lambda_2(\rho(\gamma))}} \leqslant 1,$$

and hence:

(78)
$$\sum_{\gamma \in \overrightarrow{\mathcal{C}}_{1,1}} \frac{1}{1 + e^{\tau(\gamma) + \ell_1(\gamma)}} \leqslant 1.$$

5.4. Symmetry in the $\mathcal{A}_{SL_3,S_{1,1}}(\mathbb{R}_{>0})$ case. For $(\rho,\bar{\xi})\in\mathcal{A}_{SL_3,S_{1,1}}(\mathbb{R}_{>0})$, we have the following symmetry between objects related to P_1^p and P_2^p :

Lemma 5.7. Given $k \in \mathbb{Z}$ in Figure 14, we have

$$\frac{S_{y_k,t}^{x'}+T_{y_k,t}^{x}}{R_{t,y_k}^{z_k}}=\frac{S_{t,y_k}^{z_k}+T_{t,y_k}^{z_k}}{R_{u_k,t}^{x}}=\frac{S_{x,z_k}^{t}+T_{x,z_k}^{t}}{R_{z_k,x}^{y_k}}=\frac{S_{z_k,x}^{y_k}+T_{z_k,x}^{y_k}}{R_{x,z_k}^{t}}=\frac{P_2^{\mu'}}{P_1^{\mu'}}=\frac{P_2^{\mu'}}{P_1^{\mu}}=\frac{P_2^{\mu'}}{P_1^{\mu}}=\frac{P_2^{\mu'}}{P_1^{\mu'}}=\frac{P_2^{\mu'}}=\frac{P_2^{\mu'}}{P_1^{\mu'}}=\frac{P_2^{\mu'}}{P_1^{\mu'}}=\frac{P_2^{\mu'}}$$

Proof. Firstly, we have

$$(S_{y_{k},t}^{x} + T_{y_{k},t}^{x})R_{y_{k},t}^{x} = \left(\frac{b_{k}c_{k-1}}{c_{k}d_{k-1}} + \frac{a_{1}b_{k-1}}{a_{2}d_{k-1}}\right)\frac{d_{k-1}}{a_{1}b_{k}}$$

$$= \frac{c_{k-1}}{c_{k}a_{1}} + \frac{b_{k-1}}{a_{2}b_{k}}$$

$$= \left(\frac{a_{2}c_{k-1}}{a_{1}e_{k-1}} + \frac{c_{k}b_{k-1}}{e_{k-1}b_{k}}\right)\frac{e_{k-1}}{a_{2}c_{k}} = (S_{t,y_{k}}^{z_{k}} + T_{t,y_{k}}^{z_{k}})R_{t,y_{k}}^{z_{k}},$$

thus $\frac{S_{y_k,t}^x + T_{y_k,t}^x}{R_{t,y_k}^{z_k}} = \frac{S_{t,y_k}^{z_k} + T_{t,y_k}^{z_k}}{R_{y_k,t}^{x_k}}$. By similar computation, we obtain $\frac{S_{x,z_k}^t + T_{x,z_k}^t}{R_{z_k,x}^{y_k}} = \frac{S_{z_k,x}^{z_k} + T_{z_k,x}^y}{R_{x,z_k}^t}$.

To prove that $\frac{S_{t,y_k}^{z_k} + T_{t,y_k}^{z_k}}{R_{y_k,t}^x} = \frac{S_{x,z_k}^t + T_{x,z_k}^t}{R_{z_k,x}^{y_k}}, \text{ it is equivalent to prove}$

(81)
$$\frac{a_2 e_k c_{k-1}}{a_1^2 c_k e_{k-1}} + \frac{e_k b_{k-1}}{a_1 b_k e_{k-1}} = \frac{a_2 d_{k-1} b_{k+1}}{a_1^2 b_k d_k} + \frac{d_{k-1} c_{k+1}}{a_1 c_k d_k}.$$

By mutation formulas, in the above formula, we replace b_{k+1} by $\frac{b_k d_k + a_1 e_k}{d_{k-1}}$, replace c_{k+1} by $\frac{e_k c_k + d_k a_2}{e_{k-1}}$ and replace $e_k c_{k-1}$ by $c_k e_{k-1} + a_1 d_{k-1}$. Equation (81) is then equivalent to

(82)
$$b_{k-1}d_k = a_2e_{k-1} + b_kd_{k-1},$$

which is exactly the mutation formula at dk, thus

$$\frac{S^{z_k}_{t,y_k} + T^{z_k}_{t,y_k}}{R^{x}_{u_k,t}} = \frac{S^{t}_{x,z_k} + T^{t}_{x,z_k}}{R^{y_k}_{z_k,x}}.$$

The rest is based on the fact that $\frac{\alpha}{b}=\frac{c}{d}=\frac{\alpha+c}{b+d}.$ For example

$$\frac{S_{y_k,t}^x + T_{y_k,t}^x}{R_{t,y_k}^{z_k}} = \frac{S_{x,z_k}^t + T_{x,z_k}^t}{R_{z_k,x}^{y_k}} = \frac{P_2^\mu}{P_1^\mu}.$$

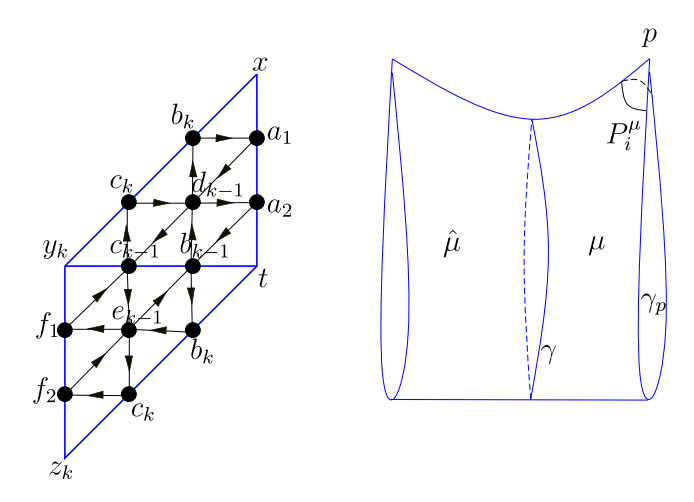


FIGURE 16. The embedded boundary-parallel pair of half-pants μ is glued to another embedded boundary-parallel pair of halfpants û.

We conclude that

$$\frac{S_{y_k,t}^x + T_{y_k,t}^x}{R_{t,y_k}^{z_k}} = \frac{S_{t,y_k}^{z_k} + T_{t,y_k}^{z_k}}{R_{y_k,t}^x} = \frac{S_{x,z_k}^t + T_{x,z_k}^t}{R_{z_k,x}^{y_k}} = \frac{S_{z_k,x}^{y_k} + T_{z_k,x}^{y_k}}{R_{x,z_k}^t} = \frac{P_2^\mu}{P_1^{\mu'}} = \frac{P_2^{\mu'}}{P_1^\mu} = \frac{P_2^\mu}{P_1^\mu}.$$

Proposition 5.8. For $(\rho, \bar{\xi}) \in \mathcal{A}_{SL_3,S_{1,1}}(\mathbb{R}_{>0})$, the P_2^p gap terms are equivalent to those obtained via P₁^p, and thus any subsequently derived McShane identities are equivalent up to index relabeling.

Proof. By the above lemma, we obtain

$$\begin{split} &\lim_{k \to +\infty} (S^{x}_{y_{k},t} + T^{x}_{y_{k},t}) = \frac{P^{p}_{2}}{P^{p}_{1}} \lim_{k \to +\infty} R^{z_{k}}_{t,y_{k}}, \lim_{k \to +\infty} (S^{z_{k}}_{t,y_{k}} + T^{z_{k}}_{t,y_{k}}) = \frac{P^{p}_{2}}{P^{p}_{1}} \lim_{k \to +\infty} R^{x}_{y_{k},t}, \\ &\lim_{k \to -\infty} (S^{t}_{x,z_{k}} + T^{t}_{x,z_{k}}) = \frac{P^{p}_{2}}{P^{p}_{1}} \lim_{k \to -\infty} R^{y_{k}}_{z_{k},x}, \lim_{k \to -\infty} (S^{y_{k}}_{z_{k},x} + T^{y_{k}}_{z_{k},x}) = \frac{P^{p}_{2}}{P^{p}_{1}} \lim_{k \to -\infty} R^{t}_{x,z_{k}}. \end{split}$$

5.5. General punctured convex real projective surfaces. We prove the McShanetype inequality on $\mathcal{A}_{SL_3,S_{g,m}}(\mathbb{R}_{>0})$ for P_1^p . We leave the similar proof for P_2^p to the readers. Notice that there is no symmetry between P_1^p and P_2^p when $(g,m) \neq 0$

Theorem 5.9. Given $(\rho, \bar{\xi}) \in \mathcal{A}_{SL_3,S_{g,m}}(\mathbb{R}_{>0})$. Let p be the puncture in m_p . Recall the collection of all boundary-parallel pairs of half-pants $\hat{H_p}$ in Definition 1.16 and $B_1(\gamma, \gamma_p)$ in Remark 1.14. Then

$$\sum_{[\gamma,\gamma_{\mathfrak{p}}]\in\overrightarrow{\mathcal{H}}_{\mathfrak{p}}}\left(\frac{B_{1}(\gamma,\gamma_{\mathfrak{p}})}{1+e^{\ell_{1}(\gamma)+\tau(\gamma,\gamma_{\mathfrak{p}})}}\right)\leqslant 1.$$

Proof. As in Figure 15, the gap term for an embedded boundary-parallel pair of half-pants $\mu=(\gamma,\gamma_p)$ corresponds to I_1 . As in right hand side of Figure 16, assume $\hat{\mu}$ is another embedded half pair of pants patching with μ along γ . Then we denote the Fock–Goncharov $\mathcal A$ coordinates after k-th Dehn twist along γ as in the left hand side of Figure 16. Then we have

(84)
$$1 \geqslant \sum_{[\gamma,\gamma_p] \in \overrightarrow{\mathcal{H}}_p} \left(\lim_{k \to +\infty} \frac{d_{k-1}}{b_k a_1 P_1^p} \right).$$

When we do Dehn twists along γ , the situation here is different from the case of $S_{1,1}$ in Figure 14, but quite similar. Here we have $t = \gamma x$, $y_k = \gamma^k y_0$, $z_k = \gamma^{k+1} y_0$. By similar arguments in Proposition 5.4, we still have

(85)
$$\lim_{k \to +\infty} \frac{d_k}{d_{k-1}} = \lambda_1(\rho(\gamma)).$$

Recall that $B_1(\gamma,\gamma_p)=\frac{P_1^{\,\mu}}{P_1^{\,p}}.$ Hence we obtain

$$\sum_{[\gamma,\gamma_{p}]\in\overrightarrow{\mathcal{H}}_{p}} \left(\lim_{k\to+\infty} \frac{d_{k-1}}{b_{k}a_{1}P_{1}^{p}} \right) \\
= \sum_{[\gamma,\gamma_{p}]\in\overrightarrow{\mathcal{H}}_{p}} \left(B_{1}(\gamma,\gamma_{p}) \lim_{k\to\infty} \frac{d_{k-1}}{b_{k}a_{1}P_{1}^{\mu}} \right) \\
= \sum_{[\gamma,\gamma_{p}]\in\overrightarrow{\mathcal{H}}_{p}} \left(B_{1}(\gamma,\gamma_{p}) \cdot \left(1 + \frac{a_{1}}{a_{2}} \cdot \lim_{k\to\infty} \frac{d_{k}}{d_{k-1}} \right)^{-1} \right) \\
= \sum_{[\gamma,\gamma_{p}]\in\overrightarrow{\mathcal{H}}_{p}} \left(B_{1}(\gamma,\gamma_{p}) \cdot \frac{1}{1 + \frac{a_{1}}{a_{2}} \cdot \lambda_{1}(\rho(\gamma))} \right) \\
= \sum_{[\gamma,\gamma_{p}]\in\overrightarrow{\mathcal{H}}_{p}} \left(\frac{B_{1}(\gamma,\gamma_{p})}{1 + T(p,\gamma_{p},\gamma^{+}) \cdot \frac{\lambda_{1}(\rho(\gamma))}{\lambda_{2}(\rho(\gamma))}} \right).$$

Finally, we conclude that

$$\sum_{[\gamma,\gamma_{\mathbf{p}}]\in\overrightarrow{\mathcal{H}}_{\mathbf{p}}}\left(\frac{B_1(\gamma,\gamma_{\mathbf{p}})}{1+e^{\tau(\gamma)+\ell_1(\gamma)}}\right)\leqslant 1.$$

Recall the set $\vec{\mathcal{P}}_p$ in Definition 1.19. We can write the above inequality in the summation of the collection $\vec{\mathcal{P}}_p$ of all boundary-parallel pairs of pants.

Theorem 5.10. Given $(\rho, \bar{\xi}) \in \mathcal{A}_{SL_3, S_{g,m}}(\mathbb{R}_{>0})$ and a distinguished puncture $p \in m_p$. Then

(87)
$$\sum_{\{\beta,\gamma\}\in\vec{\mathcal{P}}_{p}} \left(\frac{1}{1 + \frac{\cosh\frac{d_{2}(\beta,\gamma)}{2}}{\cosh\frac{d_{1}(\beta,\gamma)}{2}} \cdot e^{\frac{1}{2}(\tau(\gamma,\delta_{p}) + \ell_{1}(\gamma) + \tau(\beta,\delta_{p}) + \ell_{1}(\beta))}} \right) \leqslant 1,$$

where $d_1(\beta,\gamma) = \log D_1(x,\gamma x,\beta^+,\gamma^+)$ and $d_2(\beta,\gamma) = \log D_2(x,\gamma x,\beta^+,\gamma^+)$ and δ_p is the unique simple bi-infinite geodesic on the pair of pants $\{\bar{\beta},\bar{\gamma}\}$ with both ends going up

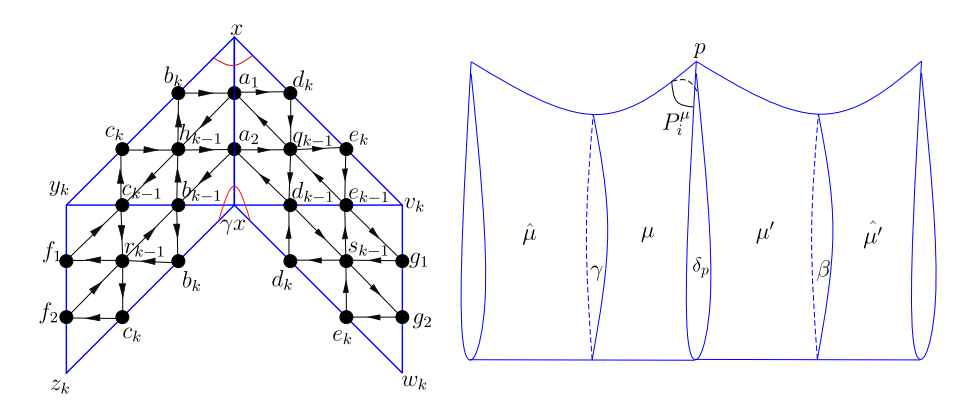


Figure 17. The embedded boundary-parallel pair of half-pants μ is glued to $\hat{\mu}$ and μ' is glued to $\hat{\mu}'$.

p. In particular, (β, δ_p) and (γ, δ_p) are boundary-parallel half-pants. Refer to Equation 6 for $\tau(\gamma, \delta_p)$ and $\tau(\beta, \delta_p)$.

Proof. As in Figure 15, the gap term for the boundary-parallel pairs of pants $[\beta, \gamma]$ corresponds to $I_1 \cup I_2$. Then we use the splitting technique for both I_1 and I_2 in Equation (86) at the same time. Figure 17 shows the resulting Fock–Goncharov $\mathcal A$ coordinates under $(tw_\beta \cdot tw_\gamma)^k$.

Firstly, we express P_1^p corresponding to two arcs at x and γx in the left hand side of Figure 17:

(88)
$$P_1^p = \frac{b_k q_{k-1} + d_k h_{k-1}}{a_1 b_k d_k} + \frac{b_k q_k + d_k h_k}{a_2 b_k d_k}$$

for simplifying our computation. Then we have

(89)
$$\begin{split} \sum_{\{\beta,\gamma\}\in\vec{\mathcal{P}}_{p}} \lim_{k\to+\infty} \left(\frac{h_{k-1}}{b_{k}a_{1}P_{1}^{p}} + \frac{q_{k-1}}{d_{k}a_{1}P_{1}^{p}} \right) \\ &= \sum_{\{\beta,\gamma\}\in\vec{\mathcal{P}}_{p}} \lim_{k\to+\infty} \frac{\frac{b_{k}q_{k-1}+d_{k}h_{k-1}}{a_{1}b_{k}d_{k}}}{\frac{b_{k}q_{k-1}+d_{k}h_{k-1}}{a_{1}b_{k}d_{k}} + \frac{b_{k}q_{k}+d_{k}h_{k}}{a_{2}b_{k}d_{k}}} \\ &= \sum_{\{\beta,\gamma\}\in\vec{\mathcal{P}}_{p}} \lim_{k\to+\infty} \frac{\frac{b_{k}q_{k-1}+d_{k}h_{k-1}}{a_{1}b_{k}d_{k}} + \frac{b_{k-1}q_{k-1}+d_{k-1}h_{k-1}}{a_{2}b_{k-1}d_{k-1}}}{\frac{b_{k}q_{k-1}+d_{k}h_{k-1}}{a_{1}b_{k}d_{k}} + \frac{b_{k-1}q_{k-1}+d_{k}h_{k-1}}{a_{2}b_{k-1}d_{k-1}}} \\ &= \sum_{\{\beta,\gamma\}\in\vec{\mathcal{P}}_{p}} \lim_{k\to+\infty} \frac{1}{1 + \frac{a_{1}d_{k}}{a_{2}d_{k-1}} \cdot \frac{1 + \frac{b_{k}-1}{b_{k-1}d_{k-1}}}{1 + \frac{d_{k}h_{k-1}}{b_{k}d_{k-1}}} \end{split}$$

After taking the limit, we obtain the above sum equals to

(90)
$$= \sum_{\{\beta,\gamma\} \in \overrightarrow{\mathcal{P}}_{p}} \frac{1}{1 + \frac{\alpha_{1}\lambda_{1}(\rho(\beta))}{\alpha_{2}} \cdot \frac{1 + \frac{1}{D_{2}(x,\gamma x,\beta+\gamma+)}}{1 + D_{1}(x,\gamma x,\beta+\gamma+)}}$$

$$= \sum_{\{\beta,\gamma\} \in \overrightarrow{\mathcal{P}}_{p}} \frac{1}{1 + \frac{\alpha_{1}\lambda_{1}(\rho(\beta))}{\alpha_{2}} \cdot e^{-\frac{d_{1}(\beta,\gamma)}{2} - \frac{d_{2}(\beta,\gamma)}{2}} \cdot \frac{\cosh\frac{d_{2}(\beta,\gamma)}{2}}{\cosh\frac{d_{1}(\beta,\gamma)}{2}}}$$

By Equation (76) and

$$D_1(x,\gamma x,\beta^+,\gamma^+) \cdot D_2(x,\gamma x,\beta^+,\gamma^+) = \frac{\lambda_1(\rho(\beta))}{\lambda_1(\rho(\gamma))},$$

the above sum equals to

$$(91) \qquad \sum_{\{\beta,\gamma\}\in\overrightarrow{\mathcal{P}}_{p}} \frac{1}{1+\sqrt{\frac{\alpha_{1}\lambda_{1}(\rho(\beta))}{\alpha_{2}}}\sqrt{\frac{\alpha_{1}\lambda_{1}(\rho(\gamma))}{\alpha_{2}}} \cdot \frac{\cosh\frac{d_{2}(\beta,\gamma)}{2}}{\cosh\frac{d_{1}(\beta,\gamma)}{2}}} \\ = \sum_{\{\beta,\gamma\}\in\overrightarrow{\mathcal{P}}_{p}} \frac{1}{1+\frac{\cosh\frac{d_{2}(\beta,\gamma)}{2}}{\cosh\frac{d_{1}(\beta,\gamma)}{2}} \cdot e^{\frac{1}{2}(\tau(\gamma,\delta_{p})+\ell_{1}(\gamma)+\tau(\beta,\delta_{p})+\ell_{1}(\beta))}}.$$

In the Fuchsian locus, $d_1(\beta,\gamma)=d_2(\beta,\gamma)$ and all the triple ratios equals to 1, thus we recover the original McShane's identity.

6. Geodesic sparsity for convex real projective surfaces

The study of positive $PGL_3(\mathbb{R})$ representations is equivalent to the study of marked convex real projective surfaces, and this geometric correspondence provides additional tools for us to work with.

We first give some background for convex real projective surfaces, before moving onto our main goal of this chapter: to generalize the Birman-Series geodesic sparsity theorem to the context of finite-area convex real projective surface context. Our proof is fundamentally geometric topological in nature, and we adjust our language accordingly. This complements the primarily algebraic treatment we give in the previous chapters via Fock–Goncharov coordinates.

6.1. Convex real projective surfaces.

Definition 6.1 (convex sets). A set $\Omega \subset \mathbb{R}P^2$ is called convex if the intersection of Ω with every line in \mathbb{R}^2 is connected. Furthermore, a convex set Ω is called

- properly convex, if the closure $\overline{\Omega}$ is convex and contained within the complement $\mathbb{R}^2 = \mathbb{R}\mathsf{P}^2 \mathbb{R}\mathsf{P}^1$ of some $\mathbb{R}\mathsf{P}^1$ linearly embedded in $\mathbb{R}\mathsf{P}^2$;
- strictly convex, if the boundary $\partial\Omega$ of Ω contains no line segments.

Definition 6.2 (convex real projective surface). A real projective surface Σ *is a topological surface* S *equipped with an atlas* $\{(U, \phi : U \to \mathbb{R}P^2)\}$, *with*

- \bullet coordinate patches U embedded as open sets in $\mathbb{R}P^2$ and
- transition maps that are (restrictions of) projective linear transformations $PGL_3(\mathbb{R})$ acting on $\mathbb{R}P^2$.

A convex real projective surface $\Sigma = (S, \{(U, \varphi)\})$ is the quotient of a properly convex open subset Ω by a discrete subgroup of $PGL_3(\mathbb{R})$ which is isomorphic to $\pi_1(S)$.

Since convex sets are contractible, every convex real projective surface Σ inherits a universal cover $\Omega \subset \mathbb{R}P^2$ from its developing map. Every such Ω lies within some copy of \mathbb{R}^2 linearly embedded in $\mathbb{R}P^2$.

The fact that Σ is equal to the quotient of Ω by a discrete subgroup Γ of $PGL_3(\mathbb{R})$ means that there is a discrete faithful representation

$$\rho: \pi_1(S) \to PGL_3(\mathbb{R}).$$

We refer to ρ as a monodromy representation for Σ . For any two compatible universal covers for Σ , one can show that their respective monodromy representations must be equal, up to conjugation.

Definition 6.3 (projective equivalence). We say that two convex real projective surfaces Σ_1 and Σ_2 are projectively equivalent if, given their respective associated universal covers $\Omega_1, \Omega_2 \subset \mathbb{R}\mathsf{P}^2$, there is a projective linear transformation $\tilde{\mathfrak{f}} \in \mathrm{PGL}_3(\mathbb{R})$ such that \mathfrak{f} maps Ω_1 to Ω_2 . The map \mathfrak{f} descends to a map between $\mathfrak{f}: \Sigma_1 \to \Sigma_2$, and we say that \mathfrak{f} is a projective equivalence between Σ_1 and Σ_2 .

Goldman-Choi [CG93, G90] studied the space of marked (finite area) convex real projective structures on a smooth surface S

$$Conv(\Sigma) := \{(\Sigma, f) \mid f : S \to \Sigma \text{ is a } C^1 \text{ homeomorphism}\} / \sim_{conv},$$

where $(\Sigma_1, f_1) \sim_{conv} (\Sigma_2, f_2)$ if and only if $f_2 \circ f_1^{-1}$ is homotopy equivalent to a projective equivalence between Σ_1 and Σ_2 . In particular, they show that the space

 $Conv(\Sigma)$ of marked convex real projective structures for a closed surface S is equivalent to the Hitchin moduli space — defined as the space of all Hitchin $PGL_3(\mathbb{R})$ representations of $\pi_1(S)$, up to conjugation.

6.2. The geometry of convex real projective surfaces.

Definition 6.4 (Hilbert distance). Given any two distinct points $x,y \in \Omega \subset \mathbb{R}^2$, extend the straight line segment running between x and y to a segment running between boundary points $p_x, p_y \in \partial \Omega$, where p_x is closer to x and p_y is closer to y. We define the Hilbert distance to be

$$d(x,y) := \log \frac{|x - p_y| \cdot |y - p_x|}{|y - p_y| \cdot |x - p_x|},$$

where |u-v| denotes the Euclidean length of the distance between $u,v\in\Omega\subset\mathbb{R}^2$. The Hilbert distance is invariant under projective linear transformations and hence descends to a distance metric on Σ . We refer to both the metric d on Ω and the metric d_{Σ} on Σ as the Hilbert metric.

Every convex real projective surface $\Sigma = \Omega/\rho(\pi_1(S))$ inherits a Hilbert distance metric d_{Σ} from its (properly convex) universal cover Ω . In the special case when Σ is a hyperbolic surface, its universal cover Ω is an ellipse, and the Hilbert metric on Ω is twice the usual hyperbolic metric on Ω with respect to the Klein model.

Remark 6.5. The Hilbert metric on any convex domain Ω is, in fact, Finsler. The Finsler metric (i.e.: the Minkowski functional) on each tangent space $T_x\Sigma$ is given by:

(92)
$$\|(x,\nu)\|_{\Omega} := \left(\frac{1}{|x-x^+|} + \frac{1}{|x-x^-|}\right) |\nu|, \text{ where:}$$

- $(x,v) \in T_x\Sigma$ is a tangent vector,
- x^+ denotes the point on $\partial\Omega$ intersected by the ray $x+t\nu$, for t>0
- and x^- denotes the point on $\partial\Omega$ intersected by the ray x tv, for t > 0.

Remark 6.6. The Hilbert distance may be written as the sum of two positive components:

(93)
$$d(x,y) = \log \frac{|x - p_y|}{|y - p_y|} + \log \frac{|y - p_x|}{|x - p_x|}.$$

Each of these two terms defines an asymmetric metric on Ω . The left term is referred to as the Funk metric [Bus74], and the right term is referred to as the reverse Funk metric [PT14]. These are (generally) distinct quantities, and the Funk metric is an asymmetric metric.

Definition 6.7 (Finsler area). The Finsler area (also known as the Busemann measure) on (Ω, d_{Ω}) is defined as the Borel measure on Ω with density

(94)
$$\frac{1}{Area(B_{d_{\Omega}}(x,1))}, where:$$

- $B_{d,o}(x,1)$ denotes the unit Hilbert distance ball centered x,
- Area (\cdot) denotes any a. priori chosen Lebesgue measure on $\Omega \subset \mathbb{R}^n$.

6.3. **Boundary regularity and convexity of** $\partial\Omega$ **.** We primarily deal with convex real projective surfaces Σ with finite area, and by the work of Marquis [Mar12], we know that the universal cover Ω for such a surface Σ is necessarily strictly convex and hence has C^1 boundary regularity.

Definition 6.8 ([Ben01, Definitions 4.1 and 4.3] Boundary regularity and convexity). Let $\Omega \subset \mathbb{R}^2$ be a convex open subset of $\mathbb{R}^2 \subset \mathbb{R}P^2$ and fix an arbitrary Euclidean metric d_E on \mathbb{R}^2 . We say that $\partial\Omega$ is C^α regular, for $\alpha \in (1,2]$, if for every compact subset $K \subset \partial\Omega$, there exists a constant $C_K > 0$ such that, for all $p, q \in K$, we have:

(95)
$$d_{E}(q, T_{p} \partial \Omega) \leqslant C_{K} \cdot d_{E}(q, p)^{\alpha};$$

and we say that $\partial\Omega$ is β -convex, for $\beta\in[2,\infty)$, if there exists a constant C>0 such that for all $p,q\in\partial\Omega$, we have:

(96)
$$d_{\mathsf{E}}(\mathfrak{q},\mathsf{T}_{\mathsf{p}}\partial\Omega)\geqslant C^{-1}\cdot d_{\mathsf{E}}(\mathfrak{q},\mathfrak{p})^{\beta}.$$

When Ω covers a compact surface Σ , the boundary regularity of $\partial\Omega$ may be extended to $C^{\alpha_{\Sigma}}$ regularity, for some $\alpha_{\Sigma} \in (1,2]$ [Ben01, Proposition 4.6]. Using an argument taught to us by Benoist, we show that this is also true when Σ is a finite area cusped convex projective surface:

Proposition 6.9 (Benoist-Hulin). *The boundary* $\partial\Omega$ *for* Ω *universally covering a finite area cusped convex projective surface* Σ *satisfies:*

- $C^{\alpha_{\Sigma}}$ -regularity for $\alpha_{\Sigma} \in (1,2]$,
- and β_{Σ} convexity for $\beta_{\Sigma} \in [2, \infty)$.

Proof. The proof of this fact relies on another famous metric for convex projective sets in \mathbb{R}^2 : Yau-Cheng's [CY77] Blaschke metric (also known as the affine metric) for strictly convex domains. This is a negatively curved Riemannian metric on Ω. Proposition 3.1 of [BH13] tells us that the curvature on Σ approaches a negative constant as one heads deeper into a cusp, and hence is bounded away from 0 on the entire surface. Combining this with [BH14, Corollary 4.7] then shows that Σ (and hence Ω) is Gromov-hyperbolic with respect to the Hilbert metric. Hence, by [Ben03, Corollary 1.5], the ideal boundary $\partial\Omega$ satisfies the desired $C^{\alpha_{\Sigma}}$ -regularity and β_{Σ} -convexity.

Benoist communicated to us the proof for Lemma 6.10 below, and it is a key estimate in our proof of the Birman-Series geodesic sparsity theorem for finite area convex real projective surfaces.

Lemma 6.10 (Exponentially shrinking balls). Fix a point $O \in \Omega = \tilde{\Sigma}$ and a number $R \in \mathbb{R}_{>0}$. For any $u \in \Omega$, let $B(u,R) \subset \Omega$ denote the ball of (Hilbert) radius R about u, and for any bounded set $U \subset \mathbb{R}^2$ let $diam_E(U)$ denote the Euclidean diameter of U. Then there exists a positive constant $c = c_{\Omega,O,R}$ such that

$$(97) \hspace{1cm} diam_{E}(B(u,R)) < c e^{\frac{-d(u,O)}{c}}.$$

Proof. We show that for the geodesic ray $\{tO+(1-t)p\mid 0< t\leqslant 1\}$ shooting out from O to an arbitrary boundary point $p\in\partial\Omega$, there exists a constant c(p)>0 such that for any point u along the ray,

(98)
$$\operatorname{diam}_{E}(B(\mathfrak{u},R)) < c(\mathfrak{p})e^{-\frac{d(\mathfrak{u},O)}{c(\mathfrak{p})}}.$$

In particular, we shall construct c(p) in such a way that $c(\cdot)$ is a function that continuously varies with respect to $p \in \partial\Omega$. Then, we may use the compactness of $\partial\Omega$ to take

$$(99) c_{\Omega,O,R} := \max_{p \in \partial \Omega} c(p).$$

Let us consider the radius R ball B(u, R) based at u, where u is a point along the geodesic ray from O to $p \in \partial \Omega$. By applying an affine (Euclidean) isometry on \mathbb{R}^2 , we assume without loss of generality that p is placed at the origin in \mathbb{R}^2 and that the tangent line $T_p \partial \Omega$ is the x-axis in \mathbb{R}^2 . Let $u = (x_0, y_0)$ with respect to this parametrization, and let p_1 and p_2 respectively denote the left and right intersection points of the line $y = y_0$ with $\partial \Omega$. Further let D denote the (closed) sector of Ω below $y = y_0$. (see Figure 18).

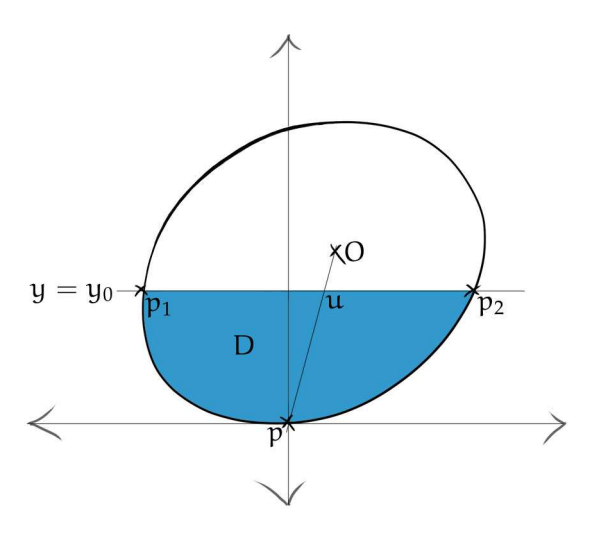


FIGURE 18. D is the shaded region below the $y = y_0$ horizontal line.

Any complete geodesic going through $\mathfrak u$ consists of two geodesic rays, at least one of which lies in D. The Euclidean length of any such geodesic ray must then be less than $diam_F(D)$, which is in turn less than:

(100)
$$diam_{E}(D \cap \{x \leq 0\}) + diam_{E}(D \cap \{x \geq 0\}) = d_{E}(p, p_{1}) + d_{E}(p, p_{2}).$$

Now invoking the β -convexity of $\partial\Omega$, we see that:

(101)
$$d_{E}(p, p_{1}) + d_{E}(p, p_{2}) \leq 2(Cy_{0})^{\frac{1}{\beta}} \leq 2(C \cdot d_{E}(u, p))^{\frac{1}{\beta}}.$$

We are now equipped to estimate the Euclidean diameter of B(u,R). The triangle inequality tells us that $diam_E(B(u,R))$ is at most 2 times the Euclidean length r of the longest geodesic segment σ joining u and the boundary of B(u,R). Such a geodesic segment lies on the unique complete geodesic in Ω joining u and some ideal boundary point $q \in D \cap \partial \Omega$. If σ lies on the geodesic ray \overline{uq} , then Equation (93) tells us that

$$(102) \hspace{1cm} R>\log\left(\frac{d_E(u,q)}{d_F(u,q)-r}\right) \text{, and hence } r<(1-e^{-R})d_E(u,q).$$

Similarly, if σ lies on the geodesic ray complementary to \overline{uq} , then

$$(103) \hspace{1cm} R> log\left(\frac{d_E(u,q)+r}{d_E(u,q)}\right) \text{, and hence } r<(e^R-1)d_E(u,q).$$

Therefore, the diameter of B(u, R) is bounded above by

$$(104) \ \ 2r < 2(e^{R} - 1)d_{E}(u, q) < 2e^{R}(d_{E}(p, p_{1}) + d_{E}(p, p_{2})) \leq 4e^{R}(C \cdot d_{E}(u, p))^{\frac{1}{\beta}}.$$

We substitute in the Hilbert length

(105)
$$d(u, O) = log\left(\frac{d_E(O, p) \cdot d_E(u, \hat{p})}{d_E(u, p) \cdot d_E(O, \hat{p}))}\right),$$

where \hat{p} is the "antipodal" ideal point to p on the opposite side of O (i.e.: p, \hat{p} and O are collinear). This then gives us $diam_E(B(u,R)) < c(p)e^{-\frac{d(u,O)}{c(p)}}$, with

$$(106) \hspace{1cm} c(\mathfrak{p}) := max \left\{ \beta, 4e^{R} \left(\frac{C \cdot d_{E}(O,\mathfrak{p}) \cdot d_{E}(\mathfrak{u},\boldsymbol{\hat{\mathfrak{p}}})}{d_{E}(O,\boldsymbol{\hat{\mathfrak{p}}})} \right)^{\frac{1}{\beta}} \right\}.$$

Since \hat{p} varies continuously with respect to p, we conclude that $c(\cdot)$ is a continuous function, as required.

- 6.4. Geodesic Sparsity for finite-area convex projective surfaces. Let Σ be a finite-area convex real projective surface, and let:
 - I_k denote the collection of complete geodesics on Σ with at most k (geometric) self-intersections (counted with multiplicity);
 - $|I_k|$ denote the subset of Σ consisting of every single point which lies on (at least one) complete geodesic in the collection I_k of geodesics with at most k self-intersections.

The goal of this subsection is to prove the following claim:

Theorem 6.11 (Geodesic sparsity). The Finsler area of $|I_k|$ is 0 and the Hausdorff dimension of $|I_k|$ is 1.

When the surface Σ is hyperbolic, the above result is referred to as the Birman–Series theorem [BS85]. They construct a descending filtration of subsets of Σ such that:

- each subset covers |I_k|,
- each subset is a union of finitely many convex geodesic quadrilaterals,
- the number of convex quadrilaterals at the k-th level of the filtration asymptotically grows as a polynomial in k,
- the Euclidean area of the quadrilaterals shrinks exponentially in k.

The polynomial growth in the number of quadrilaterals versus the exponential shrinkage their area gives us the requisite Finsler area 0 conclusion. The fact that these quadrilaterals become exponentially thin then gives the desired Hausdorff dimension 1 conclusion.

Much of the proof is topological, and we use Birman-Series' original arguments. However, we introduce the following tweaks:

• insteading of encoding geodesics as segments on a single geodesically bordered fundamental domain (such as a Ford domain), we use geodesic triangulations (Fact 6.12). This is to avoid justifying why finitely sided geodesic fundamental domains exist, to highlight the flexibility of the

Birman-Series construction and partially to use convexity to replace traditional hyperbolic geometric arguments (such as in Lemma 6.15).

• we require Lemma 6.10 to show that Hilbert radius R balls shrink uniformly exponentially as one approaches the ideal boundary.

Fact 6.12. Any finite-area strictly convex real projective surface Σ decomposes into a finite collection of (convex) geodesic triangles $\{\triangle_1, \ldots, \triangle_l\}$ glued along a finite collection of geodesic edges Γ .

For the remainder of this subsection, we fix one such collection $\{\triangle_1, ..., \triangle_l\}$ of geodesic triangles for Σ glued along Γ as described by Fact 6.12.

6.5. Polynomial growth of the number of k-diagrams.

Definition 6.13 (k-diagrams). Let J_k denote the set of geodesic arcs on Σ which:

- start and end on Γ and/or cusps,
- have at most k self-intersections.

Further let $J_k(N)$ denote the subset of geodesic arcs in J_k that are cut up into N geodesic segments by Γ . Also let $[J_k]$ denote the equivalence classes of geodesic arcs in J_k with respect to isotopies of Σ which preserve Γ as a set. Similarly define $[J_k(N)]$. We refer to the elements of $[J_k]$ as k-diagrams and the elements of $[J_0]$ as simple diagrams.

Lemma 6.14. The cardinality of $[J_k(N)]$ is bounded above by a polynomial $P_k(N)$ in N.

Proof. Every k-diagram $[\gamma] \in [J_k(N)]$ may be encoded as the ordered sequence $\sigma_1, \ldots, \sigma_N$ of elements of $[J_0(1)]$ obtained from cutting $[\gamma]$ along Γ . The key observation is that we do not need to retain the entire ordering of the sequence to recover a k-diagram: any simple diagram $[\gamma] \in [J_0(N)]$ may be completely recovered from the following data:

- the (unordered) multiset of N segments in $[J_0(1)]$ constitute $[\gamma]$;
- the starting and ending segments for $[\gamma]$ (including the direction of the starting and ending segment).

This efficient encoding is used in the original proof of the Birman–Series theorem ([BS85, Lemma 2.1]).

The consequence of this encoding is that

$$(107) \qquad \quad Card[J_0(N)] \leqslant N^2 \cdot \binom{Card[J_0(1)] + N - 1}{N - 1} =: P_0(N).$$

For general k-diagrams $[\gamma]$, we need to introduce additional data to specify the intersection loci. Since two segments may intersect at most once, the degree of freedom introduced by this intersection data is bounded above by the number of ways of designating at most k unordered pairs of segments to denote the intersections out of all possible unordered pairs of segments. Therefore:

$$(108) \qquad \quad Card[J_k(N)] \leqslant P_0(N) \cdot \left\lceil \binom{\binom{N}{2}}{0} + \ldots + \binom{\binom{N}{2}}{k} \right\rceil =: P_k(N).$$

6.6. **Topological versus geometric length.** We have so far introduced k-diagrams, which afford us topological control over geodesics with k self-intersections. We now show that the number of segments constituting a k-diagram is proportional to the Hilbert length of the segment it encodes. This promotes our topological control to geometric control.

Lemma 6.15. For any finite-area convex real projective surface Σ , there exists a positive constant $\alpha_{\Sigma,\Gamma} > 0$ so that for any complete geodesic $\hat{\gamma}$ with at most k self-intersections, the length of any geodesic subarc $\gamma \subset \hat{\gamma}$, such that γ is an element of $J_k(N)$, grows at least linearly in N for N large enough. That is: there exists an integer $N_{\Sigma,\Gamma} \geqslant 0$ such that the Hilbert length

$$\ell_{\gamma} \geqslant \alpha_{\Sigma,\Gamma} \cdot N$$
 for all $\gamma \in J_k(N)$, where $N \geqslant N_{\Sigma,\Gamma}$.

Proof of Lemma 6.15 for compact Σ . We first prove this for compact Σ . Fix a disjoint collection of embedded open balls $B_{r_i}(x_i)$ around every vertex x_i of Γ . Let $N_{\Sigma,\Gamma}$ be 3l+1 (recall here that l is the number of geodesic triangles constituting Σ) and let $\alpha_{\Sigma,\Gamma}>0$ be $\frac{\ell_{min}}{2N_{\Sigma,\Gamma}}$, where ℓ_{min} is the length of the shortest geodesic arc in $J_0(1)$ with end points on $\Gamma\setminus\cup B_{r_i}(x_i)$. The fact that ℓ_{min} is well-defined is because the subset of $J_0(1)$ with end points on $\Gamma\setminus\cup B_{r_i}(x_i)$ is a compact set. To be precise: it is the disjoint union of 3l closed (solid) rectangles. Moreover, we know that $\ell_{min}>0$ because segments have starting and ending points on distinct edges and hence cannot be of length 0.

Next observe that Γ cuts each $B_{r_i}(x_i)$ into at most 3l convex sectors. Since the intersection of convex sets is convex and hence contractible, the intersection of any contiguous subarc of γ with $B_{r_i}(x_i)$ may meet each sector at most once. This means that we may have at most 3l consecutive segments of γ lying within $B_{r_i}(x_i)$ and hence any 3l+1 consecutive segments on γ must have length strictly greater than ℓ_{min} . This in turn gives us our choice of $N_{\Sigma,\Gamma}$ and $\alpha_{\Sigma,\Gamma}$ when Σ is compact.

We now look to the situation when Σ is a (finite-area) cusped strictly convex real projective surface. We show that geodesics with k self-intersections cannot penetrate arbitrarily far into a cusp (unless it goes straight into the cusp), thus effectively reducing the analysis to being on a compact subset of the surface:

Proposition 6.16 (Cuspidal collar neighborhood). Fix a finite-area (cusped) convex real projective surface Σ and some integer $k \ge 0$. There is a compact subset $K \subset \Sigma$ which contains all (complete) compactly-supported geodesics on Σ which self-intersect at most k times when counted with multiplicity.

Remark 6.17. The complement of this compact subset K in Σ consists of annular neighborhoods around cusps and we refer to them as cuspidal collar neighborhoods — our nomenclature alludes to collar neighborhoods.

Proof. Consider a length R embedded horocycle η_R bounding an annular neighborhood C_R of a given cusp. Now choose an even shorter horocycle η_r bounding a smaller cuspidal annular neighborhood $C_r \subset C_R$, so that the minimal distance between η_r and η_R is at least $\frac{R(k+1)}{2}$ (this is always possible since C_R is infinitely long). We claim that no geodesic arc $\gamma \in J_k$ enters and then exits C_r , that is: C_r is a cuspidal collar neighborhood.

Assume otherwise that γ enters and exits C_r . The complete geodesic extension $\hat{\gamma}$ is the union of two overlapping geodesic rays $\hat{\gamma}^+$ and $\hat{\gamma}^-$ with overlap given by a subarc of γ lying within C_r and with end points on η_r . In order for the ray $\hat{\gamma}^\pm$ to lie completely within C_R , the ideal end point of any lift of $\hat{\gamma}^\pm$ would need to be the unique ideal boundary point of the horodisk in the universal cover of Σ covering C_r . This in turn characterizes $\hat{\gamma}^\pm$ as a geodesic going straight up the cusp, and therefore hitting every horocycle at most once. This is a contradiction as $\hat{\gamma}^\pm$ meets C_r in two places. Therefore, both $\hat{\gamma}^+$ and $\hat{\gamma}^-$ leave C_r at some point and hence there is a geodesic subarc $\bar{\gamma}$ of $\hat{\gamma}$ which:

- lies completely within C_R;
- has both its endpoints on η_R;
- enters and exits C_r.

Since $\bar{\gamma}$ joins η_r and η_R along two subarcs, it has length at least R(k+1). On the other hand, the geodesic arc $\bar{\gamma}$ is (endpoint-fixing) homotopy equivalent to a horocyclic path along η_R which wraps around η_R at most k times (this can be shown by unwrapping C_R to a k-fold cover of C_R that undoes the self-intersections of $\bar{\gamma}$). This in turn means that the length of $\bar{\gamma}$ must be strictly less than R(k+1), leading to a contradiction. Therefore, no geodesic arc $\gamma \in J_k$ which extends to a complete geodesic $\hat{\gamma}$ with at most k self-intersections may enter C_r .

We now return to the proof of Lemma 6.15, but addressing the cusped case.

Proof of Lemma 6.15 for cusped Σ. Finally, we complete our proof for the cusped case as follows: fix a horocyclic neighborhood C_r for each cusp on Σ and take $N_{\Sigma,\Gamma}=1$ and $\alpha_{\Sigma,\Gamma}>0$ to be the length (in the closed interval $[0,\infty]$ rather than $\mathbb{R}_{>0}$) of the shortest geodesic arc in $J_0(1)$ with endpoints outside of the horocyclic regions. Again, such a length exists due to compactness and is finite. These choices for constants clearly work because every segment on γ lies outside of C_r and hence must be at least of length $\alpha_{\Sigma,\Gamma}$.

6.7. **Geodesic sparsity: area** 0. We are now prepared to prove the geodesic sparsity theorem for finite-area convex projective surfaces. Fix a fundamental domain $F \subset \tilde{\Sigma} =: \Omega$ made up of lifts of the triangles $\Delta_1, \ldots, \Delta_l$ decomposing Σ . Represent Ω as a subset of $\mathbb{R}^2 \subset \mathbb{R}P^2$, and let \overline{F} denote the closure of F in \mathbb{R}^2 . Define the following collection of geodesic arcs

$$\hat{I}_k := \{ \sigma = \tilde{\gamma} \cap \triangle_i \mid \text{ for some } i = 1, \dots, l \text{ and where } \tilde{\gamma} \text{ is a lift of } \gamma \in J_k \},$$

and further define $|\hat{I}_k| \subset \overline{F}$ to be the collection of points lying on geodesic arcs σ in \hat{I}_k . Our goal is to show that $|\hat{I}_k| \cap F$ has zero Finsler area. However, since Finsler area on Ω is definitionally in the same measure class as the Lebesgue measure, we see that we just need to show that $|\hat{I}_k|$ occupies zero Euclidean area.

Proof of Theorem 6.11 for compact Σ – area 0. We first consider the case when Σ is compact. For each $N \geqslant N_{\Sigma,\Gamma}$, we partition $\hat{1}_k$ using the fact that any geodesic arc^1 σ is uniquely expressible as the middle (i.e.: $(N+1)^{st}$) segment of a lift of some representative of $[\gamma] \in J_k(2N+1)$. This gives us a partition of $\hat{1}_k$ into at most $P_k(2N+1)$ sets.

 $^{^1}$ We may ignore the case when σ is a vertex of F as it does not affect the measure or the Hausdorff dimension of $|\hat{1}_k|$.

We next show that the Euclidean area occupied by all the lifts of representatives of $[\gamma] \in [J_k(2N+1)]$ with the middle segment in \overline{F} is exponentially decreasing in N. Consider an arbitrary lift γ of a representative of $[\gamma]$ positioned so that its middle segment is in \overline{F} and let the endspoints of γ lie on $\overline{F'}$ and $\overline{F''}$ — two deck transformation translates of the fundamental domain \overline{F} . By the unique path lifting property, every such γ necessarily ends on the same $\overline{F'}$ and $\overline{F''}$ pair. In particular, this means that the union of every such representative of $[\gamma]$ is contained within the convex hull of $F' \cup F''$. We know from Lemma 6.15 that both $\overline{F'}$ and $\overline{F''}$ are at least distance $\alpha_{\Sigma,\Gamma}N$ away from F. We now use this fact to control the Euclidean area for the convex hull of $F' \cup F''$.

Let O be an arbitrary point on the interior of F. Since $\bar{\mathsf{F}}$ is compact, for some R>0 the domain $\bar{\mathsf{F}}\subset \mathsf{B}(0,R)$. The domains $\bar{\mathsf{F}'}$ and $\bar{\mathsf{F}''}$ are deck transform translates of $\bar{\mathsf{F}}$ and the corresponding translated points $x'\in \mathsf{F}'$ and $x''\in \mathsf{F}''$ of $O\in \mathsf{F}$ satisfy that $d(x',O),d(x'',O)>\alpha_{\Sigma,\Gamma}\mathsf{N}$. Therefore, the Euclidean diameters of F' and F'' must both be less than $ce^{\frac{-\alpha_{\Sigma,\Gamma}\mathsf{N}}{c}}$. This in turn means that the convex hull of $\mathsf{F}'\cup\mathsf{F}''$ may be covered by an Euclidean rectangle of width $ce^{\frac{-\alpha_{\Sigma,\Gamma}\mathsf{N}}{c}}$ and length $diam_{\mathsf{E}}(\Omega)$. We absorb $diam_{\mathsf{E}}(\Omega)$ into c and ignore it henceforth.

We next note that the convex hull of $F' \cup F''$ necessarily covers every representative geodesic segment in $[\gamma] \in [J_k(2N+1)]$. Since there are fewer than $P_k(2N+1)$ homotopy classes $[\gamma]$ constituting $[J_k(2N+1)]$ and each class is covered by a rectangle of area $ce^{\frac{-\alpha_{\Sigma,\Gamma}N}{c}}$, this means that the set $|\hat{I}_k|$ has Euclidean area less than $P_k(2N+1) \cdot ce^{\frac{-\alpha_{\Sigma,\Gamma}N}{c}}$. Since N may be set to be arbitrarily large, this means that $|\hat{I}_k|$ has zero Euclidean area and hence zero Finsler area. Finally observe that $|\hat{I}_k|$ is the lift of $|I_k|$ to \overline{F} (except for perhaps finitely many closed geodesics lying completely on Γ) and hence $|I_k| \cap F$ has zero Finsler area.

Proof of Theorem 6.11 for cusped Σ – area 0. We now turn to the case when Σ is non-compact, that is: we are dealing with a cusped convex real projective surface. Given a geodesic segment $\sigma \in \hat{I}_k$, when we try to geodesically extend σ using deck transform translates of segments in \hat{I}_k , one of the following three things occurs:

- (1) σ can be extended by N segments in both directions, this produces a geodesic arc in $J_k(2N+1)$;
- (2) σ can be extended by N segments in one direction and hits a cusp in the other direction, this produces an arc in $J_k(M)$, for $M \leq 2N$;
- (3) σ cannot be extended by N segments in either direction and hits a cusp in the both directions, this produces an arc in $J_k(M)$, for $M \leq 2N-1$;

This behavioral classification allows us to partition \hat{I}_k into the following three classes of objects:

- (1) σ is the middle (i.e.: $(N+1)^{st}$) segment of a lift of some representative of $[\gamma] \in J_k(2N+1)$;
- (2) σ is a segment of a lift of some representative γ of $[\gamma] \in J_k(M)$, for $M \le 2N$, where γ is a geodesic ray (i.e.: one of the ends of γ is a cuspidal ideal point) and σ is the i^{th} segment, for $1 \le i \le M (N+1)$, indexed from the cuspidal end;

(3) σ is a segment of a lift of the unique representative γ of $[\gamma] \in J_k(M)$, for $M \leqslant 2N-1$, where γ is a bi-infinite geodesic (i.e.: both end points of γ are cuspidal ideal points) and σ has index (strictly) less than N+1 indexed from both ends of γ .

Case 1 is identical to the previous compact Σ analysis, and each homotopy class $[\gamma]$ may be covered by a Euclidean rectangle of Euclidean area $ce^{\frac{-\alpha_{\Sigma,\Gamma}N}{c}}$. For Case 2, note that one end of γ is a single cuspidal ideal point on $\partial\Omega$, and therefore $[\gamma]$ may be covered by a Euclidean trapezium with area less than $ce^{\frac{-\alpha_{\Sigma,\Gamma}N}{c}}$. Case 3 concerns bi-infinite geodesics joining two cuspidal ideal points and may be covered by a single line. This means that $|\hat{1}_k|$ may be covered by a finite collection of quadrilaterals (and lines) of total area less than

$$(109) \ ce^{\frac{-\alpha_{\Sigma,\Gamma}N}{c}}(P_k(2N+1) + P_k(2N) + \ldots + P_k(1)) < ce^{\frac{-\alpha_{\Sigma,\Gamma}N}{c}} \cdot N \cdot P_k(2N+1).$$

Once again, by taking N to be arbitrarily large, we see that the Euclidean area of $|\hat{I}_k|$ is zero and hence Finsler area of $|I_k|$ is zero.

6.8. **Geodesic sparsity: Hausdorff dimension** 1. Finally, we show that $|I_k|$, or equivalently \hat{I}_k , has Hausdorff dimension 1.

Proof of Theorem 6.11 – *Hausdorff dimension* 1. Consider Ω equipped with the Hilbert (Finsler) metric d in comparison with Ω endowed with the Euclidean metric d_E (but regarded as a Finsler manifold). The Finsler metric for (Ω,d) is a C^1 rescaling of the "Finsler metric" for (Ω,d_E) due to the dependence on the boundary smoothness (which we know is at least C^1). This means that, for any (possibly non-compact) subset K of a compact subset of Ω , the identity map between (Ω,d) and (Ω,d_E) restricts to a bi-Lipschitz map between (K,d) and (K,d_E) . Combined with the fact that Hausdorff dimension is preserved under bi-Lipschitz maps, this means that when Σ (and hence \overline{F}) is compact the Hausdorff dimension of $(|I_k|,d)$ and $(|\hat{I}_k|,d_E)$ are the same. Combined with the further fact that the Hausdorff dimension is preserved with respect to taking countable unions of sets with the same Hausdorff dimension, the equivalence in Hausdorff dimension between $(|I_k|,d)$ and $(|\hat{I}_k|,d_E)$ is true when Σ is cusped.

We have reduced our Hausdorff dimension derivation problem to that of $(|I_k|,d_E)$. We first show that the $(1+\varepsilon)$ -dimensional Hausdorff content of $(|I_k|,d_E)$ is 0 for every $\varepsilon>0$. Recall from earlier in this proof that for every $N\geqslant N_{\Sigma,\Gamma}$, there we may cover $|I_k|$ with fewer than $N\cdot P_k(2N+1)$ Euclidean rectangles of length $diam_E(\Omega)$ and width $ce^{\frac{-\alpha_{\Sigma,\Gamma}N}{c}}$. Each such rectangle may be covered by $\left\lceil\frac{diam_E(\Omega)}{ce^{\frac{-\alpha_{\Sigma,\Gamma}N}{c}}}\right\rceil$ Euclidean balls of radius $\frac{3}{2}ce^{\frac{-\alpha_{\Sigma,\Gamma}N}{c}}$. The $(1+\varepsilon)$ -dimensional Hausdorff content of $(|\hat{I}_k|,d_E)$ is 0, because:

$$(110) \qquad \lim_{N\to\infty} N\cdot P_k(2N+1)\cdot \left\lceil \frac{diam_E(\Omega)}{ce^{\frac{-\alpha_{\Sigma,\Gamma}N}{c}}}\right\rceil \cdot \left(\frac{3}{2}ce^{\frac{-\alpha_{\Sigma,\Gamma}N}{c}}\right)^{1+\varepsilon} = 0.$$

This means that the Hausdorff dimension of $(|I_k|, d)$ is at most 1. On the other hand, since $|I_k|$ contains geodesic arcs, it necessarily has Hausdorff dimension at least 1.

7. McShane identities for convex projective surfaces and applications

We are now well-placed to prove our McShane identity for finite-area convex projective surfaces. We first consider a half-pants summation version of the McShane identity coming from Proposition 4.4 combined with Equation (3.7) of [Hua14].

7.1. McShane identity for finite-area convex projective surfaces.

Theorem 7.1. Let $\rho : \pi_1(S_{g,m}) \to PGL_3(\mathbb{R})$ be a positive representation with unipotent boundary monodromy and let p be a distinguished cusp on $S_{g,m}$. Then,

(111)
$$\sum_{(\gamma,\gamma_{\mathfrak{p}})\in\overrightarrow{\mathcal{H}}_{\mathfrak{p}}}\frac{B_{1}(\gamma,\gamma_{\mathfrak{p}})}{1+e^{\ell_{1}(\gamma)+\tau(\gamma,\gamma_{\mathfrak{p}})}}=1.$$

Proof. We begin with an overview of the general strategy for proving McShane's identity in the hyperbolic case. For our arguments we fix an arbitrary point $(\rho, \bar{\xi}) \in \mathcal{A}_{\mathrm{SL}_n, S_{q,m}}(\mathbb{R}_{>0})$ with $\xi = \pi \circ \bar{\xi}$.

- (1) decomposing the length 1 horocycle η based at cusp p into a countable collection of open horocylic intervals referred to as *gaps*, as well as a complementary set consisting of a Cantor set and a countable set;
- (2) observing that the Birman-Series geodesic sparsity theorem ensures that the latter complementary set is measure 0;
- (3) computing the horocyclic length measure of each gap interval in the former collection via the position of two ideal boundary points (which we denote by q₀ and q₁) of the two complete geodesics respectively connecting p and the two end points of the given horocyclic gap interval (see Figure 19));
- (4) summing the measures of these gaps gives the measure of the total horocycle (i.e.: length 1). Using the fact that the horocyclic gaps are in 2 to 1 correspondence with pairs of half-pants containing cusp p, we index our McShane identity over \mathcal{H}_p .

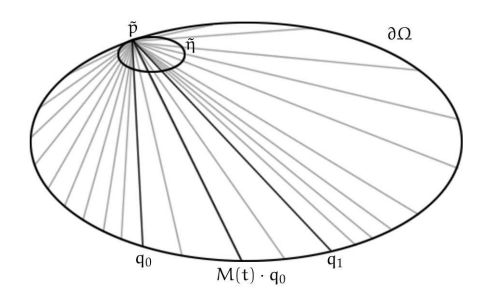


Figure 19. The lighter grey lines specify a C^1 identification between $\tilde{\eta}$ and $\partial\Omega - \{\tilde{p}\}$.

The strategy of proof for convex projective surfaces is essentially the same, but with the following adjustments for each step:

(1) instead of decomposing the length of η , we induce a C^1 measure on η obtained by representation theoretically interpreting Goncharov-Shen (partial) potentials as a *Goncharov-Shen potential measure*;

- (2) we use our generalization of the Birman-Series theorem (Theorem 6.11) to ensure that the gap-complement set has measure 0, with respect to the aforementioned Goncharov–Shen potential measure;
- (3) we compute the Goncharov–Shen potential measure for each of these gaps in Section 5 using the data of sequences of flags;
- (4) this step remains largely unchanged, but it is worth noting that the two summands associated to each pair of half-pants are generally not equal, in contrast with what occurs in the hyperbolic case. The richness of convex real projective structures forces this symmetry-breaking. We resolve this by replacing \mathcal{H}_p with the 2:1 covering set $\overrightarrow{\mathcal{H}}_p$ (Definition 1.16).

We now go through each of these steps, furnishing the necessary details.

Step 1. Let $\tilde{p} \in \partial \Omega$ be a lift of the cusp p such that $\xi_{\rho}(\tilde{p}) = \xi(p)$ and the decorated flag $^2X_{\tilde{p}} = \bar{\xi}(p)$ is used to define the A-coordinates for ρ . Now let $q_0 \in \partial \Omega$ be an arbitrarily chosen ideal point distinct from \tilde{p} and let $q_1 \in \partial \Omega$ be the point on $\partial \Omega$ obtained from translating q_0 by a single iteration of the monodromy matrix action of the loop around p. We know from Fact 4.1 that there is a unique unipotent matrix M that takes $(X_{\tilde{p}}, \xi_{\rho}(q_0))$ to $(X_{\tilde{p}}, \xi_{\rho}(q_1))$. When expressed with respect to any basis for $X_{\tilde{p}}$, the matrix M takes the form:

(112)
$$M := \begin{pmatrix} 1 & P_2 & * \\ 0 & 1 & P_1 \\ 0 & 0 & 1 \end{pmatrix}.$$

More generally, let M(t) denote the path of unipotent matrices

(113)
$$M(t) := \begin{pmatrix} 1 & m_{12}(t) & m_{13}(t) \\ 0 & 1 & tP_1 \\ 0 & 0 & 1 \end{pmatrix},$$

such that the parametrized path $M(t) \cdot q_0$ traces out the interval $[q_0, q_1]$ on $\partial\Omega$ in such a way that M(t) takes the tangent space $T_{q_0}\partial\Omega$ to $T_{M(t)\cdot q_0}\partial\Omega$. Let η be the length 1 horocycle based at p, and consider the homemorphism between the lifted horocycle $\tilde{\eta}$ based at \tilde{p} and the boundary $\partial\Omega$ given by geodesic projection from \tilde{p} (see Figure 19).

This lets us pullback the $M(t) \cdot q_0$ parametrization of $\partial \Omega - \{\tilde{p}\}$ onto η . Notice that this is a C^1 reparametrization of η (with respect to horocyclic length) because $\partial \Omega$ is C^1 -smooth. However, the $t \in [0,1]$ parameter precisely parametrizes the length of partial potentials (divided by P_1) and therefore this C^1 reparametrized length of η induces a *Goncharov–Shen measure* on η in the same measure class as horocyclic length. We decompose this probability measure to obtain McShane's identity.

As a final part of the first step, we show that η naturally decomposes into a countable union of open sets, a Cantor set $\mathfrak C$ and well as a countable set $\mathfrak A$. The structure of this decomposition is well-understood in the Fuchsian case ([McS91, McS98, Mir07a, Hua18]), and induces a topological partition of $\mathfrak d_\infty\pi_1(S)\setminus\{\tilde{\mathfrak p}\}$ via identification with a horocycle lift $\tilde{\eta}$ based at $\tilde{\mathfrak p}$. Since $\mathfrak d_\infty\pi_1(S)\cong\mathfrak d\Omega$ is independant of the geometric structure Σ imposes on S, this decomposition applies also to horocycles on convex projective surfaces. In particular, the interpretation of

²In fact, any decorated flag over $\xi_{\rho}(\tilde{p})$ suffices.

 $\mathfrak{A} \cup \mathfrak{C}$ as the collection of points on η which lie on simple (possibly non-closed) geodesics still applies.

Step 2. We showed in Theorem 6.11 that the set of simple geodesics occupies zero area on Σ . This implies that the set of points on an annular neighborhood of η which lie on simple geodesics occupies zero area. Since the annular neighborhood of takes the form of a product of $\eta \times (-\varepsilon, \varepsilon)$ and the Finsler area of Σ is in the same measure class as the product measure on this annular neighborhood, this tells us that $\mathfrak{A} \cup \mathfrak{C}$ occupies horocyclic length measure on η . Since the Goncharov–Shen potential measure on η is equal to the horocyclic length measure weighted by a \mathbb{C}^1 function, the contribution of $\mathfrak{A} \cup \mathfrak{C}$ to the Goncharov–Shen potential measure must be 0. This allows us to carry out Step 4 as per usual.

Step 3. We make the observation that the gap Goncharov–Shen potential measure computed in Section 5 depends purely on the geometry of the pair of half-pants (γ, γ_p) bounding the horocyclic gap. Therefore, the gap has measure:

(114)
$$\frac{B_1(\gamma,\gamma_p)}{1+e^{\ell_1(\gamma)+\tau(\gamma,\gamma_p)}}.$$

Step 4. As noted previously in step 2, the complement of the gap intervals on η contribute zero measure to the Goncharov–Shen potential measure, and thus the sum of the measures of all the gap intervals comes to 1. In [McS91], we see that there is a 4:1 correspondence between the collection of such gap intervals and the set of (unoriented) bi-infinite ideal geodesics with both ends up p. Two of these intervals lie on each of the two pairs of half-pants lying on each side of the aforementioned ideal geodesic (Figure 15), which creates a 2:1 correspondence between the gaps and the collection of half-pants on Σ based at p. Finally, introducing orientation on the boundaries of half-pants gives us the bijection between the set of gaps and $\overrightarrow{\mathcal{H}}_p$.

7.2. Simple spectral discreteness.

Definition 7.2 (simple spectra). Let Σ be a finite-area convex projective surface Σ with monodromy representation $\rho: \pi_1(S) \to PGL_n(R)$, and let $\vec{\mathfrak{C}}(S)$ denote the collection of oriented simple closed geodesics on S. We define the following spectra:

(1) the simple ℓ_i -spectrum:

$$\left\{\ell_{i}^{\rho}(\gamma)\mid\gamma\in\vec{\mathbb{C}}(S)\right\}$$
,

(2) the simple largest-eigenvalue spectrum:

$$\left\{\lambda_1(\rho(\gamma)) \mid \gamma \in \vec{\mathcal{C}}(S)\right\}$$
,

(3) and the simple (Hilbert) length spectrum:

$$\left\{\ell^\rho(\gamma) \mid \gamma \in \vec{\mathfrak{C}}(S)\right\}.$$

Note here that each spectra is (possibly) a multiset, that is: repeated values coming from distinct simple closed geodesics are counted as distinct elements in the spectrum.

Our goal in this subsection is to prove that the above simple spectra are discrete for any finite-area convex projective surface Σ . Our proof relies on the McShane identity (Theorem 7.1). Let $\overrightarrow{\mathcal{H}}_p(\gamma)$ denote the subset of $\overrightarrow{\mathcal{H}}_p$ consisting of all halfpants with γ as its oriented cuff.

Lemma 7.3. Given a positive representation ρ with unipotent boundary monodromy around p, there is a universal constant $b^{\rho} > 0$ such that for every oriented simple closed curve $\gamma \in \vec{\mathfrak{C}}(S)$, there exists an embedded pair of half-pants $(\gamma, \gamma_p) \in \vec{\mathfrak{H}}_p(\gamma)$ such that:

(115)
$$B_1^{\rho}(\gamma, \gamma_p) \geqslant b^{\rho}.$$

Proof. Much like the proof of the boundedness of triple ratios (Theorem 1.5), we rely on a compactness argument. Fix an arbitrarily chosen cusped hyperbolic surface Σ with topological type S. The length 1 horocycle η_p around cusp p separates Σ into two connected components: an (open) annular cuspidal neighborhood $C_p \subset \Sigma$ as well as a (closed) homotopy retract $\Sigma^{(p)} := \Sigma - C_p$. Also let $\Sigma^{\geqslant 1} \subset \Sigma^{(p)} \subset \Sigma$ denote the compact subsurface of Σ obtained from truncating every cusp of Σ at its length 1 horocycle.

Consider the following subset of the unit tangent bundle $T^1\Sigma$: (116)

$$\Xi := \left\{ (x, \nu) \in T^1 \Sigma \, \middle| \begin{array}{l} x \text{ is a point lying in } \Sigma^{\geqslant 1} \text{ and the geodesic ray } \sigma_{(x, \nu)} \\ \text{shooting out from } x \text{ with initial vector } \nu \text{ is simple,} \\ \text{approaches the cusp p, and the arc } \sigma_{(x, \nu)} \cap \Sigma^{\geqslant 1} \\ \text{realizes the distance between } x \text{ and } \eta_p \end{array} \right\}$$

We now show that Ξ is a closed subset of the restricted unit tangent bundle $\mathsf{T}^1\Sigma^{\geqslant 1}$ of $\mathsf{T}^1\Sigma$ to $\Sigma^{\geqslant 1}$, and is hence compact. Consider a sequence $\{(x_n, \nu_n) \in \Xi\}$ which converges to a point (x_∞, ν_∞) . Since $\Sigma^{\geqslant 1}$ is a closed subset of Σ , the limiting base point x_∞ must lie on $\Sigma^{\geqslant 1}$. Next, to show that the geodesic ray $\sigma_{(x_\infty, \nu_\infty)}$ approaches the cusp \mathfrak{p} , choose a fundamental domain Γ for Σ containing a lift \tilde{x}_∞ of x_∞ in the interior. The lifts to Γ of a sufficiently high subscript tail of the sequence $\{(x_n, \nu_n)\}$ necessarily all induce rays which shoot into the same lift $\tilde{\mathfrak{p}}$ of the cusp \mathfrak{p} , and hence $\sigma_{(x_\infty, \nu_\infty)}$ also shoots into \mathfrak{p} . Finally observe that the distance realization property stated for Ξ is also a closed condition, and hence Ξ is a compact set.

Now, since $\sigma_{(x,\nu)}$ shoots into cusp p, the corresponding subset to Ξ in

$$Tri(S) \cong Tri(\Sigma) \cong T^1\Sigma$$

is a compact subset with every point of the form $[\tilde{p},b,c]_S$, where \tilde{p} is a lift of p. In particular, this means that the (strictly) positive function $B_1^{\rho}(\cdot)$ given in Definition 4.13 is well-defined and continuous on a compact set and achieves its minimum. We denote this minimum by $b^{\rho}>0$.

Now, given an arbitrary oriented (essential) simple closed curve $\gamma \in \vec{\mathbb{C}}(S)$, let γ denote its geodesic realization on Σ . Further let $x_0 \in \gamma$ be the point on γ closest to η_p , let σ be one of the geodesic arcs realizing the distance between x_0 and η_p , and let v_0 denote the initial vector of σ . By construction, the geodesic ray $\sigma_{(x_0,v_0)}$ contains σ . Since σ is a distance minimizing arc, it must meet η_p perpendicularly and hence $\sigma_{(x_0,v_0)}$ shoot up straight into cusp p after passing η_p . Moreover, the arc σ must also be simple (so as to be distance minimizing), and hence $\sigma_{(x_0,v_0)}$ is the concatenation of σ and a simple geodesic ray which lies in C_p (and hence cannot intersect σ) and is thus simple. Therefore, we see that $(x_0,v_0) \in \Xi$. We denote its corresponding point in Tri(S) by $[\tilde{p},b_0,c_0]_S$. Let $(\bar{\gamma},\bar{\gamma}_p) \in \mathcal{H}_p$ denote the unique embedded pair of half pants on S containing $\bar{\gamma} \cup \sigma_{(x_0,v_0)}$ (Figure 20).

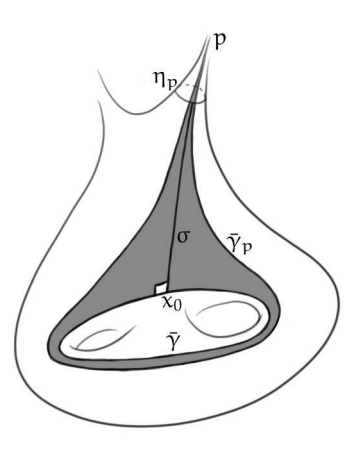


Figure 20. The pair of half-pants $(\bar{\gamma}, \bar{\gamma}_p)$ is the unique embedded pair of half-pants that contains $\bar{\gamma}$ and $\sigma(x_0, \nu_0) \supset \sigma$.

We also know that σ is perpendicular to γ , and by possibly replacing \tilde{p} with a different lift of p, the point b_0 must be of one of the two fixed points of $\rho(\gamma)$. This in turn means that $B_1^{\rho}(\gamma,\gamma_p)>B_1^{\rho}([\tilde{p},b_0,c_0]_S)>b^{\rho}$, thereby demonstrating the desired lower bound.

Theorem 7.4. Let $\rho: \pi_1(S) \to PGL_3(\mathbb{R})$ be a positive representation with unipotent boundary monodromy. Then the simple ℓ_i -spectrum, the simple largest eigenvalue spectrum and the simple length spectrum for ρ are all discrete.

Proof. We begin by rearranging the inequality (Theorem 5.9) given by McShane's identity to obtain the following expression:

(117)
$$\sum_{\gamma \in \overrightarrow{\mathcal{C}}(S)} \sum_{(\gamma, \gamma_{\mathfrak{p}}) \in \overrightarrow{\mathcal{H}}_{\mathfrak{p}}(\gamma)} \frac{B(\gamma, \gamma_{\mathfrak{p}})}{1 + e^{\ell_1(\gamma) + \tau(\gamma, \gamma_{\mathfrak{p}})}} \leqslant 1.$$

Invoking Theorem 3.4 to assert that there exists some τ_{max}^S such that $\tau(\gamma,\gamma_p)\leqslant \tau_{max}^S$, we obtain:

(118)
$$\sum_{\gamma \in \vec{\mathcal{C}}(S)} \left(\frac{1}{1 + e^{\ell_1(\gamma) + \tau_{\max}^S}} \sum_{(\gamma, \gamma_p) \in \vec{\mathcal{H}}_p(\gamma)} B(\gamma, \gamma_p) \right) \leqslant 1$$

Further invoking Lemma 7.3 to uniformly bound

(119)
$$\sum_{(\gamma,\gamma_{\mathfrak{p}})\in \overrightarrow{\mathcal{H}}_{\mathfrak{p}}(\gamma)} B_{1}(\gamma,\gamma_{\mathfrak{p}}) > \sup_{(\gamma,\gamma_{\mathfrak{p}})\in \overrightarrow{\mathcal{H}}_{\mathfrak{p}}(\gamma)} B(\gamma,\gamma_{\mathfrak{p}}) \geqslant b^{\rho}.$$

Hence:

(120)
$$\sum_{\gamma \in \overrightarrow{\mathcal{C}}(S)} \frac{b^{\rho}}{1 + e^{\ell_1(\gamma) + \tau_{\text{max}}^S}} \leqslant 1.$$

This suffices to ensure the discreteness of the simple ℓ_1 -spectrum, which is in turn equivalent to the discreteness of the simple ℓ_2 -spectrum because

$$e^{\ell_1(\gamma)} = \frac{\lambda_1(\rho(\gamma))}{\lambda_2(\rho(\gamma))} = \frac{\lambda_2(\rho(\gamma^{-1}))}{\lambda_3(\rho(\gamma^{-1}))} = e^{\ell_2(\gamma^{-1})}.$$

Furthermore, the fact that

$$\frac{\lambda_1}{\lambda_2} < \frac{\lambda_1}{\lambda_2} \cdot \frac{1}{\lambda_3} = \lambda_1^2$$

then ensures that the simple largest-eigenvalue spectrum is also discrete; the fact that the Hilbert length of a geodesic γ satisfies

$$\ell(\bar{\gamma}) = \ell(\gamma) = \ell_1(\gamma) + \ell_1(\gamma^{-1})$$

then suffices to ensure that the simple length spectrum is also discrete.

7.3. **The collar lemma.** As a first application of our McShane identity, we establish a collar lemma. This is, in some sense, slghtly premature as we also require our McShane identity for convex real projective 1-holed tori, which is established in Section 8. Note also that we do not need the full force of the McShane identity, and only require the inequality.

Lemma 7.5. Consider an arbitrary finite-area marked cusped convex projective 1-cusped torus $\Sigma_{1,1}$ with monodromy representation ρ . For distinct (oriented) simple closed geodesics $\beta, \gamma \in \stackrel{\circ}{\mathbb{C}}(\Sigma_{1,1})$, let

$$\begin{split} u_1 &= T(\beta) \frac{\lambda_1(\rho(\beta))}{\lambda_2(\rho(\beta))}, \ u_2 = T(\beta^{-1}) \frac{\lambda_1(\rho(\beta^{-1}))}{\lambda_2(\rho(\beta^{-1}))}, \\ u_3 &= T(\gamma) \frac{\lambda_1(\rho(\gamma))}{\lambda_2(\rho(\gamma))}, \ u_4 = T(\gamma^{-1}) \frac{\lambda_1(\rho(\gamma^{-1}))}{\lambda_2(\rho(\gamma^{-1}))}. \end{split}$$

Then, for any configuration of $\{i, j, k, l\} = \{1, 2, 3, 4\}$, we have:

$$\left((u_{i}u_{j})^{\frac{1}{2}}-1\right) \cdot \left((u_{k}u_{l})^{\frac{1}{2}}-1\right) >4.$$

Proof. By Theorem 5.2, we have:

$$(122) \qquad \sum_{s=1}^4 \frac{1}{1+\mathfrak{u}_s} < \sum_{\delta \in \overrightarrow{\mathfrak{C}}_{1,1}} \frac{1}{1+\mathsf{T}(\delta) \frac{\lambda_1(\rho(\delta))}{\lambda_2(\rho(\delta))}} \leqslant 1.$$

Multiplying both sides by $\prod (1 + u_s)^{-1}$ and rearranging the resulting terms, we obtain:

(123)
$$3 + 2\sum_{i=s}^{4} u_s + \sum_{s < t} u_s u_t < \prod_{s=1}^{4} u_s.$$

Further adding $(1 - u_i u_j - u_k u_l)$ to both sides, we get:

$$(124) (2 + u_i + u_i)(2 + u_k + u_1) < (1 - u_i u_i)(1 - u_k u_1).$$

By the algebraic mean-geometric mean inequality, we obtain:

$$(125) (2+2(u_iu_j)^{\frac{1}{2}})(2+2(u_ku_l)^{\frac{1}{2}})<(1-u_iu_j)(1-u_ku_l),$$

and hence:

$$\left((u_iu_j)^{\frac{1}{2}} - 1 \right) \cdot \left((u_ku_l)^{\frac{1}{2}} - 1 \right) > 4.$$

Recall that for an oriented curve β , we use $\bar{\beta}$ to denote the same curve without orientation.

Proposition 7.6. Given any finite area convex projective structure Σ on $S_{1,1}$, the Hilbert lengths of any two distinct unoriented simple closed geodesics $\bar{\beta}$ and $\bar{\gamma}$ satisfy the following inequality:

(127)
$$(e^{\frac{1}{2}\ell(\bar{\beta})} - 1)(e^{\frac{1}{2}\ell(\bar{\gamma})} - 1) > 4.$$

Proof. The finite area condition means that Σ either has unipotent or loxodromic boundary monodromy. We first consider the unipotent case. Recall from Equation (76) that

$$\begin{split} T(\delta) &= T(\tilde{p},\delta\tilde{p},\delta^+) = \lim_{k\to\infty} \frac{\alpha_1 b_{k-1} c_k}{\alpha_2 c_{k-1} b_k} = \frac{\alpha_1}{\alpha_2} \lambda_2(\rho(\delta)), \text{ and} \\ T(\delta^{-1}) &= T(\tilde{p},\delta^{-1}\tilde{p},\delta^-) = \lim_{k\to-\infty} \frac{\alpha_2 c_{k-1} b_k}{\alpha_1 b_{k-1} c_k} = \frac{\alpha_2}{\alpha_1} \lambda_2(\rho(\delta^{-1})). \end{split}$$

Thus

(128)
$$\mathsf{T}(\mathsf{p},\delta\mathsf{p},\delta^+)\cdot\mathsf{T}(\mathsf{p},\delta^{-1}\mathsf{p},\delta^-)=1.$$

This means that the product terms u_1u_2 and u_3u_4 satisfy

$$u_1u_2 = \frac{\lambda_1(\rho(\beta))}{\lambda_3(\rho(\beta))} = e^{\ell(\tilde{\beta})}$$
 and $u_3u_4 = \frac{\lambda_1(\rho(\gamma))}{\lambda_3(\rho(\gamma))} = e^{\ell(\tilde{\gamma})}$,

and hence we obtain Equation (127) as desired.

We now turn to the case where the boundary monodromy of Σ is loxodromic. For any simple closed geodesic δ on Σ , let $\mu_1^\delta, \mu_2^\delta \in \overrightarrow{\mathcal{H}}_\alpha$ denote two boundary-parallel pairs of half-pants which have δ as its oriented cuff such that their underlying half-pants are distinct. Recall Definition 8.10, we have

(129)
$$R_1(\mu_1^{\delta}) + R_2(\mu_2^{\delta}) = 1.$$

We consider two gap terms in Theorem 8.17 associated to one pair of half-pants. We require the following fact:

(130)
$$XY > 1 \Rightarrow (1 + X^2)^{-1} + (1 + Y^2)^{-1} > 2(1 + XY)^{-1}.$$

By taking $X=e^{-R_1(\mu_i^\delta)L+\ell_1(\delta)+\tau(\delta)}$ and $Y=e^{R_1(\mu_i^\delta)L+\ell_1(\delta^{-1})+\tau(\delta^{-1})}$, we obtain:

$$(131) \qquad \frac{2R_1(\mu_{i}^{\delta})}{1+e^{\frac{1}{2}\ell(\bar{\delta})}} < \frac{R_1(\mu_{i}^{\delta})e^{R_1(\mu_{i}^{\delta})L}}{e^{R_1(\mu_{i}^{\delta})L}+e^{\ell_1(\delta)+\tau(\delta)}} + \frac{R_1(\mu_{i}^{\delta})e^{-R_1(\mu_{i}^{\delta})L}}{e^{-R_1(\mu_{i}^{\delta})L}+e^{\ell_1(\delta^{-1})+\tau(\delta^{-1})}}.$$

The above inequality in turn leads to the following comparison: for L > 0,

(132)

$$\frac{2R_1(\mu_i^\delta)L}{1 + e^{\frac{1}{2}\ell(\delta)}} < log\left(\frac{e^{R_1(\mu_i^\delta)L} + e^{\ell_1(\delta) + \tau(\delta)}}{1 + e^{\ell_1(\delta) + \tau(\delta)}}\right) + log\left(\frac{1 + e^{\ell_1(\delta^{-1}) + \tau(\delta^{-1})}}{e^{-R_1(\mu_i^\delta)L} + e^{\ell_1(\delta^{-1}) + \tau(\delta^{-1})}}\right).$$

To see this, note that Equation (132) is an obvious equality when L=0 and its derivative with respect to L satisfies Equation (131) for L>0. Further replacing L

with the simple root length $\ell_1(\alpha)$ of the boundary α of Σ , we see that:

$$(133) \qquad \frac{2R_1(\mu_i^{\delta})}{1+e^{\frac{1}{2}\ell(\delta)}} < \frac{1}{\ell_1(\alpha)}\log\left(\frac{e^{R_1(\mu_i^{\delta})\ell_1(\alpha)}+e^{\ell_1(\delta)+\tau(\delta)}}{1+e^{\ell_1(\delta)+\tau(\delta)}}\right)$$

$$+ \frac{1}{\ell_1(\alpha)} \log \left(\frac{1 + e^{\ell_1(\delta^{-1}) + \tau(\delta^{-1})}}{e^{-R_1(\mu_1^\delta)\ell_1(\alpha)} + e^{\ell_1(\delta^{-1}) + \tau(\delta^{-1})}} \right).$$

There is one inequality of the same form as Equation (133) for each choice of $\delta = \beta, \gamma$ and i = 1 or 2. This makes a total of four such inequalities, and hence eight right-hand side terms. Crucially, these eight terms are distinct summands of the McShane identity for convex real projective 1-holed tori (Theorem 1.28), and hence:

$$\frac{2R_1(\mu_1^\beta)}{1+e^{\frac{1}{2}\ell(\tilde{\beta})}}+\frac{2R_1(\mu_2^\beta)}{1+e^{\frac{1}{2}\ell(\tilde{\beta})}}+\frac{2R_1(\mu_1^\gamma)}{1+e^{\frac{1}{2}\ell(\tilde{\gamma})}}+\frac{2R_1(\mu_2^\gamma)}{1+e^{\frac{1}{2}\ell(\tilde{\gamma})}}<1.$$

By Equation (129), we then obtain

$$\frac{2}{1+e^{\frac{1}{2}\ell(\tilde{\beta})}}+\frac{2}{1+e^{\frac{1}{2}\ell(\tilde{\gamma})}}<1,$$

which rearranges to give Equation (127) as desired.

Theorem 7.7 (Collar lemma). *Given any finite-area convex projective surface* Σ *, any two intersecting simple closed geodesics* β , γ *satisfy the following inequality:*

(135)
$$(e^{\frac{1}{2}\ell(\bar{\beta})} - 1)(e^{\frac{1}{2}\ell(\bar{\gamma})} - 1) > 4.$$

Proof. We first note that Proposition 7.6, coupled with the fact that the Hilbert length $\ell(\bar{\delta})$ of a curve δ is equal to

$$\ell(\bar{\delta}) = \ell(\delta) = \ell_1(\delta) + \ell_2(\delta),$$

tells us that Equation (135) is true if the convex hull of $\beta \cup \gamma$ is a 1-holed torus. Furthermore, whenever the convex-hull of $\beta \cup \gamma$ is a 4-holed sphere $\Sigma_{0,4}$, then $\Sigma_{0,4}$ is the quotient of a 4-holed torus $\Sigma_{1,4}$ with respect to the action of an isometric involution (see Figure 21):

The curve β lifts to two simple connected geodesics β_1 , β_2 in $\Sigma_{1,4}$, each of length equal to β . Likewise, the curve γ also lifts to γ_1 and γ_2 . The convex hull of $\beta_1 \cup \gamma_1$ is a 1-holed torus, and hence we once again obtain Equation (135).

The above cases cover all possibilities where there are two or fewer (geometric) intersection points between β and γ . We now turn to the case when there are at least three intersections. Let us assume without loss of generality that β is shorter than or equal to γ . We also assume that the intersection points $\beta \cap \gamma$ are generic, our arguments still apply when there are non-generic intersection points with the small caveat that some of the geodesic segments we concatenate may be of length zero.

Consider the now the geodesic subarcs $\{\sigma\}$ on γ with ends in $\beta \cap \gamma$, but not interior points. Note that this collection of subarcs may be bipartitioned into those whose endpoint tangent directions point to the same side of β (left hand side of Figure 22) and those whose endpoint directions point to opposite sides (right hand side of Figure 22). We refer to the former as a *type-A arc* and the latter as a *type-B arc*.

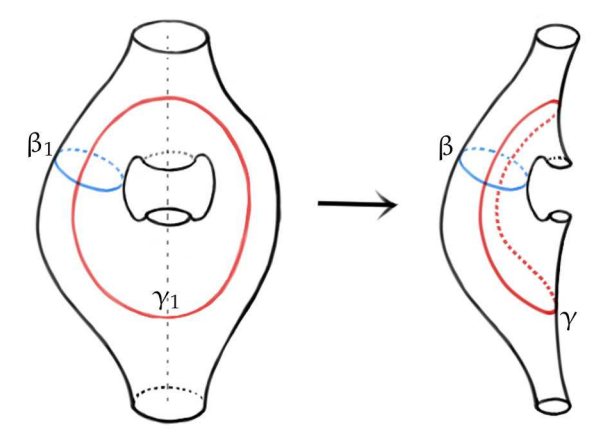


Figure 21. The left 4-holed torus double covers the right 4-holed sphere, with identification given by π -rotation about the central vertical axis. The curves β_1, γ_1 respectively cover β, γ precisely once and the convex hull of $\beta_1 \cup \gamma_1$ is a 1-holed torus.

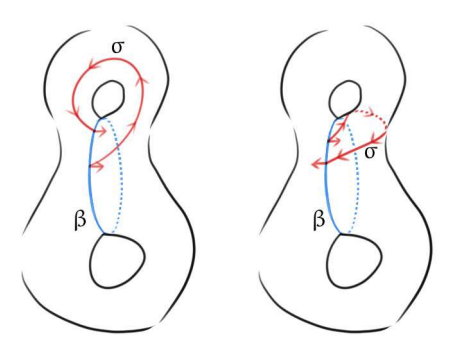


FIGURE 22. A type-A arc (left) versus a type-B arc (right).

Case 1: \exists type-A arc σ on γ of length $\ell(\bar{\sigma}) \leq \frac{1}{2}\ell(\bar{\gamma})$. Join the two ends of σ with the shorter of the two subarcs of β traversing between the endpoints of σ . The resulting concatenated broken geodesic shortens to a unique simple closed geodesic γ' which intersects β precisely once. The Hilbert length of γ' satisfies:

$$\ell(\overline{\gamma'}) \leqslant \frac{1}{2}(\ell(\bar{\beta}) + \ell(\bar{\gamma})) \leqslant \ell(\bar{\gamma}),$$

and the convex hull of $\beta \cup \gamma'$ is a 1-holed torus. Therefore:

$$(136) \qquad (e^{\frac{1}{2}\ell(\bar{\beta})} - 1)(e^{\frac{1}{2}\ell(\bar{\gamma})} - 1) \geqslant (e^{\frac{1}{2}\ell(\bar{\beta})} - 1)(e^{\frac{1}{2}\ell(\bar{\gamma}')} - 1) > 4,$$

as desired.

Case 2: no type-A arcs on γ **.** Let N denote the number of intersection points in $\beta \cap \gamma$ (non-generic intersection points are counted with multiplicity). The no type-A arcs condition forces N to be even. Hence, there are N \geqslant 4 type-B arcs $\sigma_1, \ldots, \sigma_N$ which concatenate to form γ . Consider the N geodesic arcs of the form $\sigma_i * \sigma_{i+1}$ (and $\sigma_N * \sigma_1$) obtained from concatenating consecutive type-B arcs. The

total sum of the lengths of these concatenated arcs is $2\ell(\bar{\gamma})$, and the pigeonhole principle tells us that at least one has length shorter than $\frac{2\ell(\bar{\gamma})}{N} \leqslant \frac{\ell(\bar{\gamma})}{2}$.

Let σ denote one such $\frac{\ell(\gamma)}{2}$ -short concatenated arc and consider the closed broken geodesic formed by joining the endpoints of σ with the shorter of the two arcs on β adjoining the endpoints of σ , and denote its geodesic representative by γ' . The curve γ' is either simple or may have one self-intersection. In the former case, we have two simple closed geodesics β and γ' with geometric intersection number equal to 2 but algebraic intersection number equal to 0. Hence $\beta \cup \gamma'$ lies on a 4-holed sphere, and we once again obtain Equation (136). In the latter case, the convex hull of γ' is a pair of pants. and precisely one of the two ways of resolving the intersection point on γ' produces an essential simple closed geodesic γ'' (see Figure 23). In particular, since Hilbert length is a distance metric, the triangle inequality ensures that resolving crossings results in shorter rectifiable curves with even shorter geodesic representatives. Thus, we replace γ' with γ'' , and wind up with the former case.

In either of the two cases as in Figure 23,

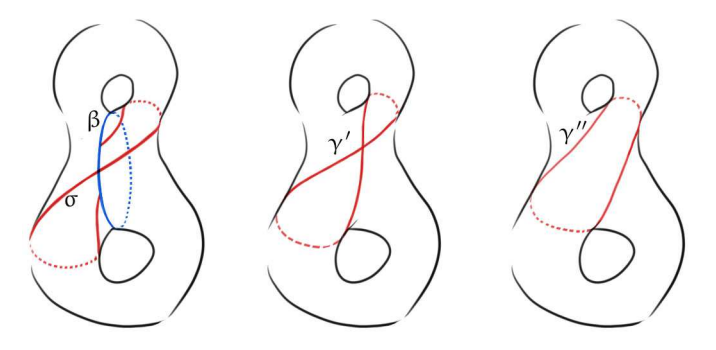


Figure 23. An example of the how the arc σ (left) is used to produce curves γ' (center) and γ'' (right).

Case 3: \exists type-A arc b on γ of length $\ell(\bar{b}) > \frac{1}{2}\ell(\bar{\gamma})$. Our argument here is similar to Case 2. Let N again denote the number of intersection points $\beta \cap \gamma$. By assuming disjointness from Case 1, we may assume without loss of generality that there are N - 1 consecutive type-B arcs $\sigma_1, \ldots, \sigma_{N-1}$ which, along with b, concatenate to form γ . The sum of the length of the following list of N concatenated arcs

$$\sigma_1 * \sigma_2, \dots, \sigma_i * \sigma_{i+1}, \dots, \sigma_{N-2} * \sigma_{N-1}, \sigma_{N-1} * b, b * \sigma_1$$

is equal to $2\ell(\bar{\gamma})$. By the pigeonhole principle, there must be at least one concatenated arc of the form $\sigma = \sigma_k * \sigma_{k+1}$ of length shorter than

$$\frac{2\ell(\bar{\gamma}) - \ell(\bar{\sigma}_{N-1} * \bar{b}) - \ell(\bar{b}) * \bar{\sigma}_1)}{N-2} < \frac{2\ell(\bar{\gamma}) - 2\ell(\bar{b})}{N-2} < \frac{\ell(\bar{\gamma})}{N-2}.$$

If N > 3, the above inequality ensures that $\ell(\bar{\sigma}) < \frac{\ell(\bar{\gamma})}{2}$. If N = 3, then σ must be $\sigma_1 * \sigma_2$, and is the complementary arc to \bar{b} . Hence σ is again of length less than $\frac{\ell(\bar{\gamma})}{2}$. We may now run the latter half of the argument for Case 3 to obtain equation (135).

Remark 7.8. Multiply both sides of Equation (135) by $(4e^{\frac{\ell(\tilde{\beta})}{4}}e^{\frac{\ell(\tilde{\gamma})}{4}})^{-1}$ and we obtain

(137)
$$\sinh\left(\frac{1}{4}\ell(\bar{\beta})\right) \cdot \sinh\left(\frac{1}{4}\ell(\bar{\gamma})\right) > e^{-\frac{\ell(\bar{\beta}) + \ell(\bar{\gamma})}{4}}.$$

Our choice of convention for Hilbert length is double hyperbolic length, and therefore our inequality is weaker than the "sharp" inequality described in [LZ17, Conjecture 3.8].

7.4. Thurston-type ratio metrics. Thurston showed in [Thu98, Theorem 3.1] that it is impossible for the simple marked length spectrum of one hyperbolic structure on a closed surface S to dominate that of another. This non-domination ensures that Thurston's simple length ratio metric on Teich(S) is positive.

Non-domination breaks down for bordered hyperbolic surfaces, and it is possible to map from a bordered surface to one where every geodesic is shorter [PT10]. The way that Papadopoulous and Théret resolve this issue is to introduce orthogeodesic arcs into the collection of objects that one takes length ratios over. We show using McShane identities that the naïve length ratio metric suffices provided that one fixes all boundary lengths.

Theorem 7.9. Given marked hyperbolic surfaces $\Sigma_1, \Sigma_2 \in Teich_{g,m}(L_1, ..., L_m)$ with fixed boundary lengths $L_1, ..., L_n \geqslant 0$. Then the marked simple geodesic spectrum for Σ_1 dominates the marked simple geodesic spectrum Σ_2 if and only if $\Sigma_1 = \Sigma_2$.

Proof. Assume without loss of generality that the simple length spectrum of Σ_1 dominates that of Σ_2 . We first consider the case where at least one of the boundaries L_i is strictly greater than 0. The summands in the McShane identities for bordered surface [Mir07a, TWZ06] have summands which are strictly decreasing with respect to increasing the lengths of (interior) simple closed geodesics. Since the simple length spectrum of Σ_1 dominates that of Σ_2 , this forces each pair of corresponding summands in the McShane identities for Σ_1 and Σ_2 to be equal. This forces the length of multicurves $\ell^{\Sigma_1}(\beta) + \ell^{\Sigma_1}(\gamma)$ to be equal to $\ell^{\Sigma_2}(\beta) + \ell^{\Sigma_2}(\gamma)$, and domination then tells us that

$$\ell^{\Sigma_1}(\beta) = \ell^{\Sigma_2}(\beta) \text{ and } \ell^{\Sigma_1}(\gamma) = \ell^{\Sigma_2}(\gamma).$$

Therefore, the marked simple length spectra for Σ_1 and Σ_2 are equal and $\Sigma_1 = \Sigma_2$.

The remaining case is where every boundary is length 0 is classically due to Thurston [Thu98], but can also be demonstrated by applying the same arguments to McShane's identities for cusped surfaces [McS98].

The above non-domination result immediately implies the following:

Corollary 7.10 (Thurston metric for bordered surfaces). *The non-negative real func*tion $d: \textit{Teich}_{g,m}(L_1, \ldots, L_m) \times \textit{Teich}_{g,m}(L_1, \ldots, L_m) \to \mathbb{R}_{\geqslant 0}$ defined by

(138)
$$d_{\mathit{Th}}(\Sigma_1, \Sigma_2) := \log \sup_{\bar{\gamma} \in \mathcal{C}(S_{q,m})} \frac{\ell^{\Sigma_2}(\bar{\gamma})}{\ell^{\Sigma_1}(\bar{\gamma})},$$

is a mapping class group invariant asymmetric Thurston-type length ratio metric on the Teichmüller space $Teich_{g,m}(L_1,\ldots,L_m)$ of surfaces with fixed boundary lengths L_1,\ldots,L_m .

For any (3-)Fuchsian representation ρ , Tholozan [Tho17] showed that it is *always* possible to find a (marked) convex projective surface whose simple Hilbert length

spectrum dominates that of ρ . Thus, the naïve length ratio expression for the Thurston metric, when extended to the space

$$Conv_{1,1}^* := \{ \Sigma \in Conv(S_{1,1}) \mid \Sigma \text{ has unipotent boundary monodromy} \}$$

of cusped convex real project tori, results in a function which may be negative. To deal with this, we reverse engineer our McShane identities-based proof for the non-negativity of the length ratio metric (Theorem 7.9) and propose the following candidate for a metric on $Conv_{1.1}^*$:

(139)
$$d_{Gap}(\Sigma_1, \Sigma_2) := \log \sup_{\gamma \in \overrightarrow{\mathcal{C}}_{1,1}} \left(\frac{\log(1 + e^{\ell_1^{\Sigma_2}(\gamma) + \tau^{\Sigma_2}(\gamma)})}{\log(1 + e^{\ell_1^{\Sigma_1}(\gamma) + \tau^{\Sigma_1}(\gamma)})} \right)$$

To show that this is a well-defined function, we use the following comparison:

Theorem 7.11 ([Ben01, Corollary 5.3] Hilbert vs. simple root length comparison). For any positive representation $\rho: \pi_1(S) \to PGL_3(\mathbb{R})$, there exists $K_{\rho} > 1$ such that for every simple closed curve γ on S, we have:

$$\ell_1(\gamma) < \ell(\bar{\gamma}) < K_{\rho} \cdot \ell_1(\gamma).$$

Remark 7.12. Although [Ben01, Corollary 5.3] is stated for compact surfaces, we believe that Benoist's proof combined with Proposition 6.9 suffices to extend this result to finite-area convex real projective surfaces. As an added insurance, we provide a proof in Appendix A.

Proposition 7.13. The gap metric d_{Gap} is well-defined.

Proof. We need to show that the supremum in (139) is bounded. If the supremum is realized by some simple geodesic γ , then obviously the gap metric is well-defined. If not, then there is a sequence of distinct geodesics $\{\gamma_k\}$ for which the expression in (139) tends to the supremum. Then, by the discreteness of the simple length spectrum (Theorem 7.4) and the uniform boundedness of triple ratios (Theorem 3.4), showing that the supremum exists is equivalent the existence of the following supremum:

$$\sup_{\gamma \in \overrightarrow{\mathcal{C}}_{1,1}} \frac{\ell_1^{\Sigma_2}(\gamma)}{\ell_1^{\Sigma_1}(\gamma)} \leqslant K_{\Sigma_1} \cdot \sup_{\gamma \in \overrightarrow{\mathcal{C}}_{1,1}} \frac{\ell^{\Sigma_2}(\bar{\gamma})}{\ell^{\Sigma_1}(\bar{\gamma})},$$

where the K_{Σ_1} in the right hand side is the coefficient in Theorem 7.11. However, we know from [Thu16, Theorem 2] that the Hilbert lengths $\ell^{\Sigma_1}(\cdot)$ and $\ell^{\Sigma_2}(\cdot)$ extend continuously to the space of (compactly supported) measured laminations on $S_{1,1}$. In particular, the homogeneity of these length functions on multicurves means that they must be homogeneous over all of measured lamination space, and hence $\ell^{\Sigma_2}/\ell^{\Sigma_1}$ defines a continuous function on the space of (compactly supported) projective measured laminations. This is a compact codomain, and hence must be bounded above. Therefore, the left-hand side supremum in (141) exists and d_{Gap} is well-defined.

Theorem 7.14 (Gap metric for $Conv_{1,1}^*$). The non-negative function d_{Gap} defines a mapping class group invariant aymmetric metric on $Conv_{1,1}^*$.

Proof. It is clear that d_{Gap} is mapping class group invariant and satisfies the triangle inequality. The McShane identity (Theorem 1.1) tells us that the gap summands of for Σ_1 cannot dominate those for Σ_2 , and this gives us the requisite non-negativity.

All that remains is to show that $d_{Gap}(\Sigma_1, \Sigma_2) = 0$ iff $\Sigma_1 = \Sigma_2$. One way is obvious. For the converse, assume that $d_{Gap}(\Sigma_1, \Sigma_2) = 0$, then the McShane identity tells us that corresponding gap summands must each be equal, and hence

$$\forall \gamma \in \vec{\mathcal{C}}_{1,1}, \quad \ell_1^{\Sigma_1}(\gamma) + \tau^{\Sigma_1}(\gamma) = \ell_1^{\Sigma_2}(\gamma) + \tau^{\Sigma_2}(\gamma).$$

Consider the sequence of curves $\{\beta\gamma^k\}_{k\in\mathbb{Z}}$ obtained from applying Dehn-twists along γ to a β which once-intersects γ . The eigenvalues for the monodromy for two matrices are minimal/maximal when they are simultaneously diagonalizable, and hence we obtain the bounds:

(143)
$$k\ell_1(\gamma) + \log \lambda_3(\beta) - \log \lambda_1(\beta) = k\ell_1(\gamma) - \ell(\bar{\beta}) < \ell_1(\beta\gamma^k)$$
 and

$$(144) \qquad k\ell_1(\gamma) + \log \lambda_1(\beta) - \log \lambda_3(\beta) = k\ell_1(\gamma) + \ell(\bar{\beta}) > \ell_1(\beta\gamma^k).$$

Hence we see that

(145)
$$\ell_1(\gamma) = \lim_{k \to \infty} \frac{1}{k} \ell_1(\beta \gamma^k).$$

Which in turn implies that:

$$(146) \qquad \frac{\ell_{1}^{\Sigma_{2}}(\gamma)}{\ell_{1}^{\Sigma_{1}}(\gamma)} = \lim_{k \to \infty} \frac{\frac{1}{k}\ell_{\beta\gamma^{k}}^{1}(\Sigma_{2})}{\frac{1}{k}\ell_{\beta\gamma^{k}}^{1}(\Sigma_{1})} = \lim_{k \to \infty} \frac{\frac{1}{k}(\ell_{1}^{\Sigma_{2}}(\beta\gamma^{k}) + \tau^{\Sigma_{2}}(\beta\gamma^{k}))}{\frac{1}{k}(\ell_{1}^{\Sigma_{1}}(\beta\gamma^{k}) + \tau^{\Sigma_{1}}(\beta\gamma^{k}))} = 1.$$

Therefore, the marked simple ℓ_1 (and ℓ_2) spectra for $\Sigma_i \in Conv_{1,1}^*$ must be congruent. Which means that the simple marked λ_1 spectra for Σ_1 and Σ_2 must be equal. By [BCL17], this means that $\Sigma_1 = \Sigma_2$.

Proposition 7.15. The restriction of the metric d_{Gap} to the Fuchsian locus of $Conv_{1,1}^*$ is precisely the Thurston metric d_{Th} .

Proof. We first note that on the Fuchsian locus, triple ratios are all equal to 1, and the simple root length $\ell_1(\gamma)$ of every geodesic γ is equal to $\frac{1}{2}\ell(\bar{\gamma})$. Since $f(x) = \log(1+x)/\log(x)$ is a monotonically decreasing for x>0, whenever $\ell_1^{\Sigma_2}(\gamma) > \ell_1^{\Sigma_1}(\gamma)$, we have

$$\frac{\log(1+e^{\ell_1^{\Sigma_2}(\gamma)})}{\log(1+e^{\ell_1^{\Sigma_1}(\gamma)})}<\frac{\log(e^{\ell_1^{\Sigma_2}(\gamma)})}{\log(e^{\ell_1^{\Sigma_1}(\gamma)})}=\frac{\ell_1^{\Sigma_2}(\gamma)}{\ell_1^{\Sigma_1}(\gamma)}=\frac{\ell^{\Sigma_2}(\gamma)}{\ell^{\Sigma_1}(\gamma)}.$$

Therefore $d_{Gap} \leq d_{Th}$. On the other hand, equation (145) gives us the converse comparison $d_{Gap} \geq d_{Th}$, hence allowing us to conclude that the two metrics are equal on the Fuchsian locus.

7.4.1. Two generalizations to $S_{g,m}$. We now turn to the space $Conv_{g,m}^*$ of (finite-area) marked cusped convex real projective surfaces with genus g and m cusps. We consider two possible generalizations, The first is equal to the Thurston metric on the Fuchsian slice and is conjecturally generalizable for rank $n \geqslant 4$ positive representations.

Definition 7.16 (Pants-gap metric for cusped real convex projective surfaces). We define the pants gap function for $PGap^{\Sigma}(\beta, \gamma)$ a pair of pants $[\beta, \gamma]$ on a marked cusped convex real projective surface $\Sigma \in Conv_{g,m}^*$ with cusps $\mathfrak{p}_1, \ldots, \mathfrak{p}_m$ as the McShane identity summand corresponding to $[\beta, \gamma]$:

$$(147) \qquad \mathsf{PGap}^{\Sigma}(\beta,\gamma) := \left(1 + \frac{\cosh\frac{d_2}{2}}{\cosh\frac{d_1}{2}} \cdot e^{\frac{1}{2}(\tau(\gamma,\delta_{\mathfrak{p}}) + \ell_1(\gamma) + \tau(\beta,\delta_{\mathfrak{p}}) + \ell_1(\beta))}\right)^{-1}.$$

We define the pants gap metric as:

(148)
$$d_{PGap}(\Sigma_1, \Sigma_2) := \log \sup_{[\beta, \gamma] \in \overrightarrow{\mathcal{P}}} \frac{-\log(PGap^{\Sigma_1}(\beta, \gamma))}{-\log(PGap^{\Sigma_2}(\beta, \gamma))},$$

where $[\beta, \gamma]$ varies over the set $\vec{\mathbb{P}} = \vec{\mathbb{P}}_{\mathfrak{p}_1} \cup \ldots \cup \vec{\mathbb{P}}_{\mathfrak{p}_m}$ of all boundary-parallel pairs of pants on $S_{g,m}$.

Definition 7.17 (Total gap metric for cusped real convex projective surfaces). *Define the* total gap function *for a marked convex real projective surface* $\Sigma \in Conv_{g,m}^*$ *with cusps* $\mathfrak{p}_1, \ldots, \mathfrak{p}_m$ *as:*

(149)
$$TGap^{\Sigma}(\gamma) := \frac{1}{m} \sum_{j=1}^{m} \left(\sum_{[\gamma, \gamma_{\mathfrak{p}}] \in \overrightarrow{\mathcal{H}}_{\mathfrak{p}_{j}}(\gamma)} \frac{B_{1}(\gamma, \gamma_{\mathfrak{p}})}{1 + e^{\ell_{1}(\gamma) + \tau(\gamma, \gamma_{\mathfrak{p}})}} \right).$$

We define the total gap metric *as:*

(150)
$$d_{TGap}(\Sigma_1, \Sigma_2) := \log \sup_{[\gamma] \in \vec{\mathcal{C}}_{q,m}} \frac{-\log(TGap^{\Sigma_2}(\gamma))}{-\log(TGap^{\Sigma_1}(\gamma))}.$$

Remark 7.18. When (g, m) = (1, 1), both of these two metrics agree with the gap metric we defined for 1-cusped convex real projective tori.

Remark 7.19. The proof that the pants gap metric and the total gap metric are both mapping class group invariant, asymmetric metrics on $Conv_{g,m}^*$ is essentially the same as for the $Conv_{1,1}^*$ case. We leave it as an exercise to show that these two metrics are well-defined. For the pants gap metric, this uses [Kim18, Theorem 1.2], which shows that the quantity $\frac{\cosh(\frac{1}{2}d_2(\beta,\gamma))}{\cosh(\frac{1}{2}d_1(\beta,\gamma))}$ is bounded as one varies over $[\beta,\gamma] \in \overrightarrow{\mathcal{P}}$. For the total gap metric, it helps to use Lemma 7.3 and the following observation:

(151)
$$\sum_{[\gamma,\gamma_{\mathfrak{p}}]\in\overrightarrow{\mathcal{H}}_{\mathfrak{p}}(\gamma)} B_{\mathfrak{i}}(\gamma,\gamma_{\mathfrak{p}}) \leqslant 1.$$

Equation (151) comes from interpreting the left hand side of the above inequality as a probability with respect to the Goncharov-Shen potential measure. Specifically, it is the probability that the portion of a geodesic launched from cusp p up to its first point of self-intersection will either:

- intersect γ, or
- be completely contained on a pair of half-pants with $\bar{\gamma}$ as its cuff.

Proposition 7.20. The restriction of the pants gap metric d_{PGap} to the Fuchsian locus is equal to the classical Thurston metric.

Proof. The proof is essentially identical to the proof of Proposition 7.15, provided that one uses the following fact:

(152)
$$d_{Th}(\Sigma_1, \Sigma_2) = \log \sup_{[\bar{\beta}, \bar{\gamma}] \in \mathcal{P}_n} \frac{\ell^{\Sigma_2}(\bar{\beta}, \bar{\gamma})}{\ell^{\Sigma_1}(\bar{\beta}, \bar{\gamma})},$$

which comes from the fact that the projection of \mathcal{P}_{p_j} regarded as a set of multicurves, in projective measured lamination space is dense.

Remark 7.21. It is unclear whether the restriction of the total gap metric d_{TGap} to the Fuchsian locus is the Thurston metric, although it is fairly straight-forward to show that $d_{TGap} \geqslant d_{Th}$.

It is also possible to extend the pants gap metric over the set of (marked) convex real projective surfaces Σ with loxodromic boundaries.

Definition 7.22 (Pants gap metric for bordered convex real projective surfaces). Let Σ denote a convex real projective surface with loxodromic boundaries $\alpha_1, \ldots, \alpha_m$. We adopt the following notation: $\vec{\mathbb{P}}^{\mathfrak{d}}_{\alpha}$ denotes the set of boundary-parallel pairs of pants in $\vec{\mathbb{P}}_{\alpha}$ which have two borders being boundary components of S_{g,m}.

- For any $[\beta,\gamma] \in \vec{\mathcal{P}}_{\alpha} \setminus \vec{\mathcal{P}}_{\alpha}^{\delta}$ we set $PGap^{\Sigma}(\beta,\gamma)$ to be $\frac{1}{\ell_{1}(\alpha)}$ times the i=1
- McShane identity summand in Equation (12); for any $[Y] \in \mathcal{P}^{\mathfrak{d}}_{\alpha}$, we set $PGap^{\Sigma}(Y)$ to be be $\frac{1}{\ell_{1}(\alpha)}$ times the $\mathfrak{i}=1$ summand in

The pants gap metric $d_{PGap}(\Sigma_1, \Sigma_2)$ *is defined as:*

$$\log \max_{j=1,\dots,m} \left\{ \sup_{[\beta,\gamma] \in \overrightarrow{\mathcal{P}}_{\alpha_{i}} \setminus \overrightarrow{\mathcal{P}}_{\alpha_{i}}} \frac{-\log(PGap^{\Sigma_{1}}(\beta,\gamma))}{-\log(PGap^{\Sigma_{2}}(\beta,\gamma))}, \sup_{[Y] \in \mathcal{P}_{\alpha_{j}}^{\delta}} \frac{-\log(PGap^{\Sigma_{1}}(Y))}{-\log(PGap^{\Sigma_{2}}(Y))} \right\}.$$

The proof that this is a well-defined metric is essentially the same as for the cusped case and we again require [Kim18, Theorem 1.2].

Remark 7.23. We expect [Kim18, Theorem 1.2] to generalize to all rank n. Provided that this can be demonstrated, it is possible to generalize the pants gap metric to define asymmetric metrics on the character variety of loxodromic-bordered positive representations of arbitrary rank. Moreover, the (n-1) different McShane identities we obtain induces a (n-1)-dimensional positive "quadrant" of such metrics.

8. McShane-type identities for higher Teichmüller space

We begin by establishing McShane identities for general rank positive representations with loxodromic boundary monodromy.

8.1. **Ordered ratios and simple root length decomposition.** We introduce a mild generalization of ordered cross ratios [LM09], called *ordered ratios*.

Definition 8.1 (Ratio). *Consider the following collection of 4-tuples*

$$\mathfrak{d}_{\infty}\pi_1(S_{g,\mathfrak{m}})^{4**} = \left\{ (x,y,z,t) \in \mathfrak{d}_{\infty}\pi_1(S_{g,\mathfrak{m}})^4 \mid x \neq y, x \neq z, x \neq t, y \neq z \right\}.$$

A ratio B: $\mathfrak{d}_{\infty}\pi_1(S_{g,\mathfrak{m}})^{4**} \to \mathbb{R}$ is a $\pi_1(S_{g,\mathfrak{m}})$ -invariant continuous real function which satisfies the following three ratio conditions:

- (1) (normalization): B(x, y, z, t) = 0 iff y = t,
- (2) (normalization): B(x, y, z, t) = 1 iff z = t,
- (3) (cocycle): $B(x, y, z, t) = B(x, y, z, w) \cdot B(x, y, w, t)$,

An ordered ratio is a ratio B on $S_{g,m}$ which satisfies two order conditions: for four different points $x, y, z, t \in \partial_{\infty} \pi_1(S_{g,m})$:

- (1) B(x,y,z,t) > 0 if z, t are on the same side of xy,
- (2) B(x, y, z, t) > 1 if x, y, z, t are cyclically ordered.

Definition 8.2 (Periods for ratios). For non-trivial $\alpha \in \pi_1(S_{g,m})$ and $y \neq \alpha^-, \alpha^+$, the period of α for the ordered ratio B is

$$\ell^{\mathrm{B}}(\alpha) := \log \mathrm{B}(\alpha^{-}, \alpha^{+}, \alpha(y), y)$$

As with periods for cross ratios, periods for ratios are also independent of the choice of y. For any $z \in \partial_{\infty} \pi_1(S_{g,m}) \setminus \{\alpha^-, \alpha^+\}$, by

- $\pi_1(S_{q,m})$ -invariance: $B(\alpha^-, \alpha^+, \alpha(y), \alpha(z)) = B(\alpha^-, \alpha^+, y, z)$,
- and the cocycle identity for the ordered ratios,

we obtain that:

$$B(\alpha^{-}, \alpha^{+}, \alpha(y), y)$$

$$=B(\alpha^{-}, \alpha^{+}, \alpha(y), \alpha(z)) \cdot B(\alpha^{-}, \alpha^{+}, \alpha(z), z) \cdot B(\alpha^{-}, \alpha^{+}, z, y)$$

$$=B(\alpha^{-}, \alpha^{+}, y, z) \cdot B(\alpha^{-}, \alpha^{+}, \alpha(z), z) \cdot B(\alpha^{-}, \alpha^{+}, z, y)$$

$$=B(\alpha^{-}, \alpha^{+}, \alpha(z), z).$$

Ordered ratios satisfy one fewer (cocycle) axiom than ordered cross ratios. As a consequence periods ℓ^B of an ordered ratio B do not necessarily satisfy $\ell^B(\gamma) \neq \ell^B(\gamma^{-1})$. One immediate advantage of ordered ratios is that simple root lengths can now be periods. In fact, we have already seen an ordered ratio in the guise of the ratio of two i-th characters (Definition 4.13).

Remark 8.3 (i-th ratio). Given $(\rho, \xi) \in \mathfrak{X}_{PGL_n, S_{\mathfrak{a}, \mathfrak{m}}}(\mathbb{R}_{>0})$, the i-th ratio:

(154)
$$B(x,y,z,t) = B_{i}(x;y,z,t) := \frac{P_{i}(x;y,t)}{P_{i}(x;y,z)},$$

is indeed an ordered ratio. By Proposition 4.14, we have that B_i is $\pi_1(S_{g,m})$ -invariant. It is easy to check the three ratio conditions. Positivity implies the two ordered conditions.

Splitting the i-th ratio using essentially the same process as in Section 5, we obtain (n-1) identities for each boundary component α .

Theorem 8.4 (McShane identity for loxodromic bordered positive representations). For positive representation ρ with loxodromic monodromy around every boundary component, define its i-th ratios via its canonical lift $(\rho, \xi) \in \mathfrak{X}_{PGL_n, S_{g,m}}(\mathbb{R}_{>0})$ (as per Definition 4.17). Given a distinguished boundary component α of $S_{g,m}$, for each $i = 1, \dots, n-1$, we have the equality:

(155)

$$\ell_{\mathfrak{i}}(\alpha) = \sum_{[\delta, \delta_{\alpha^{-}}] \in \overrightarrow{\mathcal{H}}_{\alpha}} \left| \log B_{\mathfrak{i}} \left(\alpha^{-}; \alpha^{+}, \delta(\alpha^{-}), \delta^{+} \right) \right| + \sum_{[\gamma, \gamma_{\alpha^{-}}] \in \overrightarrow{\mathcal{H}}_{\alpha}^{\mathfrak{d}}} \log B_{\mathfrak{i}} \left(\alpha^{-}; \alpha^{+}, \gamma^{-}, \gamma^{+} \right).$$

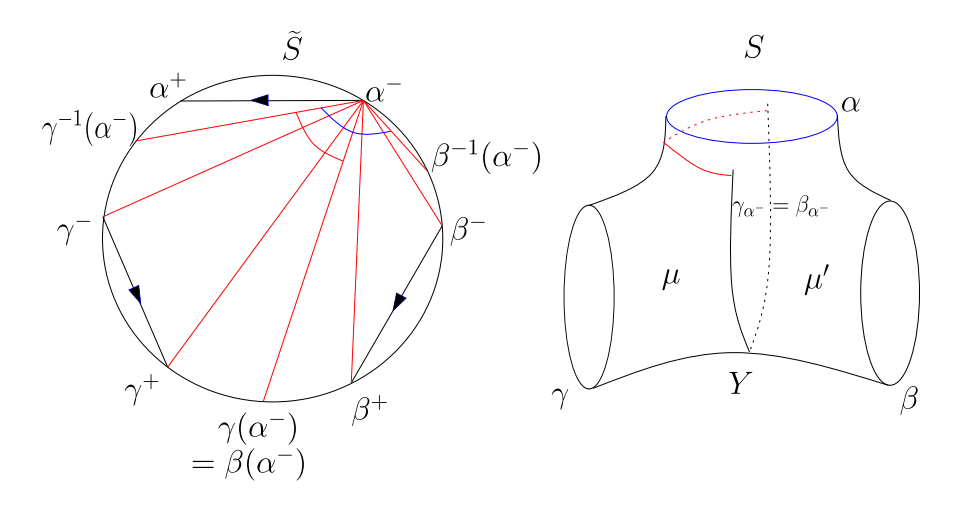


Figure 24. The pair of pants Y has the boundary components α , β , γ with $\alpha\beta^{-1}\gamma=1$ and Y is cut into μ,μ' along the simple curve $\gamma_{\alpha^-}=\beta_{\alpha^-}$ (check Figure 6 for details around α). Here $\partial\mu$ contains γ_{α^-} and γ , and $\partial\mu'$ contains γ_{α^-} and β .

Proof. Using the cocycle property of i-th ratio and Hölder property of the limit curve ξ_p , we follow the proof presented in [LM09] almost line by line and replace the ordered cross ratio $\mathbb B$ by the ordered ratio B_i . We extend Definition 1.19 to $\overrightarrow{\mathcal P}_\alpha$, Then we obtain

(156)

$$\begin{split} \ell_{\mathfrak{i}}(\alpha) &= \sum_{\{\beta,\gamma\} \in \overrightarrow{\mathcal{P}}_{\alpha}} \left(\log B_{\mathfrak{i}} \left(\alpha^{-}; \alpha^{+}, \gamma^{+}, \gamma(\alpha^{-}) \right) + \log B_{\mathfrak{i}} \left(\alpha^{-}; \alpha^{+}, \beta(\alpha^{-}), \beta^{+} \right) \right) \\ &+ \sum_{[\Upsilon] \in \mathcal{P}_{\alpha}^{\mathfrak{d}}} \log B_{\mathfrak{i}} \left(\alpha^{-}; \alpha^{+}, \gamma^{-}, \gamma^{+} \right) \\ &= \sum_{[\delta, \delta_{\alpha^{-}}] \in \overrightarrow{\mathcal{H}}_{\alpha}} \left| \log B_{\mathfrak{i}} \left(\alpha^{-}; \alpha^{+}, \delta(\alpha^{-}), \delta^{+} \right) \right| + \sum_{[\gamma, \gamma_{\alpha^{-}}] \in \overrightarrow{\mathcal{H}}_{\alpha}^{\mathfrak{d}}} \log B_{\mathfrak{i}} \left(\alpha^{-}; \alpha^{+}, \gamma^{-}, \gamma^{+} \right). \end{split}$$

As is, the identity is not expressed in terms of explicit geometric/projective invariants attached to the representation ρ . We do this crucial step later in this section.

8.2. McShane-type inequalities for unipotent bordered positive representations. We in fact have two strategies for deriving McShane-type inequalities for unipotent bordered positive representations. The first is to follow the Goncharov-Shen potential splitting idea we employed in Section 5. The second is to take the loxodromic bordered identities we just obtained and to consider them under deformation to the unipotent bordered locus in the character variety. We choose to illustrate the second strategy; the necessary ingredients for computing via the first strategy is nevertheless contained in what follows.

Theorem 8.5 (McShane-type inequality for unipotent bordered positive representations). Consider a positive representation ρ with unipotent boundary monodromy and let $p \in m_p$ be a distinguished puncture/cusp on $S_{g,m}$. Then, for $i=1,\cdots,n-1$, we have

(157)
$$\sum_{[\delta, \delta_{p}] \in \overrightarrow{\mathcal{H}}_{p}} \left(\frac{B_{i}(\delta, \delta_{p})}{1 + K_{i}(\delta, \delta_{p}) \cdot \frac{\lambda_{i}(\rho(\delta))}{\lambda_{i+1}(\rho(\delta))}} \right) \leqslant 1,$$

where γ is the oriented cuff for μ and γ_p is the oriented seam for μ , and

(158)

$$K_i(\delta,\delta_p) = \frac{1 + \sum_{c=1}^{i-1} \prod_{j=1}^{c} T_{n-i,j,i-j}(\delta p,\delta^+,p)}{1 + \sum_{c=1}^{i-1} \prod_{j=1}^{c} T_{n-i,j,i-j}(p,\delta p,\delta^+)} \cdot \frac{\prod_{j=1}^{n-i-1} T_{n-i-j,j,i}(p,\delta p,\delta^+)}{\prod_{j=1}^{i-1} T_{j,n-i,i-j}(p,\delta p,\delta^+)}.$$

Definition 8.6 (path l). For $(\rho, \xi) \in \mathcal{X}_{PGL_n, S_{g,m}}(\mathbb{R}_{>0})$ with (purely) loxodromic bordered monodromy representation ρ , we choose an analytic path l in $\mathcal{X}_{PGL_n, S_{g,m}}(\mathbb{R}_{>0})$ satisfying the following conditions:

- (1) $l(0) = (\rho, \xi)$;
- (2) every element of $l([0,1)) \subset \mathfrak{X}_{PGL_n,S_{g,m}}(\mathbb{R}_{>0})$ has loxodromic monodromy around all of its boundary components;
- (3) $l(1) = (\rho', \xi') \in \mathfrak{X}_{PGL_{\pi}, S_{g,m}}(\mathbb{R}_{>0})$ has unipotent monodromy around all of its boundary components, also arising from an element of $\mathcal{A}_{SL_{\pi}, S_{g,m}}(\mathbb{R}_{>0})$.

We denote the limit converges to l(1) along the path l by $\lim_{hyp\to para}$. Along the path l, the simple root length ℓ_i of each boundary component converges to 0 for $i=1,\cdots,n-1$. Geometrically speaking, this is tantamount to the boundary α of $S_{g,m}$ deforms to a cusp p.

Proposition 8.7. For any $[\mu] \in \overrightarrow{\mathcal{H}}^{\mathfrak{d}}_{\alpha}$ with its cuff a boundary component γ , as γ deforms to a unipotent boundary, we have:

(159)
$$\lim_{hup\to para} \frac{\log B_{i}(\alpha^{-}; \alpha^{+}, \gamma^{-}, \gamma^{+})}{\ell_{i}(\alpha)} = 0.$$

Proof. We have

$$(160) \qquad \lim_{\text{hyp}\rightarrow\text{para}}\frac{\log B_{\mathfrak{i}}\left(\alpha^{-};\alpha^{+},\gamma^{-},\gamma^{+}\right)}{\ell_{\mathfrak{i}}(\alpha)}=\lim_{\text{hyp}\rightarrow\text{para}}\frac{\frac{P_{\mathfrak{i}}\left(\alpha^{-};\alpha^{+},\gamma^{+}\right)}{P_{\mathfrak{i}}\left(\alpha^{-};\alpha^{+},\gamma^{-}\right)}-1}{\frac{P_{\mathfrak{i}}\left(\alpha^{-};\alpha^{+},\alpha^{-1}(\gamma^{-})\right)}{P_{\mathfrak{i}}\left(\alpha^{-};\alpha^{+},\gamma^{-}\right)}-1}$$

(161)
$$= \lim_{\text{hyp} \to \text{para}} \frac{P_{i}(\alpha^{-}; \gamma^{-}, \gamma^{+})}{P_{i}(\alpha^{-}; \gamma^{-}, \alpha^{-1}(\gamma^{-}))}.$$

Since γ is another boundary component which converges to a cusp along the path l, we get $P_i(\alpha^-; \gamma^-, \gamma^+) = 0$ for l(1). Hence we obtain

(162)
$$\lim_{\text{hyp}\rightarrow\text{para}}\frac{P_{i}(\alpha^{-};\gamma^{-},\gamma^{+})}{P_{i}(\alpha^{-};\gamma^{-},\alpha^{-1}(\gamma^{-}))}=0.$$

Remark 8.8. The previous result explains why there are no $\overrightarrow{\mathbb{H}}^{\mathfrak{d}}_{\alpha}$ summands in the unipotent bordered McShane identity.

Lemma 8.9. For $\delta \in \{\beta, \beta^{-1}, \gamma, \gamma^{-1}\}$ as in Figure 24, we obtain the formula (163)

$$B_{\mathfrak{i}}\left(\alpha^{-};\alpha^{+},\delta(\alpha^{-}),\delta^{+}\right)=\frac{B_{\mathfrak{i}}\left(\alpha^{-};\alpha^{+},\delta(\alpha^{-}),\delta^{-1}(\alpha^{-})\right)-B_{\mathfrak{i}}\left(\alpha^{-};\delta^{+},\delta(\alpha^{-}),\delta^{-1}(\alpha^{-})\right)}{1-B_{\mathfrak{i}}\left(\alpha^{-};\delta^{+},\delta(\alpha^{-}),\delta^{-1}(\alpha^{-})\right)}.$$

Proof. Using additivity of the i-th character, we simplify the right hand side as follows:

(164)

$$\begin{split} &\frac{B_{i}\left(\alpha^{-};\alpha^{+},\delta(\alpha^{-}),\delta^{-1}(\alpha^{-})\right) - B_{i}\left(\alpha^{-};\delta^{+},\delta(\alpha^{-}),\delta^{-1}(\alpha^{-})\right)}{1 - B_{i}\left(\alpha^{-};\delta^{+},\delta(\alpha^{-}),\delta^{-1}(\alpha^{-})\right)} \\ &= \left(\frac{P_{i}(\alpha^{-};\alpha^{+},\delta^{-1}(\alpha^{-}))}{P_{i}(\alpha^{-};\alpha^{+},\delta(\alpha^{-}))} - \frac{P_{i}(\alpha^{-};\delta^{+},\delta^{-1}(\alpha^{-}))}{P_{i}(\alpha^{-};\delta^{+},\delta(\alpha^{-}))}\right) \middle/ \left(1 - \frac{P_{i}(\alpha^{-};\delta^{+},\delta^{-1}(\alpha^{-}))}{P_{i}(\alpha^{-};\delta^{+},\delta(\alpha^{-}))}\right) \\ &= \frac{P_{i}(\alpha^{-};\alpha^{+},\delta^{-1}(\alpha^{-})) \cdot P_{i}(\alpha^{-};\delta^{+},\delta(\alpha^{-})) - P_{i}(\alpha^{-};\delta^{+},\delta^{-1}(\alpha^{-})) \cdot P_{i}(\alpha^{-};\alpha^{+},\delta(\alpha^{-}))}{P_{i}(\alpha^{-};\alpha^{+},\delta(\alpha^{-})) \cdot (P_{i}(\alpha^{-};\delta^{+},\delta(\alpha^{-})) - P_{i}(\alpha^{-};\delta^{+},\delta^{-1}(\alpha^{-})))} \\ &= \left[\left(P_{i}(\alpha^{-};\alpha^{+},\delta(\alpha^{-})) + P_{i}(\alpha^{-};\delta(\alpha^{-}),\delta^{-1}(\alpha^{-}))\right) \left(P_{i}(\alpha^{-};\delta^{+},\delta^{-1}(\alpha^{-})) + P_{i}(\alpha^{-};\delta^{-1}(\alpha^{-}),\delta(\alpha^{-}))\right) - P_{i}(\alpha^{-};\delta^{+},\delta^{-1}(\alpha^{-})) + P_{i}(\alpha^{-};\delta^{+},\delta(\alpha^{-})) + P_{i}(\alpha^{-};\delta^{-1}(\alpha^{-}),\delta(\alpha^{-}))\right) \\ &= \frac{P_{i}(\alpha^{-};\alpha^{+},\delta(\alpha^{-})) P_{i}(\alpha^{-};\delta^{-1}(\alpha^{-}),\delta(\alpha^{-})) + P_{i}(\alpha^{-};\delta^{-1}(\alpha^{-}),\delta(\alpha^{-}))}{P_{i}(\alpha^{-};\alpha^{+},\delta(\alpha^{-})) P_{i}(\alpha^{-};\delta^{-1}(\alpha^{-}),\delta(\alpha^{-}))} \\ &= \frac{P_{i}(\alpha^{-};\alpha^{+},\delta(\alpha^{-})) P_{i}(\alpha^{-};\delta^{-1}(\alpha^{-}),\delta(\alpha^{-}))}{P_{i}(\alpha^{-};\delta^{-1}(\alpha^{-}),\delta(\alpha^{-}))} \\ &= \frac{P_{i}(\alpha^{-};\alpha^{+},\delta(\alpha^{-})) P_{i}(\alpha^{-};\delta^{-1}(\alpha^{-}),\delta(\alpha^{-}))}{P_{i}(\alpha^{-};\delta^{-1}(\alpha^{-}),\delta(\alpha^{-}))} \\ &= \frac{P_{i}(\alpha^{-};\alpha^{+},\delta(\alpha^{-})) P_{i}(\alpha^{-};\delta^{-1}(\alpha^{-}),\delta(\alpha^{-}))}{P_{i}(\alpha^{-};\delta^{-1}(\alpha^{-}),\delta(\alpha^{-}))} \\ &= \frac{P_{i}(\alpha^{-};\alpha^{+},\delta(\alpha^{-})) P_{i}(\alpha^{-};\delta^{-1}(\alpha^{-}),\delta(\alpha^{-}))}{P_{i}(\alpha^{-};\alpha^{+},\delta(\alpha^{-})) P_{i}(\alpha^{-};\delta^{-1}(\alpha^{-}),\delta(\alpha^{-}))} \\ &= \frac{P_{i}(\alpha^{-};\alpha^{+},\delta(\alpha^{-})) P_{i}(\alpha^{-};\delta^{-1}(\alpha^{-}),\delta(\alpha^{-}))}{P_{i}(\alpha^{-};\alpha^{+},\delta(\alpha^{-})) P_{i}(\alpha^{-};\delta^{-1}(\alpha^{-}),\delta(\alpha^{-}))} \\ &= \frac{P_{i}(\alpha^{-};\alpha^{+},\delta(\alpha^{-})) P_{i}(\alpha^{-};\delta^{-1}(\alpha^{-}),\delta(\alpha^{-}))}{P_{i}(\alpha^{-};\alpha^{+},\delta(\alpha^{-}))} \\ &= \frac{P_{i}(\alpha^{-};\alpha^{+},\delta(\alpha^{-})) P_{i}(\alpha^{-};\delta^{-1}(\alpha^{-}),\delta(\alpha^{-}))}{P_{i}(\alpha^{-};\alpha^{+},\delta(\alpha^{-}))} \\ &= \frac{P_{i}(\alpha^{-};\alpha^{+},\delta(\alpha^{-})) P_{i}(\alpha^{-};\delta^{-1}(\alpha^{-}),\delta(\alpha^{-}))}{P_{i}(\alpha^{-};\alpha^{+},\delta(\alpha^{-}))} \\ &= \frac{P_{i}(\alpha^{-};\alpha^{+},\delta(\alpha^{-})) P_{i}(\alpha^{-};\alpha^{-},\delta(\alpha^{-}),\delta(\alpha^{-}))}{P_{i}(\alpha^{-};\alpha^{+},\delta(\alpha^{-}))} \\ &= \frac{P_{i}$$

Definition 8.10. *In the pair of pants of Figure* 24, *we obtain*

$$(165) \qquad B_{\mathfrak{i}}\left(\alpha^{-};\alpha^{+},\gamma^{-1}(\alpha^{-}),\gamma(\alpha^{-})\right)>1, \ B_{\mathfrak{i}}\left(\alpha^{-};\alpha^{+},\beta(\alpha^{-}),\beta^{-1}(\alpha^{-})\right)>1$$
 and

$$(166) \qquad \mathsf{B}_{\mathfrak{i}}\left(\alpha^{-};\alpha^{+},\gamma^{-1}(\alpha^{-}),\gamma(\alpha^{-})\right) \cdot \mathsf{B}_{\mathfrak{i}}\left(\alpha^{-};\alpha^{+},\beta(\alpha^{-}),\beta^{-1}(\alpha^{-})\right) = e^{\ell_{\mathfrak{i}}(\alpha)}.$$

When we take the limit $\lim_{hyp\to para}$ along the path 1, we have $e^{\ell_1(\alpha)}$ converges to 1. Thus both $B_i\left(\alpha^-;\alpha^+,\gamma^{-1}(\alpha^-),\gamma(\alpha^-)\right)$ and $B_i\left(\alpha^-;\alpha^+,\beta(\alpha^-),\beta^{-1}(\alpha^-)\right)$ converge to 1. For $\delta\in\{\beta,\beta^{-1},\gamma,\gamma^{-1}\}$, we define

(167)
$$R_{i}(\delta, \delta_{\alpha^{-}}) := \frac{\left| \log B_{i}(\alpha^{-}; \alpha^{+}, \delta(\alpha^{-}), \delta^{-1}(\alpha^{-})) \right|}{\ell_{i}(\alpha)}.$$

Then we have

(168)
$$R_{i}(\delta, \delta_{\alpha^{-}}) = R_{i}(\delta^{-1}, \delta_{\alpha^{-}}^{-1}) > 0,$$

and

(169)
$$R_{i}(\gamma, \gamma_{\alpha^{-}}) + R_{i}(\beta, \beta_{\alpha^{-}}) = 1.$$

In the case $S_{g,m}=S_{1,1}$, for $[\mu]\in \overrightarrow{\mathbb{H}}_{\alpha}$, we denote $R_i(\mu)$ instead.

Remark 8.11. Actually $R_1(\delta, \delta_{\alpha^-})$ has a geometric interpretation. With respect to the basis given by $\xi_{\rho}(\alpha^-)$ and $\xi_{\rho}(\alpha^+)$, consider the diagonal matrix $(g_{i,j})$ that fixes $\xi_{\rho}(\alpha^-)$ and $\xi_{\rho}(\alpha^+)$ and translate $\xi_{\rho}^1(\delta(\alpha^-))$ to $\xi_{\rho}^1(\delta^{-1}(\alpha^-))$. Then

(170)
$$R_1(\delta, \delta_{\alpha^-}) = \left| \frac{\log g_{n-1,n-1} - \log g_{n,n}}{\ell_1(\alpha)} \right|.$$

By a choice of fundamental domain, we define the normalized (μ, i) -Goncharov–Shen potential for the boundary case.

Definition 8.12. For $(\rho, \xi) \in \mathcal{X}_{PGL_n, S_{g,m}}(\mathbb{R}_{>0})$ that is a canonical lift of $\rho \in H_n(S_{g,m})$ with the loxodromic monodromy around each boundary component, for any $[Y] \in \overrightarrow{\mathcal{P}}_{\alpha}$ and a choice of its fundamental domain as in Figure 24. Choose a lift X of $\xi(\alpha^-)$ into the decorated flag variety \mathcal{A} . Then we define

(171)
$$B_{\mathfrak{i}}(\gamma,\gamma_{\alpha^{-}}) := \frac{P_{\mathfrak{i}}(\alpha^{-};\gamma^{-1}(\alpha^{-}),\gamma(\alpha^{-}))}{P_{\mathfrak{i}}(\alpha^{-};\gamma^{-1}(\alpha^{-}),\beta^{-1}(\alpha^{-}))},$$

(172)
$$B_{\mathfrak{i}}(\beta,\beta_{\alpha^{-}}) := \frac{P_{\mathfrak{i}}(\alpha^{-};\beta(\alpha^{-}),\beta^{-1}(\alpha^{-}))}{P_{\mathfrak{i}}(\alpha^{-};\gamma^{-1}(\alpha^{-}),\beta^{-1}(\alpha^{-}))}.$$

It is easy to see that

(173)
$$B_{i}(\gamma, \gamma_{\alpha^{-}}) + B_{i}(\beta, \beta_{\alpha^{-}}) = 1$$

When we take the limit $\lim_{hyp\to para}$ along the path l, α^- converges to p, the ratio $B_i(\delta,\delta_{\alpha^-})$ converges to $B_i(\delta,\delta_p)$ for $\delta\in\{\beta,\gamma\}$. Actually $B_i(\delta,\delta_p)$ does not depend on the fundamental domain that we choose.

The following lemma provides the relation between $R_i(\delta, \delta_{\alpha^-})$ and $B_i(\delta, \delta_{\alpha^-})$.

Lemma 8.13. We have

(174)
$$\frac{e^{R_{i}(\gamma,\gamma_{\alpha^{-}})\cdot\ell_{i}(\alpha)}-1}{e^{\ell_{i}(\alpha)}-1}=B_{i}(\gamma,\gamma_{\alpha^{-}}).$$

$$(175) \qquad \frac{e^{R_{i}(\beta,\beta_{\alpha^{-}})\cdot\ell_{i}(\alpha)}-1}{e^{\ell_{i}(\alpha)}-1} = \frac{B_{i}(\beta,\beta_{\alpha^{-}})}{B_{i}(\beta,\beta_{\alpha^{-}})+B_{i}(\gamma,\gamma_{\alpha^{-}})\cdot e^{\ell_{i}(\alpha)}}.$$

Proof. By direct computation

$$\frac{B_{i}\left(\alpha^{-};\alpha^{+},\beta(\alpha^{-}),\beta^{-1}(\alpha^{-})\right)-1}{e^{\ell_{i}(\alpha)}-1} = \frac{\frac{P_{i}(\alpha^{-};\alpha^{+},\beta^{-1}(\alpha^{-}))-P_{i}(\alpha^{-};\alpha^{+},\beta(\alpha^{-}))}{P_{i}(\alpha^{-};\alpha^{+},\beta(\alpha^{-}))}}{e^{\ell_{i}(\alpha)}-1}$$

$$= \frac{P_{i}(\alpha^{-};\beta(\alpha^{-}),\beta^{-1}(\alpha^{-}))}{(e^{\ell_{i}(\alpha)}-1)\cdot P_{i}(\alpha^{-};\alpha^{+},\beta(\alpha^{-}))}$$

$$= \frac{P_{i}(\alpha^{-};\beta(\alpha^{-}),\beta^{-1}(\alpha^{-}))}{P_{i}(\alpha^{-};\alpha^{+},\alpha^{-1}\beta(\alpha^{-}))-P_{i}(\alpha^{-};\alpha^{+},\beta(\alpha^{-}))}$$

$$= \frac{P_{i}(\alpha^{-};\beta(\alpha^{-}),\beta^{-1}(\alpha^{-}))}{P_{i}(\alpha^{-};\beta(\alpha^{-}),\beta^{-1}(\alpha^{-}))+P_{i}(\alpha^{-};\beta^{-1}(\alpha^{-}),\alpha^{-1}\beta(\alpha^{-}))}$$

$$= \frac{P_{i}(\alpha^{-};\beta(\alpha^{-}),\beta^{-1}(\alpha^{-}))+P_{i}(\alpha^{-};\gamma^{-1}(\alpha^{-}),\gamma(\alpha^{-}))}{P_{i}(\alpha^{-};\beta(\alpha^{-}),\beta^{-1}(\alpha^{-}))+e^{\ell_{i}(\alpha)}\cdot P_{i}(\alpha^{-};\gamma^{-1}(\alpha^{-}),\gamma(\alpha^{-}))}$$

$$= \frac{B_{i}(\beta,\beta_{\alpha^{-}})}{B_{i}(\beta,\beta_{\alpha^{-}})+B_{i}(\gamma,\gamma_{\alpha^{-}})\cdot e^{\ell_{i}(\alpha)}}.$$

Similarly for the other formula.

Then Lemma 8.9 and Lemma 8.13 allow us to compute the gap term in Theorem 8.4 as follows.

Lemma 8.14. Evaluating the function $f(A) = \frac{e^A - 1}{e^{\ell_1(\alpha)} - 1}$ at the four gap terms for $\overrightarrow{\mathbb{H}}_{\alpha}$ in Figure 24, we get:

(1)

$$(177) \qquad \frac{B_{\mathfrak{i}}\left(\alpha^{-};\alpha^{+},\gamma^{-1}(\alpha^{-}),\gamma^{-}\right)-1}{e^{\ell_{\mathfrak{i}}(\alpha)}-1} = B_{\mathfrak{i}}(\gamma,\gamma_{\alpha^{-}}) \cdot \frac{1}{1 + \frac{P_{\mathfrak{i}}(\alpha^{-};\gamma^{-},\gamma(\alpha^{-}))}{P_{\mathfrak{i}}(\alpha^{-};\gamma^{-1}(\alpha^{-}),\gamma^{-})}};$$

(2)

$$\frac{B_{\mathfrak{i}}\left(\alpha^{-};\alpha^{+},\gamma^{+},\gamma(\alpha^{-})\right)-1}{e^{\ell_{\mathfrak{i}}\left(\alpha\right)}-1}=B_{\mathfrak{i}}(\gamma,\gamma_{\alpha^{-}})\cdot\frac{1}{1+e^{R_{\mathfrak{i}}\left(\gamma,\gamma_{\alpha^{-}}\right)\cdot\ell_{\mathfrak{i}}\left(\alpha\right)}\cdot\frac{P_{\mathfrak{i}}\left(\alpha^{-};\gamma^{+},\gamma^{-1}(\alpha^{-})\right)}{P_{\mathfrak{i}}\left(\alpha^{-};\gamma(\alpha^{-}),\gamma^{+}\right)}};$$

(3)

$$(179) \qquad = \frac{\frac{B_{\mathfrak{i}}(\alpha^{-};\alpha^{+},\beta(\alpha^{-}),\beta^{+})-1}{e^{\ell_{\mathfrak{i}}(\alpha)}-1}}{B_{\mathfrak{i}}(\beta,\beta_{\alpha^{-}})+B_{\mathfrak{i}}(\gamma,\gamma_{\alpha^{-}})\cdot e^{\ell_{\mathfrak{i}}(\alpha)}} \cdot \frac{1}{1+\frac{P_{\mathfrak{i}}(\alpha^{-};\beta^{+},\beta^{-1}(\alpha^{-}))}{P_{\mathfrak{i}}(\alpha^{-};\beta(\alpha^{-}),\gamma^{-})}};$$

(4)

$$\begin{split} &\frac{B_{\mathfrak{i}}\left(\alpha^{-};\alpha^{+},\beta^{-},\beta^{-1}(\alpha^{-})\right)-1}{e^{\ell_{\mathfrak{i}}(\alpha)}-1} \\ =&\frac{B_{\mathfrak{i}}(\beta,\beta_{\alpha^{-}})}{B_{\mathfrak{i}}(\beta,\beta_{\alpha^{-}})+B_{\mathfrak{i}}(\gamma,\gamma_{\alpha^{-}})\cdot e^{\ell_{\mathfrak{i}}(\alpha)}}\cdot \frac{1}{1+e^{R_{\mathfrak{i}}(\beta,\beta_{\alpha^{-}})\cdot \ell_{\mathfrak{i}}(\alpha)}\cdot \frac{P_{\mathfrak{i}}(\alpha^{-};\beta^{-},\beta(\alpha^{-}))}{P_{\mathfrak{i}}(\alpha^{-};\beta^{-1}(\alpha^{-}),\beta^{-})}}. \end{split}$$

Proof. By direct computation, we have

(181)

$$\begin{split} &\frac{B_{i}\left(\alpha^{-};\alpha^{+},\gamma^{-1}(\alpha^{-}),\gamma^{-}\right)-1}{e^{\ell_{i}\left(\alpha\right)}-1} \\ &= \frac{\frac{B_{i}\left(\alpha^{-};\alpha^{+},\gamma^{-1}(\alpha^{-}),\gamma(\alpha^{-})\right)-B_{i}\left(\alpha^{-};\gamma^{-},\gamma^{-1}(\alpha^{-}),\gamma(\alpha^{-})\right)}{1-B_{i}\left(\alpha^{-};\gamma^{-},\gamma^{-1}(\alpha^{-}),\gamma(\alpha^{-})\right)}-1} \quad \text{by Lemma 8.9} \\ &= \frac{B_{i}\left(\alpha^{-};\alpha^{+},\gamma^{-1}(\alpha^{-}),\gamma(\alpha^{-})\right)-1}{e^{\ell_{i}\left(\alpha\right)}-1} \cdot \frac{1}{1-B_{i}\left(\alpha^{-};\gamma^{-},\gamma^{-1}(\alpha^{-}),\gamma(\alpha^{-})\right)} \\ &= \frac{B_{i}\left(\gamma,\gamma_{\alpha^{-}}\right)}{1+\frac{P_{i}\left(\alpha^{-};\gamma^{-},\gamma(\alpha^{-})\right)}{P_{i}\left(\alpha^{-};\gamma^{-1}(\alpha^{-}),\gamma^{-}\right)}} \quad \text{by Lemma 8.13} \; . \end{split}$$

Similarly for the other cases.

A direct consequence of Lemma 8.14 is the following.

Proposition 8.15. Suppose $\delta \in \{\beta, \beta^{-1}, \gamma, \gamma^{-1}\}$. For the four cases in Lemma 8.14, we have

(182)
$$\lim_{hyp \to para} \frac{|\log B_{i}(\alpha^{-}; \alpha^{+}, \delta(\alpha^{-}), \delta^{+})|}{\ell_{i}(\alpha)} = \frac{B_{i}(\delta, \delta_{p})}{1 + \frac{P_{i}(p; \delta^{+}, \delta^{-1}p)}{P_{i}(p; \delta p, \delta^{+})}}.$$

Lemma 8.16. Suppose $\delta \in \{\beta, \beta^{-1}, \gamma, \gamma^{-1}\}$. For both puncture case x = p and boundary case $x = \alpha^-$, we have

(183)
$$\frac{P_{i}(x; \delta^{+}, \delta^{-1}x)}{P_{i}(x; \delta x, \delta^{+})} = K_{i}(\delta, \delta_{x}) \cdot \frac{\lambda_{i}(\rho(\delta))}{\lambda_{i+1}(\rho(\delta))},$$

where

(184)

$$K_{i}(\delta,\delta_{x}) = \frac{1 + \sum_{c=1}^{i-1} \prod_{j=1}^{c} T_{n-i,j,i-j}(\delta x,\delta^{+},x)}{1 + \sum_{c=1}^{i-1} \prod_{j=1}^{c} T_{n-i,j,i-j}(x,\delta x,\delta^{+})} \cdot \frac{\prod_{j=1}^{n-i-1} T_{n-i-j,j,i}(x,\delta x,\delta^{+})}{\prod_{j=1}^{i-1} T_{j,n-i,i-j}(x,\delta x,\delta^{+})}.$$

Proof. Firstly, we have

(185)
$$\frac{P_{i}(x;\delta^{+},\delta^{-1}(x))}{P_{i}(x;\delta x,\delta^{+})} = \frac{P_{i}(\delta x;\delta^{+},x)}{P_{i}(x;\delta x,\delta^{+})}$$

We compute the right hand side of the above equation instead. By Proposition 4.12, we have

(186)
$$P_{x;\delta^+,\delta x}^i = \alpha_{n-i,i,0}^{x;\delta^+,\delta x} \left(1 + \sum_{c=1}^{i-1} \prod_{j=1}^{c} T_{n-i,j,i-j}(x,\delta x,\delta^+) \right),$$

(187)
$$P_{\delta x; x, \delta^+}^i = \alpha_{n-i, i, 0}^{\delta x; x, \delta^+} \left(1 + \sum_{c=1}^{i-1} \prod_{j=1}^{c} T_{n-i, j, i-j}(\delta x, \delta^+, x) \right).$$

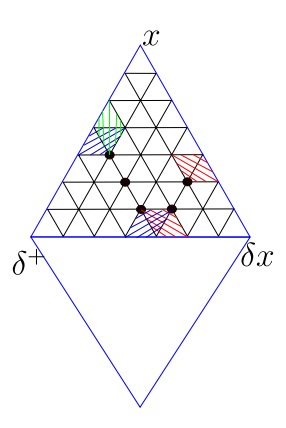


Figure 25. We draw $\alpha_{i,j,k}^{x;\delta^+,\delta x}$, $\alpha_{i,j,k}^{\delta x;x,\delta^+}$, $\alpha_{i,j,k}^{\delta^+;\delta x,x}$ to illustrate our computation.

Then

$$\frac{P_{i}(\delta x; \delta^{+}, x)}{P_{i}(x; \delta x, \delta^{+})} = \frac{P_{i}(\delta x; x, \delta^{+})}{P_{i}(x; \delta^{+}, \delta x)} = \frac{1 + \sum_{c=1}^{i-1} \prod_{j=1}^{c} T_{n-i,j,i-j}(\delta x, \delta^{+}, x)}{1 + \sum_{c=1}^{i-1} \prod_{j=1}^{c} T_{n-i,j,i-j}(x, \delta x, \delta^{+})} \cdot \frac{\alpha_{n-i,i,0}^{\delta x; x, \delta^{+}}}{\alpha_{n-i,i,0}^{x; \delta^{+}, \delta x}}.$$

Observe Figure 25, we obtain

$$(189) \begin{array}{l} \frac{\alpha_{n-i,i,0}^{\delta x;x,\delta^{+}}}{\alpha_{n-i,i,0}^{x;\beta^{+},\delta x}} \\ = \frac{\alpha_{n-i,i,0}^{\delta x;x,\delta^{+}}}{\alpha_{n-i,1,i-1}^{\delta x;x,\delta^{+}}} \cdot \frac{\alpha_{i,1,n-i-1}^{\delta^{+};\delta x,x}}{\alpha_{i,n-i,0}^{\delta^{+};\delta x,x}} \cdot \frac{\alpha_{n-i,1,i-1}^{\delta x;x,\delta^{+}}\alpha_{i,n-i,0}^{\delta^{+};\delta x,x}}{\alpha_{i,1,n-i-1}^{\delta^{+};\delta x,x}\alpha_{n-i,i,0}^{x;\delta^{+},\delta x}} \\ = \prod_{j=1}^{i-1} T_{n-i,j,i-j}(\delta x,x,\delta^{+}) \cdot \frac{1}{\prod_{j=1}^{n-i-1} T_{i,j,n-i-j}(\delta^{+},\delta x,x)} \cdot \frac{\alpha_{n-i,1,i-1}^{\delta x;x,\delta^{+}}\alpha_{i,n-i,0}^{\delta^{+};\delta x,x}}{\alpha_{i,1,n-i-1}^{\delta^{+};\delta x,x}\alpha_{i,1,n-i-1}^{x;\delta^{+};\delta x,x}} \\ = \frac{\prod_{j=1}^{n-i-1} T_{n-i-j,j,i}(x,\delta x,\delta^{+})}{\prod_{j=1}^{i-1} T_{j,n-i,i-j}(x,\delta x,\delta^{+})} \cdot \frac{\alpha_{n-i,1,i-1}^{\delta x;x,\delta^{+}}\alpha_{i,n-i,0}^{\delta^{+};\delta x,x}}{\alpha_{n-i,1,i-1}^{\delta^{+};\delta x,x}\alpha_{n-i,i,0}^{x;\delta^{+},\delta x}}. \end{array}$$

By Lemma 4.8, we get

$$\begin{split} &\frac{\alpha_{n-i,1,i-1}^{\delta x;x,\delta^+}\alpha_{i,n-i,0}^{\delta^+;\delta x,x}}{\alpha_{i,1,n-i-1}^{\delta^+;\delta x,x}\alpha_{i,i,0}^{\delta^+;\delta x,x}} \\ &= \frac{\frac{\Delta\left((\delta x)^{n-i+1}\wedge\delta^{i-1}\right)\cdot\Delta\left((\delta x)^{n-i-1}\wedge\delta^{i}\wedge x^1\right)}{\Delta\left((\delta x)^{n-i}\wedge\delta^{i-1}\wedge x^1\right)\cdot\Delta\left((\delta x)^{n-i-1}\wedge\delta^{i}\wedge x^1\right)}}{\frac{\Delta\left((\delta x)^{n-i}\wedge\delta^{i-1}\wedge x^1\right)\cdot\Delta\left((\delta x)^{n-i-1}\wedge\delta^{i}\wedge x^1\right)}{\Delta\left((\delta x)^{n-i-1}\wedge\delta^{i-1}\wedge x^1\right)\cdot\Delta\left((\delta x)^{n-i-1}\right)}} \cdot \frac{\frac{\Delta\left(\delta^{i+1}\wedge(\delta x)^{n-i-1}\right)\cdot\Delta\left(\delta^{i-1}\wedge x^1\wedge(\delta x)^{n-i}\right)}{\Delta\left(\delta^{i}\wedge x^{n-i-1}\wedge(\delta x)^1\right)\cdot\Delta\left(\delta^{i}\wedge x^{n-i}\right)}}{\frac{\Delta\left(\delta^{i+1}\wedge x^{n-i-1}\wedge(\delta x)^1\right)\cdot\Delta\left(\delta^{i}\wedge x^{n-i-1}\right)}{\Delta\left(\delta^{i}\wedge x^{n-i-1}\wedge(\delta x)^1\wedge\delta^{i-1}\right)}} \\ &= \frac{\frac{\Delta\left((\delta x)^{n-i+1}\wedge\delta^{i-1}\right)}{\Delta\left((\delta x)^{n-i+1}\wedge\delta^{i-1}\right)}\cdot\frac{\Delta\left(\delta^{i+1}\wedge(\delta x)^{n-i-1}\right)}{\Delta\left(\delta^{i}\wedge x^{n-i-1}\right)}}{\frac{\Delta\left((\delta x)^{n-i}\wedge\delta^{i}\right)}{\Delta\left(x^{n-i}\wedge\delta^{i}\right)}\cdot\frac{\Delta\left(\delta^{i}\wedge(\delta x)^{n-i}\right)}{\Delta\left(\delta^{i}\wedge x^{n-i}\right)}} \\ &= \frac{\frac{1}{\lambda_1\cdots\lambda_{i-1}(\rho(\delta))}\cdot\frac{1}{\lambda_1\cdots\lambda_{i+1}(\rho(\delta))}}{\frac{1}{\lambda_1\cdots\lambda_{i}(\rho(\delta))}\cdot\frac{1}{\lambda_1\cdots\lambda_{i}(\rho(\delta))}}} \\ &= \frac{\lambda_i\left(\rho(\delta)\right)}{\lambda_{i+1}(\rho(\delta))}. \end{split}$$

We conclude that

(191)
$$\frac{P_{i}(x; \delta^{+}, \delta^{-1}(x))}{P_{i}(x; \delta x, \delta^{+})} = K_{i}(\delta, \delta_{x}) \cdot \frac{\lambda_{i}(\rho(\delta))}{\lambda_{i+1}(\rho(\delta))}.$$

Proof of Theorem 8.5. For any $[\delta, \delta_{\alpha^-}] \in \overrightarrow{\mathcal{H}}_{\alpha}$, when we take the limit $\lim_{hyp\to para}$ in Definition 8.6 along the path l, by Proposition 8.15 and Lemma 8.16, for $\delta \in \{\beta, \beta^{-1}, \gamma, \gamma^{-1}\}$, the gap term $|\log B_i(\alpha^-; \alpha^+, \delta(\alpha^-), \delta^+)|$ over $\ell_i(\alpha)$ in Theorem 8.4 deforms to

(192)
$$\frac{B_{i}(\delta, \delta_{p})}{1 + K_{i}(\delta, \delta_{p}) \cdot \frac{\lambda_{i}(\rho(\delta))}{\lambda_{i+1}(\rho(\delta))}}.$$

For any $[\mu] \in \overrightarrow{\mathcal{H}}^{\mathfrak{d}}_{\alpha}$, by Proposition 8.7, when we take the limit $\lim_{hyp \to para}$, the gap term $\log B_{\mathfrak{t}}(\alpha^-; \alpha^+, \gamma^-, \gamma^+)$ over $\ell_{\mathfrak{t}}(\alpha)$ is 0. We conclude that

(193)
$$\sum_{[\delta,\delta_{\mathfrak{p}}]\in\overrightarrow{\mathcal{H}}_{\mathfrak{p}}}\left(\frac{B_{\mathfrak{i}}(\delta,\delta_{\mathfrak{p}})}{1+K_{\mathfrak{i}}(\delta,\delta_{\mathfrak{p}})\cdot\frac{\lambda_{\mathfrak{i}}(\rho(\delta))}{\lambda_{\mathfrak{i}+1}(\rho(\delta))}}\right)\leqslant 1.$$

8.3. Expressing the hyperbolic bordered McShane identity summand. The following corollary gives a geometric expression of the gap term in the summation $\overrightarrow{\mathcal{H}}_{\alpha}$ of Theorem 8.4. Let us define

(194)
$$\kappa_{i}(\delta, \delta_{x}) := \log K_{i}(\delta, \delta_{x}).$$

Theorem 8.17. In Theorem 8.4, the gap terms in $\overrightarrow{\mathbb{H}}_{\alpha}$ for Figure 24 are geometrically expressed in the following form: for $\delta \in \{\beta, \beta^{-1}, \gamma, \gamma^{-1}\}$, we have

(195)
$$\left|\log B_{\mathfrak{i}}\left(\alpha^{-};\alpha^{+},\delta(\alpha^{-}),\delta^{+}\right)\right| = \left|\log \frac{e^{R_{\mathfrak{i}}(\delta,\delta_{\alpha^{-}})\cdot\ell_{\mathfrak{i}}(\alpha)} + e^{\kappa_{\mathfrak{i}}(\delta,\delta_{\alpha^{-}})+\ell_{\mathfrak{i}}(\delta)}}{1 + e^{\kappa_{\mathfrak{i}}(\delta,\delta_{\alpha^{-}})+\ell_{\mathfrak{i}}(\delta)}}\right|.$$

Proof. Directly derive from Lemma 8.9 and Lemma 8.16.

Definition 8.18. We generalize d_1 and d_2 in Theorem 5.10 using i-th ratios:

$$(196) \qquad d_1:=\log\frac{P_{\mathfrak{t}}(\alpha^-;\gamma^+,\gamma(\alpha^-))}{P_{\mathfrak{t}}(\alpha^-;\beta(\alpha^-),\beta^+)}, \quad d_2:=\log\frac{P_{\mathfrak{t}}(\alpha^-;\gamma^{-1}(\beta^+),\gamma^{-1}(\alpha^-))}{P_{\mathfrak{t}}(\alpha^-;\gamma^{-1}(\alpha^-),\gamma^+)}.$$

Let

(197)
$$e^{d} := \frac{\cosh \frac{d_2}{2}}{\cosh \frac{d_1}{2}}.$$

Lemma 8.19.

(198)

$$\frac{e^{\ell_{\mathfrak{i}}(\alpha)} \cdot P_{\mathfrak{i}}(\alpha^-; \gamma(\beta^+), \gamma^+)}{P_{\mathfrak{i}}(\alpha^-; \gamma^+, \beta^+)} = \frac{\cosh \frac{d_2}{2}}{\cosh \frac{d_1}{2}} \cdot e^{\frac{1}{2}(\kappa_{\mathfrak{i}}(\gamma, \gamma_{\alpha^-}) + \ell_{\mathfrak{i}}(\gamma) + \kappa_{\mathfrak{i}}(\beta, \beta_{\alpha^-}) + \ell_{\mathfrak{i}}(\beta) + \ell_{\mathfrak{i}}(\alpha))}.$$

Proof. By Lemma 8.16 we have

$$e^{d_1+d_2+\kappa_i(\gamma,\gamma_{\alpha}-)+\ell_i(\gamma)}$$

$$\begin{aligned} \text{(199)} \quad &= \frac{P_{\mathfrak{i}}(\alpha^{-};\gamma^{+},\gamma(\alpha^{-}))}{P_{\mathfrak{i}}(\alpha^{-};\beta(\alpha^{-}),\beta^{+})} \cdot \frac{P_{\mathfrak{i}}(\alpha^{-};\gamma^{-1}(\beta^{+}),\gamma^{-1}(\alpha^{-}))}{P_{\mathfrak{i}}(\alpha^{-};\gamma^{-1}(\alpha^{-}),\gamma^{+})} \cdot \frac{P_{\mathfrak{i}}(\alpha^{-};\gamma^{+},\gamma^{-1}(\alpha^{-}))}{P_{\mathfrak{i}}(\alpha^{-};\gamma(\alpha^{-}),\gamma^{+})} \\ &= \frac{P_{\mathfrak{i}}(\alpha^{-};\gamma^{-1}(\beta^{+}),\gamma^{-1}(\alpha^{-}))}{P_{\mathfrak{i}}(\alpha^{-};\beta(\alpha^{-}),\beta^{+})}. \end{aligned}$$

By $\alpha^{-1}\gamma^{-1} = \beta^{-1}$ and Proposition 4.16, the above equation equals to

$$(200) \qquad \frac{e^{-\ell_{\mathfrak{i}}(\alpha)} \cdot P_{\mathfrak{i}}(\alpha^{-}; \beta^{+}, \beta^{-1}(\alpha^{-}))}{P_{\mathfrak{i}}(\alpha^{-}; \beta(\alpha^{-}), \beta^{+})} = e^{\kappa_{\mathfrak{i}}(\beta, \beta_{\alpha^{-}}) + \ell_{\mathfrak{i}}(\beta) - \ell_{\mathfrak{i}}(\alpha)}.$$

Thus

(201)

$$\frac{\cosh\frac{d_2}{2}}{\cosh\frac{d_1}{2}} \cdot e^{\frac{1}{2}(\kappa_{\mathfrak{i}}(\gamma,\gamma_{\alpha}-)+\ell_{\mathfrak{i}}(\gamma)+\kappa_{\mathfrak{i}}(\beta,\beta_{\alpha}-)+\ell_{\mathfrak{i}}(\beta)+\ell_{\mathfrak{i}}(\alpha))} = \frac{1+e^{-d_2}}{1+e^{d_1}} \cdot e^{\kappa_{\mathfrak{i}}(\beta,\beta_{\alpha}-)+\ell_{\mathfrak{i}}(\beta)}$$

$$= \frac{\frac{P_{\mathfrak{i}}(\alpha^-;\gamma^{-1}(\beta^+),\gamma^+)}{P_{\mathfrak{i}}(\alpha^-;\gamma^+,\beta^+)}}{\frac{P_{\mathfrak{i}}(\alpha^-;\beta^+,\beta^+)}{P_{\mathfrak{i}}(\alpha^-;\beta(\alpha^-),\beta^+)}} \cdot \frac{P_{\mathfrak{i}}(\alpha^-;\beta^+,\beta^{-1}(\alpha^-))}{P_{\mathfrak{i}}(\alpha^-;\beta(\alpha^-),\beta^+)} = \frac{e^{\ell_{\mathfrak{i}}(\alpha)} \cdot P_{\mathfrak{i}}(\alpha^-;\gamma^{-1}(\beta^+),\gamma^+)}{P_{\mathfrak{i}}(\alpha^-;\gamma^+,\beta^+)}.$$

Theorem 8.20. *In Figure* 24, *the gap term for one* $\{\beta, \gamma\} \in \vec{\mathbb{P}}_{\alpha}$ *is expressed geometrically in the following way:*

(202)
$$\log B_i(\alpha^-; \alpha^+, \gamma^+, \beta^+)$$

$$(203) \qquad = \log \left(\frac{e^{\ell_{\mathfrak{i}}(\alpha)} + \frac{\cosh\frac{d_{\mathfrak{j}}}{2}}{\cosh\frac{d_{\mathfrak{j}}}{2}} \cdot e^{\frac{1}{2}(\kappa_{\mathfrak{i}}(\gamma,\gamma_{\alpha^{-}}) + \ell_{\mathfrak{i}}(\gamma) + \kappa_{\mathfrak{i}}(\beta,\beta_{\alpha^{-}}) + \ell_{\mathfrak{i}}(\beta) + \ell_{\mathfrak{i}}(\alpha))}}{1 + \frac{\cosh\frac{d_{\mathfrak{j}}}{2}}{\cosh\frac{d_{\mathfrak{j}}}{2}} \cdot e^{\frac{1}{2}(\kappa_{\mathfrak{i}}(\gamma,\gamma_{\alpha^{-}}) + \ell_{\mathfrak{i}}(\gamma) + \kappa_{\mathfrak{i}}(\beta,\beta_{\alpha^{-}}) + \ell_{\mathfrak{i}}(\beta) + \ell_{\mathfrak{i}}(\alpha))}} \right).$$

Remark 8.21. The relation between the ordered cross ratio $\mathbb B$ used in Labourie–McShane identity [LM09] and the i-th ratio is provided by Corollary 4.15. Combing with Theorem 8.20, we also have geometrical expression for the Labourie–McShane identities.

Proof. We show two sides of the above equation are equal by evaluating two sides at the strictly increasing function $f(A) = \frac{e^A - 1}{e^{\ell_1}(\alpha) - 1}$. Then the left side becomes into

$$\frac{P_{\mathfrak{t}}(\alpha^-;\gamma^+,\beta^+)}{P_{\mathfrak{t}}(\alpha^-;\alpha^+,\gamma^+)\cdot(e^{\ell_{\mathfrak{t}}(\alpha)}-1)}\text{, and the right side becomes into }\frac{1}{1+\frac{e^{\ell_{\mathfrak{t}}(\alpha)}\cdot P_{\mathfrak{t}}(\alpha^-;\gamma^{-1}(\beta^+),\gamma^+)}{P_{\mathfrak{t}}(\alpha^-;\gamma^+,\beta^+)}}$$

by Lemma 8.19. By Proposition 4.16, we have

(204)
$$\begin{aligned} P_{i}(\alpha^{-}; \alpha^{+}, \gamma^{+}) \cdot (e^{\ell_{i}(\alpha)} - 1) \\ = P_{i}(\alpha^{-}; \alpha^{+}, \alpha^{-1}(\gamma^{+})) - P_{i}(\alpha^{-}; \alpha^{+}, \gamma^{+}) \\ = P_{i}(\alpha^{-}; \gamma^{+}, \alpha^{-1}(\gamma^{+})). \end{aligned}$$

Then this theorem is equivalent to show

$$(205) \qquad P_{i}(\alpha^{-};\gamma^{+},\alpha^{-1}(\gamma^{+})) = e^{\ell_{i}(\alpha)} \cdot P_{i}(\alpha^{-};\gamma^{-1}(\beta^{+}),\gamma^{+}) + P_{i}(\alpha^{-};\gamma^{+},\beta^{+}),$$
 or equivalently

(206)
$$P_{i}(\alpha^{-};\beta^{+},\alpha^{-1}(\gamma^{+})) = e^{\ell_{i}(\alpha)} \cdot P_{i}(\alpha^{-};\gamma^{-1}(\beta^{+}),\gamma^{+}),$$

which is a consequence of Proposition 4.16.

Proposition 8.22. In Figure 24, the gap term for one $[Y] \in \overrightarrow{\mathcal{H}}^{\mathfrak{d}}_{\alpha}$ is expressed geometrically in the following way:

Let

(207)
$$d_1' := \log \frac{P_i(\alpha^-; \gamma^-, \gamma(\alpha^-))}{P_i(\alpha^-; \beta(\alpha^-), \beta^+)}, \quad d_2' := \log \frac{P_i(\alpha^-; \gamma^{-1}(\beta^+), \gamma^{-1}(\alpha^-))}{P_i(\alpha^-; \gamma^{-1}(\alpha^-), \gamma^-)}.$$

Let

(208)
$$e^{\mathbf{d}'} := \frac{\cosh \frac{\mathbf{d}'_2}{2}}{\cosh \frac{\mathbf{d}'_1}{2}}.$$

Then

(209)
$$\log B_i\left(\alpha^-;\alpha^+,\gamma^-,\gamma^+\right) = \log\left(\frac{\cosh\frac{1}{4}A + \cosh\frac{1}{4}B}{\cosh\frac{1}{4}A + \cosh\frac{1}{4}C}\right),$$

where

(210)

$$\overset{.}{A}=\overset{.}{2}\kappa_{\mathfrak{i}}(\beta,\beta_{\alpha^{-}})+2\ell_{\mathfrak{i}}(\beta)+\kappa_{\mathfrak{i}}(\gamma,\gamma_{\alpha^{-}})+\ell_{\mathfrak{i}}(\gamma)-\kappa_{\mathfrak{i}}(\gamma^{-1},\gamma_{\alpha^{-}}^{-1})-\ell_{\mathfrak{i}}(\gamma^{-1})+2d+2d',$$

$$(211) \qquad B=2\ell_{\mathfrak{i}}(\alpha)+\kappa_{\mathfrak{i}}(\gamma,\gamma_{\alpha^{-}})+\ell_{\mathfrak{i}}(\gamma)+\kappa_{\mathfrak{i}}(\gamma^{-1},\gamma_{\alpha^{-}}^{-1})+\ell_{\mathfrak{i}}(\gamma^{-1})+2d-2d',$$

$$(212) \hspace{0.5cm} C = -2\ell_{\mathfrak{i}}(\alpha) + \kappa_{\mathfrak{i}}(\gamma,\gamma_{\alpha^{-}}) + \ell_{\mathfrak{i}}(\gamma) + \kappa_{\mathfrak{i}}(\gamma^{-1},\gamma_{\alpha^{-}}^{-1}) + \ell_{\mathfrak{i}}(\gamma^{-1}) + 2d - 2d'.$$

Proof. Similar to the prove of Theorem 8.20, we have

$$(213) \quad = \log \left(\frac{e^{\ell_{\mathfrak{i}}(\alpha)} + \frac{\cosh \frac{d_{\mathfrak{i}}'}{2}}{\cosh \frac{d_{\mathfrak{i}}'}{2}} \cdot e^{\frac{1}{2} \left(-\kappa_{\mathfrak{i}}(\gamma^{-1}, \gamma_{\alpha^{-}}^{-1}) - \ell_{\mathfrak{i}}(\gamma^{-1}) + \kappa_{\mathfrak{i}}(\beta, \beta_{\alpha^{-}}) + \ell_{\mathfrak{i}}(\beta) + \ell_{\mathfrak{i}}(\alpha) \right)}{1 + \frac{\cosh \frac{d_{\mathfrak{i}}'}{2}}{\cosh \frac{d_{\mathfrak{i}}'}{2}} \cdot e^{\frac{1}{2} \left(-\kappa_{\mathfrak{i}}(\gamma^{-1}, \gamma_{\alpha^{-}}^{-1}) - \ell_{\mathfrak{i}}(\gamma^{-1}) + \kappa_{\mathfrak{i}}(\beta, \beta_{\alpha^{-}}) + \ell_{\mathfrak{i}}(\beta) + \ell_{\mathfrak{i}}(\alpha) \right)} \right).$$

Then the formula is obtained through

$$\begin{array}{l} \left(214\right) \\ \log B_{i}\left(\alpha^{-};\alpha^{+},\gamma^{-},\gamma^{+}\right) = \log B_{i}\left(\alpha^{-};\alpha^{+},\gamma^{-},\beta^{+}\right) - \log B_{i}\left(\alpha^{-};\alpha^{+},\gamma^{+},\beta^{+}\right). \end{array}$$

8.4. A strategy for establishing the unipotent bordered McShane identity.

Theorem 8.23 (equality under assumption). *Assume that we have the following property, denoted by* (*):

For ρ on the path 1 with the loxodromic monodromy around each boundary component, let $D_i(N,\rho)=\#[\delta]\in \vec{\mathbb{C}}_{g,m}\mid \log\frac{\lambda_i(\rho(\delta))}{\lambda_{i+1}(\rho(\delta))}\leqslant N\}$ where $\vec{\mathbb{C}}_{g,m}$ is the set of free homotopy classes of simple closed curves on $S_{g,m}$, or equivalently, the set of $\pi_1(S_{g,m})$ conjugacy classes of simple homotopy classes. Then

(215)
$$D_{i}(N,\rho) = c(\rho) \cdot N^{6g-6+2m} + o(N^{6g-6+2m}),$$

where $c(\rho)$ is a continuous function.

Then the inequality in theorem 8.5 is an equality.

Remark 8.24. *The assumption generalizes Mirzakhani's result for Teichmüller space into the* $PGL(n, \mathbb{R})$ *-Hitchin component.*

Proof. Given $(\rho', \xi') \in \mathcal{A}_{SL_n, S_{g,m}}(\mathbb{R}_{>0})$, let l be the path in Definition 8.6 such that $l(1) = (\rho', \xi')$. Since the path l is compact, we have the following bounds in the path l:

- (1) the limit of $\frac{e^{\ell_{\mathfrak{i}}(\alpha)}-1}{\ell_{\mathfrak{i}}(\alpha)}$ under $\lim_{hyp\to para}$ is 1, so $\frac{e^{\ell_{\mathfrak{i}}(\alpha)}-1}{\ell_{\mathfrak{i}}(\alpha)}$ is upper bounded by a constant $C_0>0$;
- (2) by Theorem 3.4, the triple ratios in the mapping class group orbit in the closed path l is bounded away from 0, thus $K(\delta, \delta_{\alpha^-})$ is lower bounded by a constant K>0.

Moreover, fix $\delta \in \pi_1(S_{g,m})$, the sum over different δ_{α} :

$$\sum_{[\delta,\delta_{\alpha^{-}}]\in\overrightarrow{\mathcal{H}}_{\alpha}}B_{\mathfrak{i}}(\delta,\delta_{\alpha^{-}})\leqslant 1$$

for any $l(s) \in \mathfrak{X}_{PGL_n,S_{q,m}}(\mathbb{R}_{>0})$. Thus we get

$$\sum_{\substack{[\delta,\delta_{\alpha^{-}}]\in\overrightarrow{\mathcal{H}}_{\alpha}}} \frac{|\log B_{i}\left(\alpha^{-};\alpha^{+},\delta(\alpha^{-}),\delta^{+}\right)|}{\ell_{i}(\alpha)}$$

$$\leqslant \frac{e^{\ell_{i}(\alpha)}-1}{\ell_{i}(\alpha)} \cdot \sum_{\substack{[\delta,\delta_{\alpha^{-}}]\in\overrightarrow{\mathcal{H}}_{\alpha}}} \left(\frac{B_{i}(\delta,\delta_{\alpha^{-}})}{1+K_{i}(\delta,\delta_{\alpha^{-}})\cdot e^{\ell_{i}(\delta)}}\right) \quad \text{Lemma 8.14}$$

$$\leqslant C_{0} \cdot \sum_{\substack{[\delta]\in\overrightarrow{\mathcal{C}}_{g,m}}} \sum_{\substack{[\delta,\delta_{\alpha^{-}}]\in\overrightarrow{\mathcal{H}}_{\alpha}}} \left(\frac{B_{i}(\delta,\delta_{\alpha^{-}})}{1+K_{i}(\delta,\delta_{\alpha^{-}})\cdot e^{\ell_{i}(\delta)}}\right)$$

$$\leqslant C_{0} \cdot \sum_{\substack{[\delta]\in\overrightarrow{\mathcal{C}}_{g,m}}} \sum_{\substack{[\delta,\delta_{\alpha^{-}}]\in\overrightarrow{\mathcal{H}}_{\alpha}}} \left(\frac{B_{i}(\delta,\delta_{\alpha^{-}})}{1+K\cdot e^{\ell_{i}(\delta)}}\right)$$

$$\leqslant C_{0} \cdot \sum_{\substack{[\delta]\in\overrightarrow{\mathcal{C}}_{g,m}}} \frac{1}{K\cdot e^{\ell_{i}(\delta)}}$$

$$\leqslant C_{0} \cdot \sum_{t=1}^{+\infty} \frac{\left(D_{i}(t,\rho)-D_{i}(t-1,\rho)\right)}{K\cdot e^{t}}.$$

Since the continuous function $c(\rho)$ is also bounded by a constant Q>0 in the path l, we have $C_0\cdot\sum_{t=1}^{+\infty}\frac{(D_{\iota}(t,\rho)-D_{\iota}(t-1,\rho))}{C_1\cdot K\cdot e^t}$ is uniform convergent. Thus

(217)
$$\sum_{[\delta,\delta_{\alpha^{-}}]\in\overline{\mathcal{H}}_{\alpha}} \frac{|\log B_{i}(\alpha^{-};\alpha^{+},\delta(\alpha^{-}),\delta^{+})|}{\ell_{i}(\alpha)}$$

converges uniformly to 1 on the path l. Thus on l(1), we conclude that

(218)
$$\sum_{[\delta,\delta_{\alpha}-]\in\overrightarrow{\mathcal{H}}_{p}}\left(\frac{B_{i}(\delta,\delta_{p})}{1+K_{i}(\delta,\delta_{p})\cdot\frac{\lambda_{i}(\rho(\delta))}{\lambda_{i+1}(\rho(\delta))}}\right)=1.$$

ACKNOWLEDGEMENTS

The authors wish to thank Yves Benoist, Vladimir Fock, Maxim Kontsevich, François Labourie, Robert Penner, Andres Sambarino, Linhui Shen, Nicolas Tholozan, Binbin Xu, Yunhui Wu and Tengren Zhang for your active interest in our project and for helpful and stimulating discussions. We also wish to thank many, *many* others in the community whose support has sustained us throughout this long project: your words have been truly encouraging. The bulk of this work was conducted at the Yau Mathematical Sciences Center (Tsinghua University), but key insights were also developed thanks to the generous hospitality of the Institut des Hautes Études Scientifique, the Institute for Mathematical Sciences (National University of Singapore) and the University of Melbourne.

FUNDING

The first author wishes to state that this work was supported by the China Post-doctoral Science Foundation [grant numbers 2016M591154, 2017T100058]. The

second author wishes to state that this work was supported by the China Postdoctoral Science Foundation 2018T110084 and FNR AFR bilateral grant COALAS 11802479-2. The second author also acknowledges support from U.S. National Science Foundation grants DMS-1107452, 1107263, 1107367 "RNMS:GEometric structures And Representation varieties" (the GEAR Network).

APPENDIX A. HILBERT LENGTH VERSUS SIMPLE ROOT LENGTH COMPARISON

This is a proof of Theorem 7.11:

Theorem A.1 (Hilbert vs. simple root length comparison). For any positive representation $\rho: \pi_1(S) \to PGL_3(\mathbb{R})$, there exists $K_{\rho} > 1$ such that for every simple closed curve γ on S, we have:

(219)
$$\ell_1(\gamma) < \ell(\gamma) < K_o \cdot \ell_1(\gamma).$$

Proof. The left inequality is obvious. For the right inequality, we first consider the case when S is closed. In this case, let K_{ρ} be the supremum of the ratio between the infinitesimal expansion rates for the Hilbert length flow and the simple root length flow [BCLS18] for ρ . The fact that K_{ρ} exists is due to the compactness of the unit tangent space T¹S. When S has boundary components, we double [Lab07] ρ along its hyperbolic boundaries to a positive representation dρ on a doubled surface dS. If dS is closed, we invoke the previous argument, and thus we have reduced ourselves to the case when every boundary of ρ is unipotent.

Consider a positive representation ρ with (only) unipotent boundary monodromy, and let $\{\gamma_k\}$ denote a sequence of simple closed curves for which $\ell^{\rho}(\gamma_k)/\ell_1^{\rho}(\gamma_k)$ tends to the supremum of $\ell^{\rho}(\cdot)/\ell_1^{\rho}(\cdot)$. The compactness of $\mathcal{PML}(S_{1,1})$ means that we may replace $\{\gamma_k\}$ with a subsequence such that there are lifts $\tilde{\gamma}_k$ in the universal cover Ω for the cusped convex real projective surface Σ with monodromy representation ρ converge to an (oriented) lifted leaf $\tilde{\gamma}_{\infty}$ of some geodesic lamination on Σ . By possibly conjugating ρ , we assume without loss of generality that the flag at $\tilde{\gamma}_{\infty}^{+}$ is given by

$$U_1 = Span\left\{\left[\begin{smallmatrix}1\\0\\1\end{smallmatrix}\right]\right\} \subset U_2 = Span\left\{\left[\begin{smallmatrix}1\\0\\1\end{smallmatrix}\right], \left[\begin{smallmatrix}0\\0\\1\\1\end{smallmatrix}\right]\right\} \subset U_3 = \mathbb{R}^3$$

and the flag at $\tilde{\gamma}_{\infty}^{-}$ is given by

$$V_1 = Span\left\{\left[\begin{smallmatrix}0\\1\\1\end{smallmatrix}\right]\right\} \subset V_2 = Span\left\{\left[\begin{smallmatrix}0\\1\\1\end{smallmatrix}\right], \left[\begin{smallmatrix}0\\0\\1\end{smallmatrix}\right]\right\} \subset V_3 = \mathbb{R}^3.$$

We also fix an arbitrary point $[x : y : 1]^t \in \partial\Omega$ which is somewhere below the geodesic from $\tilde{\gamma}_{\infty}^-$ to $\tilde{\gamma}_{\infty}^+$. Note in particular that $x+y\in(0,1).$ Now consider the sequence of (unique) projective linear transformations $M_k \in PGL_3(\mathbb{R})$ which

- maps the flag at $\tilde{\gamma}_k^+$ to $U_1 \subset U_2 \subset U_3$,
- maps the flag at $\tilde{\gamma}_k$ to $V_1 \subset V_2 \subset V_3$, and fixes $[x:y:1]^t \in \partial \Omega$.

We observe that k tends to infinity, the matrices M_k approach the identity matrix.

We know from Proposition 6.9 that Ω satisfies β_{ρ} -regularity for some (finite) $\beta_{\rho}\geqslant 2$. This means that there exists C>0 such that for all $p,q\in\partial\Omega,$ we have:

$$d_{\mathsf{E}}(\mathsf{q},\mathsf{T}_{\mathsf{p}}\partial\Omega)\geqslant C^{-1}\cdot d_{\mathsf{E}}(\mathsf{q},\mathsf{p})^{\beta_{\mathsf{p}}}.$$

The regularity coefficient β_{ρ} is preserved under projective linear transformations, and by applying M_k sufficiently close to the identity matrix (i.e.: for all k sufficiently high) to with $p = \tilde{\gamma}_k^+$, we have:

(220)
$$d_{E}(M_{k} \cdot q, U_{2}) > (2C)^{-1} \cdot d_{E}(M_{k} \cdot q, U_{1})^{\beta_{\rho}}.$$

Explicit computation shows that $M_k \cdot \rho(\gamma_k) \cdot M_k^{-1}$ acts as the matrix

and hence $M_k \cdot \rho(\gamma_k) \cdot [x:y:1]^t = M_k \cdot \rho(\gamma_k) \cdot M_k^{-1} \cdot [x:y:1]^t$ is equal to

$$\left[\frac{x\lambda_1}{x(\lambda_1 - \lambda_2) + y(\lambda_3 - \lambda_2) + \lambda_2} : \frac{y\lambda_3}{x(\lambda_1 - \lambda_2) + y(\lambda_3 - \lambda_2) + \lambda_2} : 1 \right]^t.$$

We now consider equation (220) after taking $q = \rho(\gamma_k) \cdot [x:y:1]^t$ in. The left hand side of the inequality satisfies

(223)
$$d_E(M_k \cdot q, U_2) = \frac{y\lambda_3}{x(\lambda_1 - \lambda_2) + y(\lambda_3 - \lambda_2) + \lambda_2} < \frac{2y\lambda_3(\gamma_k)}{x\lambda_1(\gamma_k)}$$
, for sufficiently large k.

Similarly, the right hand side term $d_E(M_k \cdot q, U_1)$ satisfies

(224)
$$d_E(M_k \cdot q, U_1) > 1 - \frac{x\lambda_1}{x(\lambda_1 - \lambda_2) + y(\lambda_3 - \lambda_2) + \lambda_2} = \frac{-x\lambda_2 + y(\lambda_3 - \lambda_2) + \lambda_2}{x(\lambda_1 - \lambda_2) + y(\lambda_3 - \lambda_2) + \lambda_2}$$

(225)
$$> \frac{(1-x-y)\lambda_2(\gamma_k)}{2x\lambda_1(\gamma_k)}$$
, for sufficiently large k.

Putting all of this together, we obtain that

$$\frac{2y\lambda_3}{x\lambda_1} > \frac{(1-x-y)^{\beta} \rho \lambda_2^{\beta} \rho}{2C(2x)^{\beta} \rho \lambda_1^{\beta} \rho},$$

and therefore $\beta_{\rho}\ell_1(\gamma_k) > \ell(\gamma_k) - \log(C')$ for some constant C'. Since

(227)
$$\beta_{\rho} \geqslant \lim_{k \to \infty} \frac{\ell(\gamma_k) - \log(C')}{\ell_1(\gamma_k)} = \lim_{k \to \infty} \frac{\ell(\gamma_k)}{\ell_1(\gamma_k)},$$

we see that K_o not only exists, but is bounded above by β_o .

REFERENCES

[AC15] Ilesanmi Adeboye and Daryl Cooper, *The area of convex projective surfaces and Fock–Goncharov coordinates*, Journal of Topology and Analysis (2018). 5

[AMS04] Hirotaka Akiyoshi, Hideki Miyachi, and Makoto Sakuma, A refinement of McShane's identity for quasifuchsian punctured torus groups, Contemporary Mathematics 355 (2004), 21–40. 2, 12

[AMS06] —, Variations of McShane's identity for punctured surface groups, Spaces of Kleinian groups, London Math. Soc. Lecture Note Ser., vol. 329, Cambridge Univ. Press, Cambridge, 2006, pp. 151–185. 2, 12

[Bas93] Ara Basmajian, *The orthogonal spectrum of a hyperbolic manifold*, American Journal of Mathematics 115 (1993), no. 5, 1139–1159. 2

[BCL17] Martin Bridgeman, Richard Canary, and François Labourie, *Simple length rigidity for Hitchin representations*, arXiv preprint arXiv:1703.07336. (2017). 70

[BCLS18] Martin Bridgeman, Richard Canary, François Labourie, and Andres Sambarino, Simple root flows for Hitchin representations, Geometriae Dedicata 192 (2018), no. 1, 57–86. 86

[BD14] Francis Bonahon and Guillaume Dreyer, *Parameterizing Hitchin components*, Duke Mathematical Journal **163** (2014), no. 15, 2935–2975. 2, 4

[BD17] —, Hitchin characters and geodesic laminations, Acta Mathematica 218 (2017), no. 2, 201-295. 2

[Ben01] Yves Benoist, *Convexes divisibles I*, Algebraic groups and arithmetic. Tata Inst. Fund. Res. Stud. Math. 17 (2004), 339-374. 10, 29, 50, 69

[Ben03] —, Convexes hyperboliques et fonctions quasisymétriques, Publications Mathématiques de l'IHÉS 97 (2003), no. 1, 181–237. 50

[BS85] Joan S. Birman and Caroline Series, Geodesics with bounded intersection number on surfaces are sparsely distributed, Topology 24 (1985), no. 2, 217–225. 3, 52, 53

[BH13] Yves Benoist and Dominique Hulin, *Cubic differentials and finite volume convex projective surfaces*, Geometry & Topology **17** (2013), no. 1, 595–620. 5, 7, 50

[BH14] —, Cubic differentials and hyperbolic convex sets, Journal of Differential Geometry 98 (2014), no. 1, 1–19. 50

[BK10] Martin Bridgeman and Jeremy Kahn, Hyperbolic volume of manifolds with geodesic boundary and orthospectra, Geometric and Functional Analysis 20 (2010), no. 5, 1210–1230. 2

[Bon96] Francis Bonahon, Shearing hyperbolic surfaces, bending pleated surfaces and Thurston's symplectic form, Ann. Fac. Sci. Toulouse Math. (6) 5 (1996), no. 2, 233–297. 4

[Bow97] Brian H Bowditch, A variation of McShane's identity for once-punctured torus bundles, Topology **36** (1997), no. 2, 325–334. 2, 12

[Bow98] B. H. Bowditch, Markoff triples and quasi-Fuchsian groups, Proc. London Math. Soc. (3) 77 (1998), no. 3, 697–736. 2, 12

[Bri11] Martin Bridgeman, Orthospectra of geodesic laminations and dilogarithm identities on moduli space, Geom. Topol. 15 (2011), no. 2, 707–733. 2

[BCS18] Martin Bridgeman, Richard Canary, and Andrés Sambarino, *An introduction to pressure metrics for higher Teichmüller spaces*, Ergodic Theory Dynam. Systems **38** (2018), no. 6, 2001–2035. **23**

[Bus74] Herbert Busemann, Spaces with homothetic spheres, Journal of Geometry 4 (1974), no. 2, 175–186, 49

[CG93] Suhyoung Choi and William M Goldman, Convex real projective structures on closed surfaces are closed, Proceedings of the American Mathematical Society 118 (1993), no. 2, 657–661. 4, 48

[CY77] Shiu-Yuen Cheng and Shing-Tung Yau, On the regularity of the monge-ampère equation det $(\partial^2 u/\partial x_i \partial x_j) = f(x,u)$, Communications on Pure and Applied Mathematics **30** (1977), no. 1, 41–68. 50

[FG06] Vladimir Fock and Alexander Goncharov, *Moduli spaces of local systems and higher Teichmüller theory*, Publications Mathématiques de l'Institut des Hautes Études Scientifiques **103** (2006), no. 1, 1–211. 2, 4, 15, 16, 17, 18, 19, 20, 21

[FG07] Vladimir V Fock and Alexander B Goncharov, Moduli spaces of convex projective structures on surfaces, Advances in Mathematics 208 (2007), no. 1, 249–273. 4, 19, 26

[G90] William M Goldman, Convex real projective structures on compact surfaces, Journal of Differential Geometry 31 (1990), no. 3, 791–845. 4, 48

[GS15] Alexander Goncharov and Linhui Shen, Geometry of canonical bases and mirror symmetry, Inventiones mathematicae 202 (2015), no. 2, 487–633. 1, 4, 6, 31, 32, 40

[Guo13] Ren Guo, Characterizations of hyperbolic geometry among Hilbert geometries: a survey, Handbook of Hilbert Geometry. IRMA Lectures in Mathematics and Theoretical Physics 22 (2013), 147–158. 6

[Hit92] Nigel J. Hitchin, Lie groups and Teichmiler space, Topology 31(1992), no. 3, 449-473. 4

[Hua14] Yi Huang, Moduli spaces of surfaces, Ph.D. thesis, The University of Melbourne, June 2014. 7, 40, 58

[Hua15] —, A McShane-type identity for closed surfaces, Nagoya Mathematical Journal **219** (2015), 65–86.

[Hua18] —, McShane-type identities for quasifuchsian representations of nonorientable surfaces, arXiv preprint arXiv:1802.03069 (2018). 2, 12, 59

[Kim18] Inkang Kim, Degeneration of strictly convex real projective structures on surface, arXiv preprint arXiv:1811.11841 (2018). 5, 9, 71, 72

[Kim19] Inkang Kim, Primitive stable representations in higher rank semisimple Lie groups, arXiv preprint arXiv:1504.08056v4 (2019). 10

[Lab06] François Labourie, *Anosov flows, surface groups and curves in projective space*, Inventiones mathematicae, **165** (2006), no. 1, 51–114. 4

[Lab07] François Labourie, Cross ratios, surface groups, $PSL(n, \mathbb{R})$ and diffeomorphisms of the circle, Publications mathématiques **106** (2007), no. 1, 139–213. 86

[LM09] François Labourie and Gregory McShane, Cross ratios and identities for higher Teichmüller-Thurston theory, Duke Math. J. 149 (2009), no. 2, 279–345. 1, 10, 11, 14, 22, 23, 35, 36, 73, 74, 82

[LS13] Donghi Lee and Makoto Sakuma, A variation of McShane's identity for 2-bridge links, Geometry & Topology 17 (2013), no. 4, 2061–2101. 2, 12

[LT11] Feng Luo and Ser Peow Tan, A dilogarithm identity on moduli spaces of curves, preprint (2011), arXiv:1102.2133. 2

[LZ17] Gye-Seon Lee and Tengren Zhang, Collar lemma for Hitchin representations, Geometry & Topology 21 (2017), no. 4, 2243–2280. 12, 68

[Mar12] Ludovic Marquis, Surface projective convexe de volume fini, Ann. Inst. Fourier (Grenoble) 62 (2012), no. 1, 325–392. 25, 50

[McS91] Greg McShane, A remarkable identity for lengths of curves, Ph.D. thesis, may 1991. 2, 41, 59, 60 [McS98] —, Simple geodesics and a series constant over Teichmüller space, Invent. Math. 132 (1998), no. 3, 607–632. 2, 8, 59, 68

[Mir07a] Maryam Mirzakhani, Simple geodesics and Weil-Petersson volumes of moduli spaces of bordered Riemann surfaces, Invent. Math. 167 (2007), no. 1, 179–222. 2, 12, 59, 68

[Mir07b] Maryam Mirzakhani, Weil-Petersson volumes and intersection theory on the moduli space of curves, J. Amer. Math. Soc. 20 (2007), no. 1, 1-23. 1

[Miy05] Hideki Miyachi, The limit sets of quasifuchsian punctured surface groups and the Teichmüller distances, Kodai Mathematical Journal 28 (2005), no. 2, 301–309. 12

[Nor08] Paul Norbury, Lengths of geodesics on non-orientable hyperbolic surfaces, Geom. Dedicata 134 (2008), 153–176. 2

[Pen87] R. C. Penner, The decorated Teichmüller space of punctured surfaces, Comm. Math. Phys. 113 (1987), no. 2, 299–339. 4, 6, 15, 21

[PS17] Rafael Potrie and Andrés Sambarino, Eigenvalues and entropy of a Hitchin representation, Inventiones mathematicae 209 (2017), no. 3, 885–925. 29

[PT10] Athanase Papadopoulos and Guillaume Théret, Shortening all the simple closed geodesics on surfaces with boundary, Proceedings of the American Mathematical Society 138 (2010), no. 5, 1775–1784. 13, 68

[PT14] Athanase Papadopoulos and Marc Troyanov, From Funk to Hilbert Geometry, Handbook of Hilbert geometry, IRMA Lectures in Mathematics and Theoretical Physics, vol. 22, European Mathematical Society Publishing House, 2014, pp. p. 33–68. 49

[Sun15] Zhe Sun, Rank n swapping algebra for PGL_n Fock–Goncharov X moduli space, Preprint, arXiv:1502.03769 (2015). 34

[SWZ17] Zhe Sun, Anna Wienhard, and Tengren Zhang, Flows on the PGL(V)-Hitchin component, arXiv preprint arXiv:1709.03580 (2017). 5

[SZ17] Zhe Sun and Tengren Zhang, The Goldman symplectic form on the PGL(V)-Hitchin component, arXiv preprint arXiv:1709.03589 (2017). 5

[Tho17] Nicolas Tholozan, *Volume entropy of Hilbert metrics and length spectrum of Hitchin representations into* PSL(3, ℝ), Duke Mathematical Journal **166** (2017), no. 7, 1377–1403. 68

[Thu98] William P Thurston, Minimal stretch maps between hyperbolic surfaces, arXiv preprint math/9801039 (1998). 13, 19, 68

[Thu16] Dylan P Thurston, From rubber bands to rational maps: a research report, Research in the Mathematical Sciences 3 (2016), no. 1, 15. 69

[TWZ06] Ser Peow Tan, Yan Loi Wong, and Ying Zhang, Generalizations of McShane's identity to hyperbolic cone-surfaces, J. Differential Geom. 72 (2006), no. 1, 73–112. 2, 68

[TWZ08] —, McShane's identity for classical Schottky groups, Pacific Journal of Mathematics 237 (2008), no. 1, 183–200, 2

[WZ18] Anna Wienhard, and Tengren Zhang, Deforming convex real projective structures, Geometriae Dedicata 192 (2018), no. 1, 327–360. 5

[Zha15] Tengren Zhang, The degeneration of convex \mathbb{RP}^2 structures on surfaces, Proceedings of the London Mathematical Society 111 (2015), no. 5, 967–1012. 5

YAU MATHEMATICAL SCIENCES CENTER, TSINGHUA UNIVERSITY

 ${\it Email address: \tt yihuang@math.tsinghua.edu.cn}$

MATHEMATICS RESEARCH UNIT, UNIVERSITY OF LUXEMBOURG

Email address: sunzhe1985@gmail.com